INVESTIGATION INTO THE ROLE OF R2R3-MYB TRANSCRIPTION FACTORS RELATED TO FLOWER SHAPE AND COLOUR IN *DENDROBIUM* ORCHIDS

MUHAMMAD ASYRAF BIN KHAIRUL ANUAR

INSTITUTE FOR ADVANCED STUDIES
UNIVERSITI MALAYA
KUALA LUMPUR

2023

INVESTIGATION INTO THE ROLE OF R2R3-MYB TRANSCRIPTION FACTORS RELATED TO FLOWER SHAPE AND COLOUR IN *DENDROBIUM* ORCHIDS

MUHAMMAD ASYRAF BIN KHAIRUL ANUAR

DISSERTATION SUBMITTED IN FULFILMENT OF THE REQUIREMENTS FOR THE DEGREE OF MASTER OF PHILOSOPHY

INSTITUTE FOR ADVANCED STUDIES
UNIVERSITI MALAYA
KUALA LUMPUR

2023

UNIVERSITY OF MALAYA

ORIGINAL LITERARY WORK DECLARATION

Name of Candidate: **MUHAMMAD ASYRAF BIN KHAIRUL ANUAR**

Matric No: **HMA 180014 (old) and 17081565/3 (new)**

Name of Degree: **MASTER OF PHILOSOPHY**

Title of Project Paper/Research Report/Dissertation/Thesis ("this Work"):

Investigation into the role of R2R3-MYB transcription factors related to flower shape and colour in *Dendrobium* orchids

Field of Study: **Molecular Biology (Biology and Biochemistry)**

I do solemnly and sincerely declare that:

(1) I am the sole author/writer of this Work;
(2) This Work is original;
(3) Any use of any work in which copyright exists was done by way of fair dealing and for permitted purposes and any excerpt or extract from, or reference to or reproduction of any copyright work has been disclosed expressly and sufficiently and the title of the Work and its authorship have been acknowledged in this Work;
(4) I do not have any actual knowledge nor do I ought reasonably to know that the making of this work constitutes an infringement of any copyright work;
(5) I hereby assign all and every rights in the copyright to this Work to the University of Malaya ("UM"), who henceforth shall be owner of the copyright in this Work and that any reproduction or use in any form or by any means whatsoever is prohibited without the written consent of UM having been first had and obtained;
(6) I am fully aware that if in the course of making this Work I have infringed any copyright whether intentionally or otherwise, I may be subject to legal action or any other action as may be determined by UM.

Candidate's Signature Date:

Subscribed and solemnly declared before,

Witness's Signature Date:

Name :

Designation:

Investigation into the role of R2R3-MYB transcription factors related to flower shape and colour in *Dendrobium* orchids

ABSTRACT

During flower development, a set of structural genes are regulated to control the flower's colour and shape. R2R3-MYB transcription factors are important for controlling many different biological processes. However, we still don't know which members of this large family of transcription factors are involved in pigment and, in particular, organ shape development in a popular *Dendrobium* orchid with a dark purple flower. Phylogenetic analysis was used to find *Dendrobium catenatum R2R3-MYB* (*DcaMYB*) sequences that are likely to be involved in the development of pigment and cell shape. The expression of candidate *DhMYB* genes in *Dendrobium* hybrid was silenced by directly applying dsRNA to the developing flowers together with observation of the gene expression level and flower phenotypes. As a comparison, the structural pigment-related gene, *chalcone synthase*, was also silenced. Flowers treated with dsRNA of *DhMYB22* and *DhMYB60* sequences had less colour and low expression of anthocyanin biosynthesis genes (*DFR* and *F3'H*). They also had lower total anthocyanin and much lower cyanidin-3-glucoside and cyanidin-3-rutinoside content. The most significant difference in colour was seen in the petals of *DhMYB22*-treated flowers and the sepals of *DhMYB60*-treated flowers compared to the same organs of untreated flowers. The lips of flowers treated with *DhMYB22* were narrow and constricted, also observed in the sepals of flowers treated with *DhMYB60*. No significant difference was seen in the shape of flowers that were untreated or were treated with *DhCHS*. The results showed that *Dendrobium*'s *DhMYB22* and *DhMYB60* control the amount of pigment and the shape of the flower organs. This is the first report that the shape of flower organs in orchids has been linked to MYB.

Keywords: *Dendrobium*, anthocyanin, floral organ shape, gene silencing, R2R3-MYB

Penyiasatan terhadap peranan faktor transkripsi R2R3-MYB yang berkaitan dengan bentuk bunga dan warna dalam orkid *Dendrobium*

ABSTRAK

Pigmen dan bentuk bunga ditentukan oleh ekspresi terkoordinasi satu set gen struktur semasa perkembangan bunga. Faktor transkripsi R2R3-MYB memainkan peranan penting dalam mengawal selia proses biologi yang pelbagai, namun, lebih banyak lagi yang tidak diketahui tentang faktor transkripsi ini yang mempunyai peranan dalam pigmen terutamanya dalam pembangunan bentuk organ orkid *Dendrobium* yang sangat terkenal dengan pigmen gelap berwarna ungu. Analisis filogenetik digunakan untuk mengenal pasti jujukan *Dendrobium catenatum R2R3-MYB* (*DcaMYB*) yang berkaitan dengan pembangunan bentuk pigmen dan sel. Penguncian gen *DhMYB* dalam *Dendrobium* hibrid dengan dsRNA untuk melihat perkembangan bunga diikuti dengan tahap ekspresi gen dan fenotip bunga. Mengunci gen struktur *chalcone synthase* digunakan sebagai kawalan perbandingan. Bunga yang dirawat dengan dsRNA *DhMYB22* dan *DhMYB60* menyebabkan kurang pigmen dengan ekspresi gen biosintesis antosianin yang rendah (*DFR* dan *F3'H*) dan mempunyai jumlah kandungan antosianin yang lebih rendah seiring dengan paras cyanidin-3-glukosida dan cyanidin-3-rutinosida yang lebih rendah. Kelopak bunga yang dirawat *DhMYB22* dan sepal bunga dirawat *DhMYB60* menunjukkan perbezaan warna yang paling besar berbanding organ yang sama dalam bunga yang tidak dirawat. Bunga yang dirawat *DhMYB22* mempunyai bibir yang agak tirus dan mengecil, manakala bunga yang dirawat *DhMYB60* mempunyai sepal yang tirus dan mengecil. Tiada perbezaan ketara dalam bentuk diperhatikan untuk bunga *DhCHS* yang dirawat atau tidak dirawat. Keputusan menunjukkan bahawa *DhMYB22* dan *DhMYB60* mengawal keamatan pigmen dan bentuk organ bunga dalam *Dendrobium*. Ini adalah laporan pertama peraturan MYB tentang bentuk organ bunga dalam orkid.

Kata kunci: *Dendrobium*, antosianin, bentuk organ bunga, penguncian gen, R2R3-MYB

ACKNOWLEDGEMENTS

All praise be to Allah. I have completed my Master's degree and am now composing my thank you note as the final step in my dissertation. Much of my life has changed since I began working on this dissertation. I'd want to take a moment to thank all of the people who have helped and supported me throughout my Master's degree journey.

To begin, I want to convey my heartfelt gratitude to my supervisors, Professor Dr. Jennifer Ann Harikrishna and Professor Dr. Rofina Yasmin Othman, for taking me under their wing. Their assistance and insightful comments have kept me on track toward completing this study throughout these years. I want to express my gratitude to Dr. Purabi Mazumdar, Senior Lecturer, CEBAR, for assisting me with experimental design, technical guidance, and paper preparation.

Besides, I'd like to take this opportunity to thank current and former members of CEBAR Molecular Lab, CEBAR Biochemistry Lab, PBF members, CEBAR Admins, 'Geng The Usual Bunch', 'Geng Karok Part Timer', 'Geng Hiking', and my friends for always being my morale boosters and source of laughter throughout my Master's degree journey.

Finally, I would like to express my gratitude to my dear wife, Syafi Alia Marsan, parents, En. Khairul Anuar Daud and Pn. Norpatiah Mohd Luding, as well as my family, for their unwavering support, persistent prayers, and words of encouragement in helping me accomplish my study. Once again, I want to express my gratitude to everyone who has motivated me to be the best version of myself, whether directly or indirectly. May Allah shower you all with goodness and unending happiness

TABLE OF CONTENTS

LIST OF FIGURES

LIST OF TABLES

LIST OF SYMBOLS AND ABBREVIATIONS

+ve	:	Positive
-ve	:	Negative
AM	:	After midnight
bp	:	Base Pair
ºC	:	Celsius
Ca^{2+}	:	Calcium ions
CTAB	:	Cetyltrimethylammonium bromide
d	:	Day
K^{+}	:	Potassium ions
kb	:	Kilobase
L	:	Litre
Mbp	:	Mega base pair
mg	:	Milligram
min	:	Minute
mL	:	Millilitre
mM	:	Millimolar
mm	:	Millimetre
µg	:	Microgram
µM	:	Micromolar
µmol	:	Micromole
ng	:	Nanogram
nm	:	Nanometre
OD	:	Optical density
%	:	Percentage

P	:	Probability
s	:	Second
V	:	Voltage
v/v	:	Volume per volume
w/v	:	Weight per volume
C3G	:	Cyanidin-3-glucoside
C3R	:	Cyanidin-3-rutinoside
$CaCl_2$	:	Calcium chloride
cDNA	:	Complementary deoxy ribonucleic acid
CDS	:	Coding DNA sequence
CI	:	Chloroform Isoamyl
CTAB	:	Cetyltrimethylammonium bromide
ddH_20	:	Sterile distilled water
DEPC	:	Diethyl Pyrocarbonate
DNA	:	Deoxy ribonucleic acid
dNTPs	:	Deoxyribonucleotide triphosphate
dsRNA	:	Double stranded RNA
DW	:	Dry weight
EV	:	Empty Vector
FW	:	Fresh weight
gDNA	:	Genomic DNA
HCl	:	Hydrochloric acid
HiFi	:	High Fidelity
IPTG	:	Isopropyl-beta-D-thiogalactopyranoside
LB	:	Luria Bertani
$MgCl_2$	:	Magnesium chloride

mRNAs	:	Messenger ribonucleic acid
MYB	:	Myeloblastosis
NaCl	:	Sodium chloride
NaOH	:	Sodium hydroxide
OD	:	Optical density
P:C:I	:	Phenol Chloroform Isoamyl
PCR	:	Polymerase chain reaction
RT-PCR	:	Reverse transcriptase PCR
qRT-PCR	:	Quantitative real time PCR
RH	:	Relative humidity
RM	:	Ringgit Malaysia
RNA	:	Ribonucleic acid
RNAi	:	Ribonucleic acid interference
rpm	:	Revolutions per minute
RT	:	Room temperature
siRNAs	:	Small interfering ribonucleic acid
spp.	:	Species
SPSS	:	Statistical package for social sciences
Tris-HCl	:	Trisaminomethane hydrochloride
UV	:	Ultraviolet
WT	:	Wild type

LIST OF APPENDICES

CHAPTER 1: INTRODUCTION

Malaysia is located in the tropics, which encompass the most diverse flora in the world. Thus, Malaysia has an advantage for generating income by exporting floriculture products worldwide. According to the National Agrofood Policy (2011-2020) and the 11th Malaysian Plan (2016-2020), floriculture is recognised as a high-value industry (Nik Rozana et al., 2016). Orchids account for a large share in the global floriculture trade as cut flowers and potted plants. Malaysia exported about RM 337.7 million worth of orchids in 2017 (Department of Agriculture, Malaysia, 2017).

Hybrids of *Dendrobium* (Family Orchidaceae) are popular orchids grown in Malaysia and have attracted consumers worldwide. However, there is an increasing demand for novel flower colours and patterns. The generation of novel traits in orchids is constrained by the long breeding time and the lack of information on suitable candidate genes responsible for colours and shapes. *R2R3-MYB* genes encode a family of transcription factors, widely reported as key regulators of plant development, including floral morphogenesis and pigment biosynthesis.

Lau et al. (2015) have shown the involvement of *DhMYB1* (an *R2R3-MYB* gene) in determining cell shape in *Dendrobium* hybrid flowers, via knockdown of *DhMYB1* expression using bacterially produced dsRNA. A related *R2R3-MYB* gene, *DhMYB2* supported by another transcription factor *DhbHLH1* has been shown to regulate pigment biosynthesis in *Dendrobium* hybrid flowers using a transient overexpression study (Li et al., 2017). The recently published complete genome sequence of a *Dendrobium* species, *Dendrobium catenatum*, showed the presence of many *R2R3-MYB* genes with as yet undetermined function (Zhang et al., 2016). The main aim of the research proposed for this thesis is to determine the roles of selected *R2R3-MYB* genes from *Dendrobium* hybrid

in flower development, by using the direct dsRNA-mediated knockdown of candidate *R2R3-MYB* genes to reveal their function.

The specific objectives are:

1) To identify and select two candidate *R2R3-MYB* genes related to flower colour and/or shape.
2) To optimise the isolation of RNA from *Dendrobium* hybrid floral tissue.
3) To investigate the stage-specific expression of two selected *R2R3-MYB* genes related to flower colour and/or shape in different developmental stages of *Dendrobium* flower buds.
4) To prepare dsRNA expression constructs for the knockdown of two selected *R2R3-MYB* genes.
5) To determine the role of the two selected *R2R3-MYB* genes on flower development *via* quantification of phenotypic changes, biochemical assays and expression analysis (qRT-PCR assay) of plants with knocked-down expression.

CHAPTER 2: LITERATURE REVIEW

2.1 Orchid industry in Malaysia

Malaysia is an abundant reservoir of flowering plant species because of its climate and topography. Malaysia was listed as one of the top countries in exporting floriculture products worldwide (Nik Rozana et al., 2016). Malaysia's floriculture industry contributes more than RM 500 million a year from its export markets (Abu Dardak et al., 2020). The National Agrofood Policy (NAP) 2011-2020 expects further increase in floriculture exportation value from RM 449 million in 2010 to RM 857 million in 2020. The primary export markets for Malaysian floriculture products were Japan, Thailand, Singapore, Australia, and the United Arab Emirates in 2018 (https://ap.fftc.org.tw/article/1924).

Orchids are a floriculture product that account for a significant share in global trade as cut flowers and potted plants. The total production value for orchids in Malaysia has been increasing from RM 72,692 million in 2012 to RM 95,775 million in 2017, as shown in Table 2-1 (Department of Agriculture, Malaysia, 2017). Japan, Singapore, Australia, and Saudi Arabia are the major export destinations for fresh orchids (https://ap.fftc.org.tw/article/1924). The three (3) types of orchids considered enormous variety of exported orchids encompasses *Dendrobium*, Aranda, and Mokara (De et al., 2014). Realising the value of orchids in the floriculture industry, the Malaysian Agriculture Research and Development Institute (MARDI) has embarked on an Orchid Breeding Programme to assist the industry. Their main projects for this programme are the germplasm collection and hybridisation program. Therefore, MARDI is able to produce new orchid hybrids to ensure consistent supply for high demand in the market (Mahmood 2006).

Table 2-1 : Number of plants and total production value for orchid from 2012 – 2017

Years	Number of plants	Total Production Value (RM Million)
2012	158,026,488	72,692
2013	182,274,565	91,157
2014	187,742,802	93,871
2015	192,003,297	96,002
2016	188,163,231	94,082
2017	191,550,169	95,775

Data source from the Department of Agriculture, Malaysia (http://www.doa.gov.my/index.php/pages/view/622?mid=239)

2.2 *Dendrobium*

Orchidaceae with an estimated >28,000 species in 736 genera are considered as one of the largest flower families (Christenhusz et al., 2016; Pridgeon et al., 2015) with diverse flower shapes and exotic colours (Hsiao et al., 2011). *Dendrobium* is one of the large genera of the Orchidaceae family noted for their profuse, delicate and vibrant coloured blooms with a long shelf life (Sheehan, 1992). Olaf Swartz classified the *Dendrobium* genus in 1979 in an article "Dianome Epidendri Generis Linn' where he included 1500 species mainly distributed in the tropics and subtropics in the south of Asia and Oceanica. *Dendrobium* species are mostly epiphytes or lithophytes while a few species are terrestrial. *Dendrobium*s are sympodial orchids with cylindrical roots usually arising from the base of a pseudobulb. The pseudobulbs or stem, when present, are hard, sometimes cane-like, cylindrical or cone-shaped and more or less covered with the bases of the leaves. Leaves are arranged in two rows and flowers are arranged along an unbranched flowering stem (Figure 2-1) (Hew et al., 2004). *Dendrobium* species are warm climate orchids and although able to withstand direct sunlight to some extent, a partially shaded environment is more conducive for growth and flowering and to prevent scorching of

leaves and flowers. Hence, growing *Dendrobium* indoors or in a greenhouse is highly recommended for better growth (Fitch, 2004). A suitable growing temperature for *Dendrobium* is around 21 – 25 °C with a relative humidity of 70 – 75% (Ding et al., 2018).

In this study a *Dendrobium* hybrid orchid is used for functional study of R2R3-MYBs. This *Dendrobium* hybrid, the crossbreed from *Dendrobium* Burmese Ruby, Bee Lian 1989 with *Dendrobium* Mae-Klong River, S. Semachai 1975. Table 2-2 show the seed parent and pollen parent for the crossbreed *Dendrobium* hybrid. This research will use a *Dendrobium* hybrid orchid which has not been studied before.

Table 2-2 : Seed parent and pollen parent for *Dendrobium* cross breed *Dendrobium* hybrid (Source: The Royal Horticultural Society 2016)

***Dendrobium* hybrid**	**Seed Parent**	**Pollen Parent**
Dendrobium Burmese Ruby	*Dendrobium* Norma Jackson	*Dendrobium* Bobby Mesina
Dendrobium Mae-Klong River	*Dendrobium* Srisomboon	*Dendrobium* Yaowamal

Figure 2-1 : *Dendrobium* hybrid orchid (*Dendrobium* Burmese Ruby × *Dendrobium* Mae-Klong River)

2.3 *MYB* genes

Almost all biological processes in eukaryotic cells or organisms are regulated by transcriptional control of gene expression. Transcription factors (TFs) are proteins which act as a regulator in the processing of genetic information from DNA to mRNA. TFs alone or complexed with other proteins bind to specific DNA sequences and activate or repress the production of mRNA transcripts from genes (Stracke, et al., 2001; Chen, et al., 2006).

MYB (myeloblastosis) transcription factors, form one of the largest gene families in plants. The MYB proteins have a structure of an N-terminal DNA-binding domain, a central transactivation domain, and a C-terminal regulatory domain (reviewed in Oh & Reddy, 1999). The MYB domain comprises of up to four imperfect amino acid sequence repeats (R) that are 1R, 2R (R2R3), 3R, and 4R (Figure 2-2). These repeats are of about 50-53 amino acids, each forming three alpha-helices (Dubos et al., 2010). The second and third helices of each repeat build a helix-turn-helix (HTH) structure with three regularly spaced tryptophan (or hydrophobic) residues, forming a hydrophobic core (Ogata et al., 1996). The third helix of each repeat was identified as the DNA recognition helix that binds directly to the target DNA (Jia et al., 2004). During DNA contact, two MYB repeats are closely packed in the major groove, so that the two recognition helices bind cooperatively to the specific DNA recognition sequence motif.

Most plant *MYB* genes encode R2R3-MYB class proteins, containing two repeats (Dubos et al., 2010; Jin et al., 1999). Genome-wide analyses of the *R2R3-MYB* gene family has been investigated in several plant species such as *Arabidopsis thaliana* (Stracke et al., 2001), *Zea mays* (maize) (Riaz et al., 2019), *Gossypium* spp. (cotton) (An et al., 2008) , *Oryza sativa* (rice) (Suzuki et al., 1997), *Petunia* hybrid (petunia) (Shimada et al., 2006), *Antirrhinum majus* (snapdragon) (Baumann et al., 2007), *Vitis vinifera L.* (grapevine) (Deluc et al., 2006), *Populus tremuloides* (poplar) (Wilkins et al., 2009) and

Malus domestica (apple) (Xie et al., 2018), using both bioinformatic and molecular analyses. The functions of R2R3-MYB transcription factors are widely studied for plant development regulation, light, hormone, signalling, cell morphogenesis, and defence response and stress responses (Jin and Martin et al., 1999).

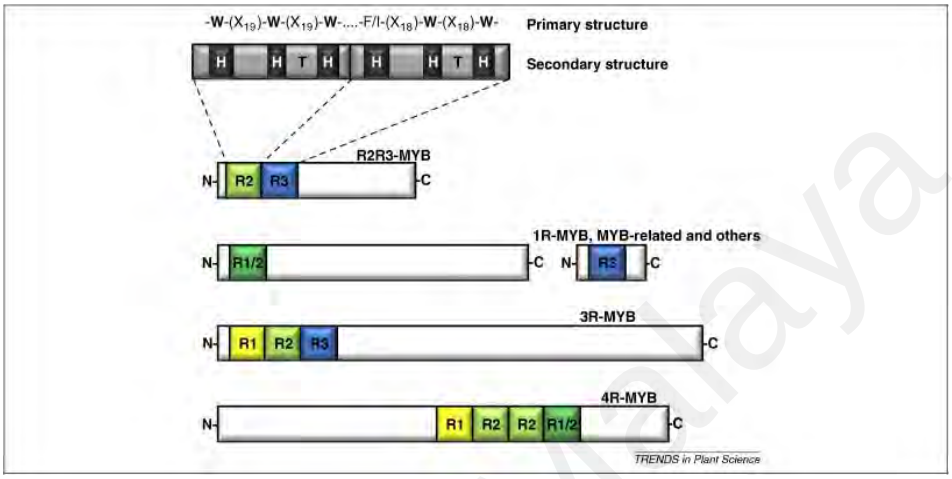

Figure 2-2 : Classes of the MYB transcription factor according to the number of repeats (R). Each MYB contains primary and secondary structures. MYB repeats, R; helix, H; turn, T; tryptophan, W; any amino acid, X. Source: Dubos et al. (2010).

2.3.1 *MYB* genes associated with flower colour

Breeding hybrid flowers with altered colours, hues and patterns is an important research area to fulfil consumer needs (Li et al., 2017). The colour of a flower is from the accumulation of pigments such as anthocyanins, a group of water-soluble vacuolar pigments. The colour of an anthocyanin depends on the pH and may appear red in acidic aqueous solution while purple or blue in a pH neutral solution (Ibrahim et al., 2011).

Anthocyanin pigment synthesis is branched from the flavonoid biosynthesis pathway, which has been well studied and is conserved within a wide range of plants (Higashi et al., 2013). The first key enzyme, which acts on the precursor for all classes of flavonoids is chalcone synthase (CHS). CHS catalyses the stepwise condensation of three acetate units from malonyl-CoA using coumaroyl-CoA as a starter CoA to yield naringenin

chalcone. Chalcone isomerase (CHI) is needed for the subsequent enzymatic reaction from naringenin chalcone to naringenin, which is further converted to dihydrokaempferol by flavone 3-hydroxylase (F3H). Finally, three classes of anthocyanidin end products; pelagornidin-3-glucoside, cyanidin-3-glucoside and delphinidin-3-glucoside are completed by consecutive late anthocyanin biosynthetic genes (Kim et al., 2017) (Figure 2-3).

Diversification of anthocyanidins is related to the structure, quantity and position of conjugated sugar and acyl moieties. Anthocyanidins consist of two rings of aromatic benzene, separated by an oxygenated heterocycle (Tanaka et al., 2008). Cyanidin, pelargonidin and delphinidin are the main anthocyanidins and differ at their B-rings by the number of hydroxyl groups (Figure 2-4). Blue/violet flowers tend to contain delphinidin-based anthocyanins, magenta/red flowers contain predominantly cyanidin-based anthocyanins and orange/brick red flowers contain pelargonidin-based anthocyanins. Methylation of 3′- or 5′-hydroxyl groups tends to yield slightly redder colours (Figure 2-3 and 2-4) (Tanaka et al., 2013).

The expression of anthocyanin biosynthetic genes is mostly controlled by two families of transcription regulators, MYB and bHLH proteins (Holton et al., 1995; Koes et al., 2005). MYB proteins are the main components which trigger anthocyanin structural genes (Davies et al., 2003) and bHLH proteins can have overlapping regulatory targets (Zhang et al., 2003; Zimmermann et al., 2004). WD-repeat proteins also form part of the regulatory protein complex which uniquely binds to target genes to initiate gene expression (Koes et al., 2005). The R2R3-MYB protein family members which can be found in most plants are among the main regulators of the anthocyanin pathway (Stracke et al., 2007).

Several studies have been conducted to elucidate the mechanism of the regulatory genes for flower colour and pigmentation in orchids. Transient expression of *OgMYB1* resulted in mosaic red pigmentation in yellow tissue of *Oncidium* Gower Ramsay. *OgCHI* and *OgDFR* expression were regulated by *OgMYB1* (Chiou et al., 2008). Transient expression of *PsMYB8* induced anthocyanin pigmentation in *Phalaenopsis amabilis* petals and sepals (Hongmei et al., 2009). High levels of *PsMYBs* and *Dfr* transcripts were present in purple flowers of *Phalaenopsis* 'Everspring Fairy' but not in the white sector of petals and sepals (Hongmei et al., 2009). Hsu et al. (2015) identified that three R2R3-MYB transcription factors; *PeMYB2*, *PeMYB11*, and *PeMYB12* could activate the expression of three downstream structural genes of *Flavanone 3-hydroxylase 5*, *Dihydroflavonol 4-reductase 1* and *Anthocyanidin synthase 3* of *Phalaenopsis* spp. Silencing of these genes resulted in the loss of the full-red pigmentation, red spots, and venation patterns in the sepals/petals. In the *Dendrobium* hybrid 'Burana charming',transient over-expression of *DhMYB2* and *DhbHLH1* resulted in ability to recover the purple coloration for anthocyanin production in white petals (Li et al., 2017).

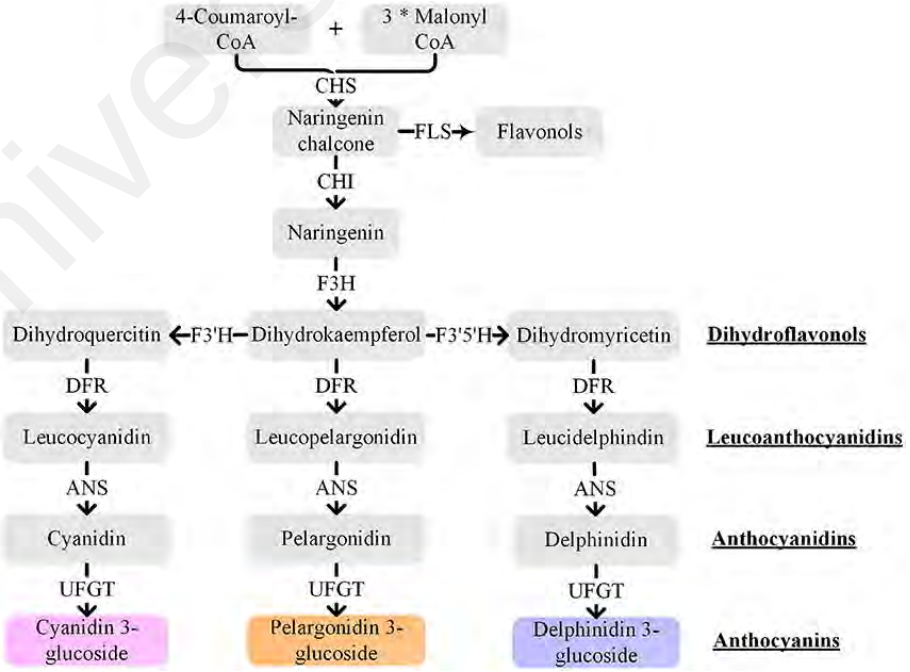

Figure 2-3 : Schematic representation of the anthocyanin biosynthetic pathway. Source: Liu et al. (2018).

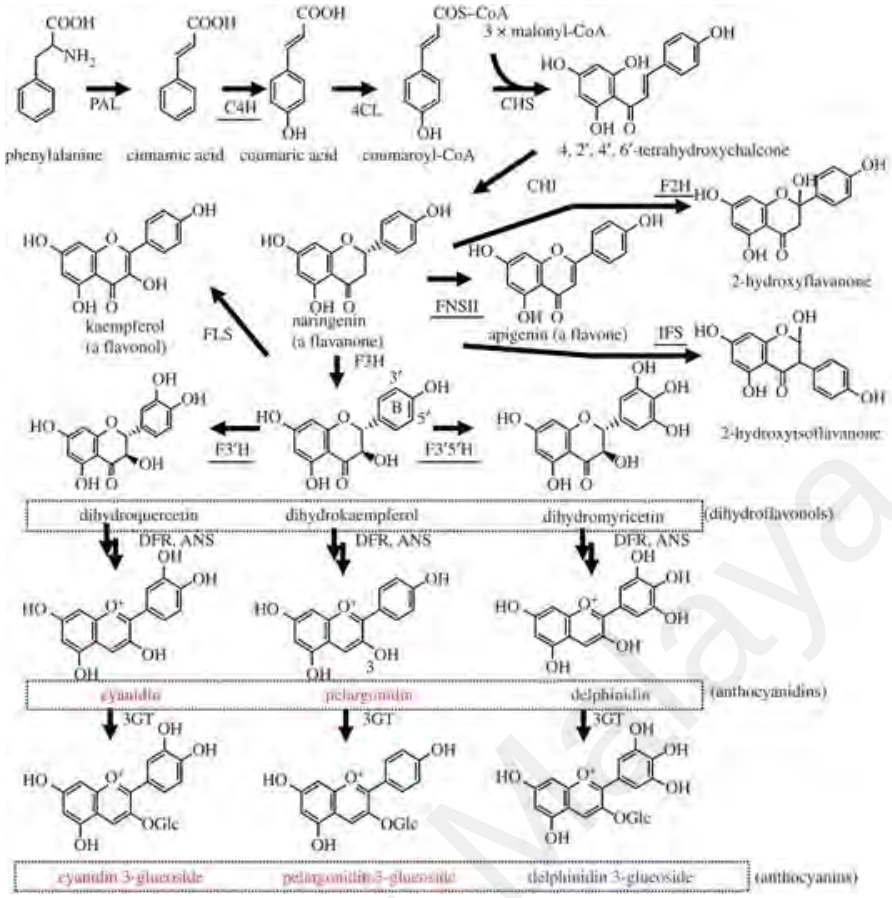

Figure 2-4 : Structures of anthocyanin compounds. Source: Tanaka et al. (2013)

2.3.2 *MYB* genes associated with flower shape

Flower size and shape vary across species and depends on epidermal cell development. These variations are affected by biotic and abiotic environments (Vega et al., 2015). Cell shape provides visual signals to pollinators with stimulation by temperature and light capture of the plants (Miller et al., 2011; Whitney et al., 2011). On the other hand, different cell shapes such as conical, flat or pointed can affect flower colour differently (Baumann et al., 2007; Miller et al., 2011; Noda et al., 1994). For example, conical cell shape can enhance light absorption by the pigments by increasing the amount of incident light that enters the epidermal cells (Baumann et al., 2007; Yoshida et al., 2006).

Several studies have been conducted to describe various cell types based on cell shape and size in several species of orchid. Rasika et al. (2003) reported the presence of flat epidermal cells in petals and sepals for *Dendrobium* Autumn Lace, *Dendrobium* Betty Goto, *Dendrobium canaliculatum* X *Dendrobium taurinum*, *Dendrobium gouldii* and *Dendrobium lasianthera*. Flat epidermal cells can also be seen in petals and sepals of *Dendrobium* hybrid (Lau et al., 2015). However, this contrasts with findings by Pan et al. (2014) that the adaxial epidermal cells of the sepal of *Phalaenopsis* orchid were conical in shape. This suggests that different genera of orchids such as *Dendrobium* and *Phalaenopsis* may have different cell shape patterns (Lau et al., 2015).

Many studies have reported that MYB transcription factors, mainly R2R3-MYB, can regulate plant development and secondary metabolism, light and hormone signaling, cell morphogenesis as well as defence and stress responses (Dubos et al., 2010; Jin et al., 1999). For regulation of epidermal cell development in *Antirrhinum majus*, *AmMYBML1* expression was reported to induce the production of both trichomes and conical cells in floral tissues (Perez-Rodriguez et al., 2005). Furthermore, *AmMYBML2* gene expression was able to extend the growth of conical petal epidermal cells (Baumann et al., 2007) while *AmMYBML3* gene expression can enhance cellular out-growth from the epidermis of all aerial organs (Jaffé et al., 2007). In *Thalictrum thalictroides*, the expression of the MIXTA related *R2R3-MYB* gene *TtMYMML2* was able to promote conical cell growth in the petal and carpel epidermal cells (Di Stilio et al., 2009). Besides, *AmMIXTA*, *AtMYB16* and *PhMYB1* were reported to control cell differentiation and also able to activate anthocyanin biosynthetic gene expression in *Antirrhinum majus*, *Arabidopsis thaliana* and *Petunia* hybrida respectively (Baumann et al., 2007; Noda et al., 1994). Lau et al. (2015) observed that dsRNA silencing of *DhMYB1* affected epidermal cell shape in the labellum of *Dendrobium* hybrid by changing from (wild type) conical shaped cells to flattened cells. This finding by Lau et al. (2015) was very similar to the finding for flowers

of MIXTA mutants in *Anthirrhinum majus* (Glover et al., 1998; Noda et al., 1994) and *PhMYB1* mutants in *Petunia* hybrida (Baumann et al., 2007).

2.4 RNA silencing in plants

2.4.1 RNA silencing

RNA silencing, also known as RNA interference or "RNAi", results from natural mechanisms in eukaryotes that can be applied as a powerful research tool to study gene function and development of novel traits in plants. This is because the biological process in RNA silencing in which RNA molecules inhibit the transcription or translation of a targeted gene can be triggered using dsRNA. Probably, the first documented observation of an RNA silencing effect was in 1928 by Wingard. Wingard described tobacco plants in which only the initial leaves infected with tobacco ringspot virus were necrotic and diseased (Wingard et al., 1928) reviewed by Balcombe (2004). However, the upper leaves were asymptomatic and resistant to secondary infection, which is now understood through the subsequent work of Hamilton and Baulcombe (1999), to be due to RNA silencing triggered by the presence of viral RNA in the plants. Throughout the years, there has been growing knowledge to understand the mechanism of RNA silencing. Napoli et al. (1990) discovered that RNA silencing, which they described as co-suppression, occurred in *Petunia* hybrida plants when they introduced transgene copies of the flower pigmentation gene, *chalcone synthase* (CHS) into *Petunia* hybrida flowers aiming to produce a more intense purple colouration in this flower. However, this introduction produced intense purple, patterns of purple and white, and flowers that were completely white (Napoli et al., 1990). Andrew Fire and Craig C. Mello also discovered RNA interference (RNAi) mechanism in a nematode species; *Caenorhabditis elegans*, which they published in 1998 (Fire et al., 1998). The RNAi mechanism has been used successfully in several research studies such as in inhibition of the proliferation of foreign sequences (transposable elements) and development of resistance against plant viruses (Broecker et al., 2019;

Obbard et al., 2009), to validate the function of novel genes (Tenea et al., 2012) and generation of novel traits (Saurabh et al., 2014).

Plants exhibit two types of gene silencing: transcriptional gene silencing (TGS), which involves reduced RNA synthesis as a result of promoter methylation or histone modification, and posttranscriptional gene silencing (PTGS), which involves sequence-specific RNA degradation (Hoffer et al., 2011). TGS occurs during the transcription stage in the nucleus, whereas PTGS is thought to act in the cytoplasm via mRNA cleavage or inhibition of translation (Ruiz-Ferrer et al., 2009). TGS can be caused by DNA pairing or dsRNA-mediated promoter inactivation, while PTGS can resulted from either intentional or unintentional creation of double-stranded RNA (dsRNA) (Hoffer et al., 2011).

Figure 2-5 illustrates RNAi schematically. The procedure involves the processing of dsRNA into shorter units, which results in the recognition and targeted cleavage of homologous mRNA (reviewed in Fellmann et al., 2014). The ribonuclease called DICER, or Dicer-like enzyme, cleaves dsRNA and creates small non-coding RNAs called microRNA (miRNA) and small interfering RNA (siRNA) (reviewed in Song et al., 2017). The RNAi phenomenon is caused by short non-coding RNAs in combination with an RNA-induced silencing complex (RISC), Argonaute (AGO), and other effector proteins. Small RNAs are made up of cleaved double-stranded RNA that silence the target mRNA transcript, resulting in gene expression suppression (reviewed in Song et al., 2017).

RNAi is a natural process of gene regulation that employs silencing mechanisms (Andrade & Hunter 2016) to silence gene expression, and introduction of dsRNA can also be utilised in biotechnology to make complementary siRNA, that can trigger posttranscriptional gene silencing in the cell or organism being targeted. There are extensive studies on silencing of cytoplasmic RNA (siRNA) by direct application of dsRNA for functional analysis of plant endogenous genes because it is rapid and

circumvent the tedious steps of plant transformation (Tenllado et al., 2003). The knockdown of genes by direct use of dsRNA overcomes the limitation of host specificities and is applicable to a wide range of plant species at minimal cost. By processing dsRNA into 21 to 23 nucleotides small interfering RNAs (siRNAs), the RNAi mediators are able to induce cognate degradation of mRNA (Bernstein et al., 2001; Zamore et al., 2000). These processes were shown by Lau et al. (2015), to be a simple and efficient method of direct application of dsRNA for functional analysis of endogenous genes in *Dendrobium* hybrid.

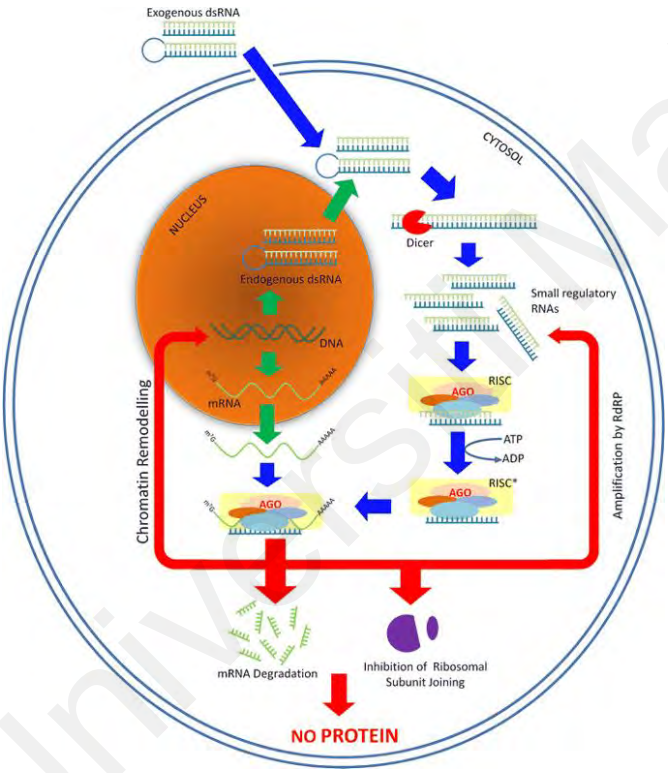

Figure 2-5 : Schematic representation of biogenesis of small regulatory RNAs (siRNAs, miRNAs) pathways and their role in mechanisms for RNA interference. Green arrows: natural pathway of molecular biology; Blue arrows: biogenesis pathway of activated small regulatory RNAs from double stranded RNA (dsRNA); Red arrows: RNA interference-mediated pathways toward gene silencing. RISC: RNA induced silencing complex; RISC*: activated RNA induced silencing complex; AGO: argonaut proteins; RdRP: RNA-dependent RNA polymerase. Source: Saurabh et al., (2014).

2.4.2 Delivery of RNAi

RNA interference (RNAi) has been widely utilised in crop defence systems since its discovery more than 20 years ago. Until now, RNAi approaches have commonly been focused on the use of transgenic plants expressing double-stranded RNAs (dsRNAs) against selected targets. Nevertheless, there has been growing scientific and public concern with the use of transgenes and genetically modified organisms (GMOs). Thus, the need for alternative strategies to avoid using transgenes and instead resort to direct exogenous application of RNA molecules with the potential to trigger RNAi (Dalakouras et al., 2020).

There are various methods to apply dsRNA in plants (Dubrovina et al., 2019). Several studies reported on the usefulness of exogenously applied *in vitro* synthesised or bacterially produced long dsRNAs, hairpin RNAs (hpRNAs), or small interfering RNAs (siRNAs) that target essential genes of the plant pathogens and protecting plants against viral, fungal and plant pathogens (Dubrovina et al., 2019) (Figure 2-6). The efficient delivery of exogenous hpRNAs and siRNAs into woody and herbaceous plants by means of trunk injections, soil/root drench, and petiole absorption has been reported (Dalakouras et al., 2018). The conjugation of RNA molecules to nanoparticles and carrier peptides greatly enhances their resistance to nucleases and improves the efficiency of delivery (Dalakouras et al., 2018). A recent study demonstrated that the efficiency of RNAi in plants can be enhanced by the addition of chemical enhancers such as Sortin 1, Isoxazolone and [5-(3,4-dichlorophenyl) furan-2-yl]-piperidine-1-ylmethanethione (DFPM) (Jay et al., 2019). These three molecules increased the RNAi potency of the inverted-repeat construct, in large part by enhancing 21-nt siRNA accumulation and loading into AGO1, and concomitantly reducing AGO4 and DCL3 levels in plant (Jay et al., 2019).

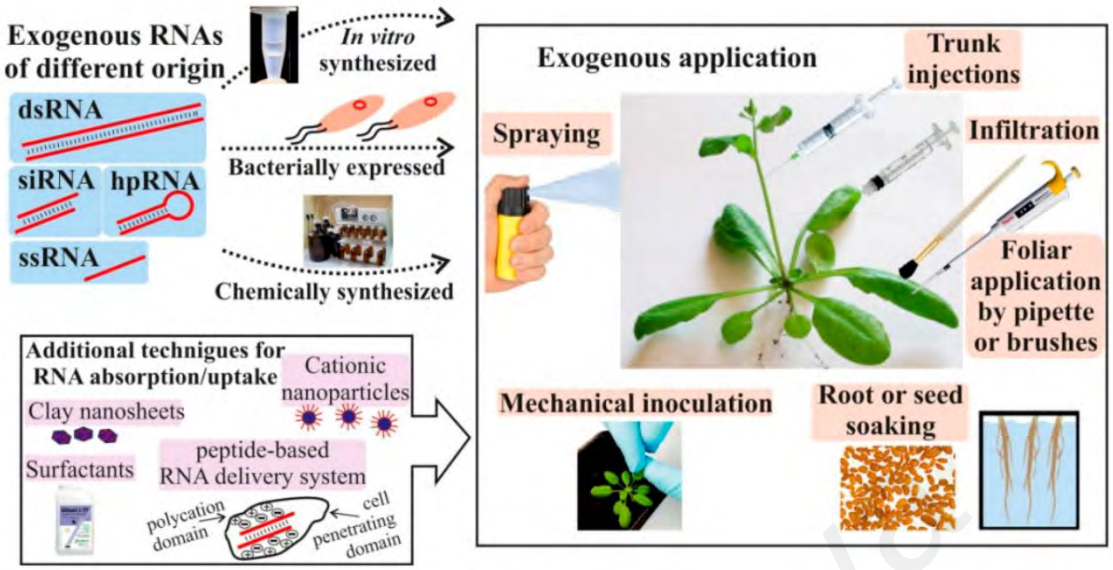

Figure 2-6 : Methods for RNAi delivery to plants. Source: Dubrovina et al. (2019)

2.5 Analysis of flower shape using geometric morphometrics

Geometric morphometrics is widely used to analyze biological shapes. It is used to address a range of questions about evolution and development of organisms. Recent breakthroughs in morphometrics and the statistical analysis of shapes have seen an increasing emphasis on identifying and explicitly describing the multidimensional spaces that underlie geometric morphometric analysis (Klingenberg 2020). The techniques used for geometric morphometrics are based on configurations of landmarks in two or three dimensions. Most approaches are based either on relative shifts of landmark positions in starting and target shapes after superimposition or on D'Arcy Thompson's idea of transformation grids (Klingenberg, 2013).

A study has been done by coupling geometric morphometrics with virus induced gene silencing (VIGS) in *Fedia graciliflora* to statistically analyze shape and symmetry changes that result from knocking down the *CYCLOIDEA2A*-like (*CYC2A*) ortholog of the *CYC2* (Berger et al., 2017). Successfully knockdown of *CYC2A* by Berger et al. (2017) resulted in a consistent shift in petal position of the corolla and a more radially

symmetrical flower. This application of geometric morphometrics analysis opens new possibilities for studying the genetics and developmental origins of morphological diversity in flowers, especially in the context of symmetry and asymmetry, which is thought to have a key role in flowers adaptive evolution (Berger et al., 2017).

CHAPTER 3: MATERIALS AND METHODS

3.1 Plant materials and growth conditions

Dendrobium hybrid (*Dendrobium* Burmese Ruby × *Dendrobium* Mae-Klong River) plants at the early flower bud stage were obtained from Cheah Wah Sang Orchid Farm in Shah Alam, Selangor, Malaysia. The plants were maintained at the GP-BSL2 greenhouse (Plant Biotech Facility), University of Malaya, Malaysia under natural light (12 hours photoperiod) in a controlled temperature (25±2°C) and relative humidity (65±5%). Floral buds of *Dendrobium* hybrid were collected at five different developmental stages according to Lau et al. (2015); Stage 1: 0-0.5 cm; Stage 2: 0.51-1.0 cm; Stage 3: 1.1-2.0 cm; Stage 4: 2.1-3.0 cm and Stage 5: 3.1-4.0 cm). Mature flowers (stage 6) were separated into three different parts: sepal, petal and lip. At the time of collection, floral tissues were immediately frozen in liquid nitrogen and then were stored at -80°C until further analysis.

3.2 Identification of *MYB* gene sequences and conserved motifs in the genome sequence of *Dendrobium catenatum*

The protein coding sequences (CDS) of the *Dendrobium catenatum* were obtained from National Center for Biotechnology Information (NCBI) database (https://ftp.ncbi.nlm.nih.gov/genomes/all/GCA/001/605/985/GCA_001605985.2_ASM160598v2/). The CDS of *Dendronium catenatum* of *R2R3-MYB* genes were extracted by using the Basic Local Alignment Search Tool (BLAST) (Mount, 2007) to the *R2R3-MYB* gene sequences from *Arabidopsis thaliana* (Stracke et al., 2001) with the command line: blastall –p blastn –d (CDS *Dendrobium*. txt) –i (query. Txt) –e 1e-10 –o (output.txt) –m8 to find putative orthologous *Dendrobium R2R3-MYB* gene sequences. The *R2R3-MYB* candidates was translated to amino acid sequences using MEGA 7.0 (Kumar et al., 2016). The translated sequences were validated by checking for the presence of an R2R3-MYB domain using the SMART database (Letunic et al., 2021) (Appendix A).

370 **3.3 Alignment and phylogenetic analysis of *Dendrobium* MYB protein**
371 **sequences**

372 Molecular Evolutionary Genetics Analysis (MEGA) version 7.0 (Kumar et al., 2016)
373 was used to perform multiple sequence alignment and phylogenetic analysis of the amino
374 acid sequences predicted from *Dendrobium MYB* genes. Multiple sequence alignments of
375 60 putative *Dendrobium* R2R3-MYB proteins and orthologues from *Arabidopsis thaliana*
376 (Stracke et al., 2001), *Dendrobium* hybrid (Lau et al., 2015; Li et al., 2017), *Dendrobium*
377 hybrid Woo Leng (Wu et al., 2003), *Dendrobium crumenatum* (Gilding & Marks, 2010),
378 Oncidium Gower Ramsey (Chiou & Yeh, 2011), Phalaenopsis (Hongmei et al., 2009;
379 Hsu et al., 2015), *Petunia* hybrida (Avila et al., 1993; Quattrocchio et al., 1999),
380 *Antirrhinum majus* (Noda et al., 1994; Perez-Rodriguez et al., 2005; Schwinn et al., 2006;
381 Baumann et al., 2007; Jaffé et al., 2007), *Zea mays* (Paz-Ares et al., 1986; Cone et al.,
382 1993), *Lilium* spp. (Yamagishi et al., 2010), *Oryza sativa* (Gao et al., 2011), *Mimulus*
383 *guttatus* (Scoville et al., 2011), *Thalictrum filamentosum* (Di Stilio et al., 2009), *Ipomoea*
384 *batatas* (Deng et al., 2020), *Nicotiana tabacum* (Pattanaik et al., 2010), *Gerbera* hybrid
385 (Elomaa et al., 2003), *Malus domestica* (Takos et al., 2006), *Vitis vinifera* (Azuma et al.,
386 2007), *Capsicum annuum* (Zhang et al., 2015) and *Solanum lycopersicum* (Hassanin et
387 al., 2017) (Appendix C) were performed using Multiple Sequence Comparison by Log-
388 Expectation (MUSCLE) (Edgar, 2004). A phylogenetic tree for *Dendrobium* MYB and
389 orthologues was constructed using a neighbour-joining statistical method with parameters
390 of pairwise gap deletion. A bootstrap value of 1000 replicates was set to assure the
391 statistical reliability of the result.

392 **3.4 Reconstruction of the anthocyanin pathway for *Dendrobium***

393 The set of 29,149 protein sequences of *Dendrobium catenatum* (Genbank:
394 GCA_001605985.2) were analysed using KEGG's GhostKOALA annotation server
395 (https://www.kegg.jp/ghostkoala/) to assign KEGG ortholog ID and map the sequences

396 in KEGG pathways (Kanehisa et al., 2016). The KEGG GhostKOALA tool mapped
397 29.9% of the functional category according to KEGG ortholog groups (Appendix D). The
398 anthocyanin pathway for *Dendrobium* was reconstructed and simplified based on KO
399 value as shown in Figure 4-18 and Table 4-12.

400 **3.5 Off-target prediction for *Dendrobium* MYB dsRNA**

401 Off-target gene predictions were made using siRNA-Finder (si-Fi) software (Lück et
402 al., 2019) with a parameter for the size of siRNA set as 19 nucleotides. The algorithm
403 used in this software to search for sequence similarity is BOWTIE (Ben et al., 2009). The
404 dsRNA construct for *DhMYB22*, *DhMYB60* and *DhCHS* were used as query subject to
405 search the possible hits or sequence to be silenced towards CDS sequences of MYB from
406 *Dendrobium catenatum*.

407 **3.6 RNA isolation**

408 Total RNA was isolated from floral bud tissues using our optimised CTAB method.
409 The method comprises grinding 500 mg flower samples using liquid nitrogen and add 12
410 ml of prewarmed extraction buffer into powdered tissue. Then, the mixture was incubated
411 at 65℃ for 45 min, cooled to room temperature and centrifuged at 7000× g for 5 min and
412 the supernatant collected. An equal volume of P:C:I (125:24:1, pH 4.5) was added to the
413 supernatant and the mixture vortexed for 5 min at room temperature. Following that the
414 mixture was centrifuged for 15 min at 4℃, 17500×g and the supernatant was collected.
415 An equal volume of C:I (24:1) was added and the mixture vortexed and centrifuged for
416 15 min at 4℃, 17500×g and the supernatant was collected. This C:I extraction step was
417 repeated twice. One third sample volume of 8M LiCl was added to the collected
418 supernatant and the mixture was incubated at -20°C overnight. The mixture was
419 centrifuged for 30 min at 4 °C , 17500×g after the overnight incubation. The supernatant
420 was discarded and 500 µl of 70% ethanol was added and the mixture was centrifuged for

421 15 min at 4°C, 17500 × g. The ethanol washing step was repeated twice and the pellet
422 formed was air dried. The pellet then was resuspended in 25 µl RNase-free water and
423 stored at -80°C (Appendix E).

424 3.7 Deoxyribonuclease (DNase) treatment of extracted RNA

425 This procedure used the DNase I amplification grade (Invitrogen, United States)
426 according to the manufacturer's instructions and as follows. The following reagents were
427 mixed in a 1.5 ml tube, on ice. The mixture was incubated at room temperature for 15
428 minutes. Then, 1 µl of 25 mM EDTA was added to the mixture and incubated at 65 °C
429 for 15 minutes to heat inactivate the DNase I. Next, the mixture was replaced on ice for
430 1 minute before use for reverse transcription.

431 **Table 3-1:** Reaction mixture set up for DNase I treatment
432

Components	Volume (µL)	Final Concentration
RNA	Variable	1 µg
10X Reaction Buffer	1	1X
DNase I (1 U/µl)	1	1 U
ddH20	Up to 10 µl	-

433

434 3.8 cDNA reverse transcription

435 Reverse transcription of RNA was carried out using a commercial kit, SuperScript®
436 III First-Strand Synthesis System (Invitrogen, USA). Samples of 1 µg of RNA, primer
437 and dNTPs were mixed together in a 0.1 ml microtube (Table 3-2) and incubated in 65°C
438 for 5 minutes. After 5 minutes, the tube containing the mixture was placed in ice for 1
439 minute. During the incubation time, the cDNA Synthesis Mix was prepared following the
440 manufacturer's instructions. The cDNA Synthesis Mix consisted of 2 µl 10X RT buffer,
441 4 µl 25nM $MgCl_2$, 2 µl 0.1M DTT, 1 µl RNaseOUT (40 U/ µl) and 1 µl SuperScript III
442 RT (200 U/ µl) (Table 3-3). The prepared cDNA Synthesis Mix (Table 3-3) was added to

20 µl cDNA synthesis components 0.1 ml microtube and mixed gently before incubating at 50°C for 50 minutes. The reactions were terminated at 85°C for 5 minutes. 1 µl of RNase H was added to each tube and the tube was incubated for 20 minutes at 37°C. The cDNA product was then stored at -30°C.

Table 3-2: cDNA synthesis components

Components	Amount
1 µg total RNA	10 µl
Primer* *50 µM oligo(dT)20, or 2 µM gene-specific primer (GSP), or 50 ng/µl random hexamers	1 µl
10 mM dNTP mix	1 µl
ddH20	to 20 µl

Table 3-3: cDNA synthesis mix

Components	Volume (µl), 1X Reaction
10X RT buffer	2 µl
25 mM $MgCl_2$	1 µl
0.1 M DTT	2 µl
RNaseOUT™ (40 U/µl)	1 µl
SuperScript® III RT (200 U/µl)	1 µl
Total volume	10 µl

3.9 Construction of RNA expression vectors

Primers to amplify the *Dendrobium* homologues of Dca003829 and Dca008884 which we named DhMYB22 and DhMYB60 (following the numbering assigned in Zhang et al., 2021) were designed using Primer3 online software (Untergasser et al., 2012). *DhCHS* primers were designed based on the *CHS* sequence of *Dendrobium* hybrid cultivar Sonia Earsakul [GenBank: KC345011.1] (Table 3-4). cDNAs were synthesised from 1 µg RNA using the SuperScript® III First-Strand Synthesis System (Invitrogen, USA). PCR

460 amplification was carried by using *TransTaq*®HiFi DNA Polymerase (Transgenbiotech,
461 China) in a total of 25 µL reaction volume as shown in Table 3-5. The thermoprofile was
462 as follows: initial denaturation at 95 °C for 3 min, 35 cycles of 94 °C for 30 s, 53 °C for
463 30 s, and 72 °C for 1 min followed by the final extension for 10 min at 72 °C. The PCR
464 products containing an 'A' nucleotide overhang were ligated into pGEM®-T Easy Vector
465 (Promega, USA in a reaction mixture) as shown in Table 3-6 then transformed into *E.*
466 *coli* DH5α for plasmid propagation. Bacterial dsRNA expression vector pL4440
467 (Timmons et al., 2001a/b) was used for preparation of constructs for three genes
468 (pL4440/*DhMYB22*, pL4440/*DhMYB60* and pL4440/*DhCHS*) under the control of two
469 inverted T7 RNA polymerase promoters. *Sac* I and *Sac* II were used for digestion of
470 *DhMYB22* and *DhMYB60* from the pGEM®-T Easy Vector as in Table 3-7 while *Not*I
471 was used for digestion of *DhCHS* as shown in the Table 3-7. The digestion is occurred at
472 37 °C for 4 hours. Then, the inserts were ligated to pL4440 plasmid as in Table 3-8 and
473 incubated at -20 °C overnight. The plasmids were then introduced into RNase III-
474 deficient *E.coli* strain HT115 (DE3) (Timmons et al., 2001b) using a standard $CaCl_2$
475 transformation protocol (Sambrook et al., 2006). Colony PCR screening for
476 pL4440/*DhMYB22*, pL4440/*DhMYB60* and pL4440/*DhCHS* were performed for
477 validation. Bacterial colonies were picked using sterile tips, touched lightly into the inner
478 side of PCR tubes, and streaked onto appropriate selection plate based on the bacterial
479 species and strain used to establish "plate library". The plate was incubated in the dark at
480 37 °C for E. coli. PCR was carried out as described previously.

481

482

483

484 **Table 3-4:** Primer sequences used for PCR (cloning) and qRT-PCR

Primers used in PCR (cloning)		
Primer name	**Primer Sequence**	**Amplicon size (bp)**
DhMYB22	Forward:5'GAATTCGTGCAGTTTCAAGGAAG-3' Reverse:5'-ATTATTGCACCTTATTGCCGTTG-3'	501 bp
DhMYB60	Forward: 5'-GGCTCAGGTGGACAAATTAC-3' Reverse: 5'-GGTTGGCGACTCAAGATCAA-3'	530 bp
DhCHS	Forward: 5'-GCCCAAATCTCGCATAACTC-3' Reverse: 5'-GGTTAGTCCCATCTCGCGTA-3'	436 bp
Primers used in qRT-PCR (gene expression analysis)		
Primer name	**Primer Sequence**	**Amplicon size (bp)**
DhMYB22	Forward: 5'-TCCAAAGCAGCTTCCATCTT-3' Reverse: 5'-CTTTCGGGCATCTCACTAGC-3'	102 bp
DhMYB60	Forward: 5'-GCTGTGTGGATGTGGAAGAA-3' Reverse: 5'-GTGGTGAATTTGAGGGAGATGA-3'	105 bp
DhCHS	Forward: 5'- GCTCAAGGAGAAGTTCAAACG-3' Reverse: 5'- ATGAATGCGCATATGTTTGG-3'	108 bp
PAL	Forward: 5'-AAGCCGGAATACACAGACCA-3' Reverse: 5'-GGAGCTTCTTCGCCATCTTC-3'	124 bp
CHI	Forward: 5'-TGGAGAAGAAGAAGCAGCCA-3' Reverse: 5'-CGCATTCGTCAGCTTCTTGT-3'	106 bp
F3'H	Forward: 5'-ATCTCACGCTAGGCCTCAAG-3' Reverse: 5'-CTGAACGGTGATCCAGGTTG-3'	119 bp
F3'5'H	Forward: 5'-GTGAGGATGGAGAAGGGCTT-3' Reverse: 5'-CCATCGCCCACTCTATGACT-3'	105 bp
DFR	Forward: 5'-GATACGTGGCAGCATTGGAG-3' Reverse: 5'-CAAGACCTCAAGATGCCCAG-3'	120 bp
β-actin	Forward: 5'- GTCAGGGACATCAAGGAGAAG-3' Reverse: 5'- TGGGCACCTAAATCTCTCAGC-3'	150 bp

485
486
487
488
489
490
491
492
493
494
495
496
497
498
499 **Table 3-5:** Master mix of *TransTaq*®HiFi DNA Polymerase PCR

Components	Volume (µL)	Final Concentration
cDNA Template	1	100 ng/µL
Forward Primer (10 µM)	1	0.2 µM
Reverse Primer (10 µM)	1	0.2 µM
10X *TransTaq*®HiFi Buffer	2.5	1x
2.5 mM dNTPs	2	0.25 mM
TransTaq®HiFi DNA Polymerase	0.8	2.5 units
ddH20	16.7	-
Total volume	25	-

Table 3-6: Ligation mixture of PCR product into pGEM®-T Easy Vector

Components	Volume (µl)
2X Rapid Ligation Buffer, T4 DNA Ligase (100 Weiss units)	10
pGEM®-T Easy Vector (50 ng)	1
PCR Product (500 ng)	7.9
T4 DNA Ligase (100 Weiss Units)	1.1
Nuclease-Free water to final volume of	20

Table 3-7: Digestion of pL4440 and pGEM®-T Easy Vector harbouring *DhMYB22*, *DhMYB60* and *DhCHS* cDNA

Components	Volume (µL)
Vector (pL4440 and pGEM®-T Easy) (0.5µg)	5
For *DhMYB22* and *DhMYB60* using *Sac*I and *Sac*II	
*Sac*I (NEB) (2,000 units)	0.5
*Sac*II (NEB) (2,000 units)	0.5
Buffer CutSmart (NEB) (10X)	2.5
Nuclease-Free water to final volume of	25
For *DhCHS* using *Not*I	
*Not*I (NEB) (2,500 units)	0.5
Buffer 3.1 (NEB) (10X)	2.5
Nuclease-Free water to final volume of	25

Table 3-8: Ligation mixture of digested pL4440, *DhMYB22*, *DhMYB60* and *DhCHS*

514

Components	Volume (µl)
Digested pL4440	2
Digested *DhMYB22* and *DhMYB60* (*Sac*I and *Sac*II) Digested *DhCHS* (*Not*I)	19.5
T4 DNA Ligase Reaction buffer (10X)	2.5
T4 DNA Ligase (100 Weiss Units)	1
Total reaction mixture	25

515

516 **3.10 Production of crude bacterial lysates containing dsRNA of *DhMYB22*,**
517 ***DhMYB60* and *DhCHS***

518 For each of the transformed RNase III-deficient *E. coli* strain HT115 (DE3) with the
519 vector construct pL4440/*DhMYB22* or pL4440/*DhMYB60* or pL4440/*DhCHS,* a single
520 colony was used as inoculum and grown overnight in LB broth containing 100 µg/ml
521 ampicillin and 12.5 µg/ml tetracycline with 220 rpm agitation in an incubator shaker at
522 37°C. Then, the overnight culture was then diluted 100-fold by transferring 1ml of
523 overnight culture into 99 ml fresh 2-YT Broth (Invitrogen™) with 100 µg/ml ampicillin
524 and 12.5 µg/ml tetracycline. The mixture was allowed to grow in an incubator shaker with
525 220 rpm at 37°C for 3 hours 30 minutes until the OD_{600} reading reached around 0.7. Next
526 400 µl Isopropyl-D-1-thiogalactopyranoside (IPTG) was added to induce dsRNA
527 expression and the culture incubated for an additional two hours. After the incubation,
528 the cells were collected by centrifugation at 16,000 x g for 14 minutes at 4°C. The cell
529 pellet was resuspended in 500 µl resuspension buffer containing 10mM
530 Ethylenediaminetetraacetic acid (EDTA) and 50mM Tris Base (pH8.0) and incubated
531 with 500 µl of 1 mg/ml lysozyme for 5 minutes with mixing by vortex for few seconds at
532 2 min intervals. The lysed cell mixture was then centrifuged for 5 minutes in 4°C, 16,000
533 x g. The supernatant was collected and quantified using a nanophotometer (Implen,
534 Germany) and stored at -80°C. The supernatant was separated by gel electrophoresis in
535 1% (w/v) agarose gel pre-stained with 0.8 µl of 0.5 µg/ml Ethidium bromide (EtBr) run

536 at 100 V for 30 min. After the run is complete, the gel was visualized and photographed
537 using a Gel documentation system AlphaImager (Alpha Innotec, USA).

538 **3.11 Degradation Study**

539 The stored supernatant solution of *DhMYB60* dsRNA (from 3.10) was thawed and
540 1500 ng/µL was transferred into 0.2 mL PCR tubes (Eppendorf, Germany) and tightly
541 sealed with Parafilm ® M (Parafilm, USA). The sealed tubes were subjected to different
542 temperature treatment at 4°C and room temperature for a period of 0 days, 1 day, 2 days,
543 3 days, and 6 days. After the treatment, the concentration of dsRNA for each temperature
544 and period was measured using a nanophotometer (Implen, Germany) followed by gel
545 electrophoresis using 1.0% agarose gel, stained with EtBr (0.5 µg/ml) and visualised with
546 Gel documentation system AlphaImager (Alpha Innotec, USA).

547 **3.12 dsRNA treatment of *Dendrobium* hybrid plants**

548 Before treated with dsRNA of DhMYB22 and DhMYB60, DhCHS which act as a
549 positive control treatment was used to optimise the delivery of dsRNA. Crude bacterial
550 extracts containing dsRNA of DhCHS were inoculated separately onto floral buds at stage
551 1 (i.e., approximately 0.5 cm in length) of 30 *Dendrobium* plants (10 biological replicates
552 ×3 experimental repeats). Each *Dendrobium* plant blooms twice a year and produces ~7
553 flowers per raceme. Mechanical inoculation was carried out by gently brushing 50 µl of
554 crude bacterial extract containing 2 µg/µl dsRNA onto each flower bud at 3-day intervals
555 (around 10 treatments) starting from the stage 1 bud until the flower opened (after stage
556 5) using a flat paintbrush (0.8 mm wide). The plants were treated at around 10am on each
557 day of treatment then left for 30 min before rinsing off any debris under slow running tap
558 water. Images of floral buds were captured at stages 1 to stage 6 with samples harvested
559 at the same stages for phenotypic measurements. Time points of sampling from the start
560 of treatments (or start of experiment for untreated control) were after 5 days (stage 1), 10

561 days (stage 2), 15 days (stage 3), 20 days (stage 4), 25 days (stage 5) and 30 days (stage
562 6). Repeat the optimised step of treatment dsRNA of DhCHS with dsRNA of DhMYB22
563 and DhMYB60.

564 **3.13 Quantitative real time PCR (qRT-PCR)**

565 cDNAs were synthesised from 1 µg RNA using the SuperScript® III First-Strand
566 Synthesis System (Invitrogen, USA) according to the manufacturer's instructions and
567 using the primers shown in Table 3-4. RNA extracted from floral buds was used for
568 cDNA systhesis and qRT-PCR analysis by using Power SYBR® Green PCR Master Mix
569 kit (Applied Biosystems, USA). The reaction prepared mixture was as shown in Table 3-
570 9. Amplification conditions used an initial DNA Polymerase activation at 95 °C for 10
571 min, followed by 40 cycles of amplification with denaturing at 95 °C for 15 s, annealing
572 and extension at 60 °C for 1 min using a 7500 Real Time PCR System (Applied
573 Biosystems). SDS 1.3.1 (Sequence Detection Software) was used to create a relative
574 quantification (ddCt) plate and the dissociation curves. *Dendrobium* β-actin (Forward
575 Primer: 5'-GTCAGGGACATCAAGGAGAAG-3' and Reverse Primer: 5'-
576 TGGGCACCTAAATCTCTCAGC-3') was used as the endogenous reference for the
577 normalisation of the expression levels of the target CP gene (Livak et al., 2001) and the
578 non-treated control sample was used as the calibrator. The relative quantification
579 minimum (RQmin) ratio relative quantification maximum (RQmax) limit was set at 95
580 % confidence. qRT-PCR analysis was done with three biological replicates and 4
581 technical replicates for each sample.

582 **Table 3-9:** Reaction mixture for qRT-PCR
583

Components	Volume (µL)	Final Concentration
cDNA template	2	10 ng/µL
Forward Primer (10 µM)	1	0.5 µM
Reverse Primer (10 µM)	1	0.5 µM
Power SYBR Master Mix (5X)	10	1X
Sterile Distilled water	6	-

Total volume	20

584

585 **3.14 Anthocyanin quantification using spectroscopy and HPLC analysis**

586 Total anthocyanin was extracted using a methanol-HCL method (Lee & Wicker,
587 1991). Samples (0.2 g fresh weight) of *Dendrobium* hybrid floral buds were homogenized
588 in liquid nitrogen, after which they were soaked and incubated overnight in 5 mL
589 methanol and 0.1% (v/v) HCL in the dark at room temperature. The absorbance of each
590 extract was measured at 530, 620, and 650 nm with a nanophotometer (Implen, Germany).
591 The relative anthocyanin concentration will be determined by the formula: optical density
592 (OD) = $(OD_{530} - OD_{620}) - 0.1(OD_{650} - OD_{620})$. Anthocyanin content will be expressed
593 as a change of 0.1 optical density (unit × 10^3 g−1 fresh weight) followed Li et al. (2012)
594 method.

595 For LC-MS/MS analysis, an Agilent 1100 series HPLC system (Agilent Technologies,
596 United States) coupled with Sciex 3200 QTrap hybrid tandem mass spectrometer system
597 (AB Sciex Pte. Ltd., Canada) was used for quantification of cyanidin-3-glucoside and
598 cyanidin-3-rutinoside for each sample. Water (HPLC grade containing 0.1% v/v formic
599 acid) and acetonitrile (HPLC grade containing 0.1% v/v formic acid) were used as mobile
600 phase solvents A and B, respectively. All samples were centrifuged at 10 000 rpm for 5
601 min and filtered using a 0.45 µm nylon syringe filter before injection into the LC-MS/MS
602 system. The total runtime for LC-MS/MS system was 8 min. A gradient was applied:
603 min/A%/B% as 0/90/10, 0.5/90/10, 3/40/60, 4/40/60, 4.1/15/85, 5/15/85, 5.1/90/10, and
604 8/90/10 with a flow rate of 400 µl min^{-1}. A total of 20 µl was injected into LC-MS/MS
605 system using the autosampler. Data acquisition and analysis were performed using
606 Analyst® 1.5.2 software (AB Sciex Pte. Ltd., Canada). Appendix F shows the extracted-
607 ion chromatogram and calibration curve for anthocyanin compounds.

608 **3.15 Geometric analysis of floral bud and organ shape**

609 A geometric morphometric method combined with multivariate statistical shape
610 analysis was used to examine the difference in flower bud and floral organ shape between
611 buds and flowers from the various treatments. A total of 180 floral buds and open flowers
612 (sepals, petals and lips) with 3 images from 10 biological replicates for each stage, were
613 photographed in an identical manner using a Dino-lite Edge Digital Microscope AM4515
614 (AnMo Electronic Corporation, Taiwan). Flower organ parts were pressed flat on to
615 double-sided tapes and images taken were used for analysis. Image analysis followed the
616 method of Rohlf & Slice (1990). Briefly, following capture, images were superimposed
617 (untreated versus DhMYB22, untreated versus DhMYB60, untreated versus empty
618 vector, DhMYB60 versus empty vector, empty vector versus DhMYB22 and DhMYB60
619 versus DhMYB22) using tpsSuper64 version 2.06 (Rohlf, 2015). Then, an outline was
620 drawn, before landmarks were placed on the outline (Appendix G). The output images of
621 floral buds and open flowers parts were converted from JPEG format to TPS format using
622 tpsUtil32 version 1.78 (Rohlf, 2019) (http://www.sbmorphometrics.org/). The TPS
623 output images were analysed for Procrustes coordinates using MorphoJ tool
624 (Klingenberg, 2011) and the shape data were extracted using a generalized Procrustes fit.
625 A mean form configuration (consensus) is computed, and variance is decomposed into
626 biologically important components around this mean by averaging the Procrustes
627 coordinates for the original and properly transformed and relabelled versions of each
628 individual's landmarks (Rohlf & Slice, 1990; Goodall, 1991; Dryden & Mardia, 1998;
629 Slice, 2001). The mean value of Procrustes coordinates obtained were plotted in bar
630 diagrams as shape distance.

631 **3.16 Field emission scanning electron microscopy (FESEM) and Cell Count**

632 Abaxial surfaces of fresh *Dendrobium* hybrid sepals, petals and lip were mounted on
633 specimen stubs and the adaxial surface was examined using a Field Emission Scanning

Electron Microscope (FESEM, Quanta™ 450 FEG, Austria) at 1000-times magnification in low vacuum secondary electron detector mode. Cell count is being conducted by observing the images from dsRNA of *DhCHS*, *DhMYB22* and *DhMYB60*.

3.17 Statistical analysis

All statistical analyses were performed using SPSS Statistics 23 for Windows (IBM, United States). Significant tests were conducted for applicable datasets with Tukey HSD test where the significant value is $p < 0.05$. by using One-way ANOVA.

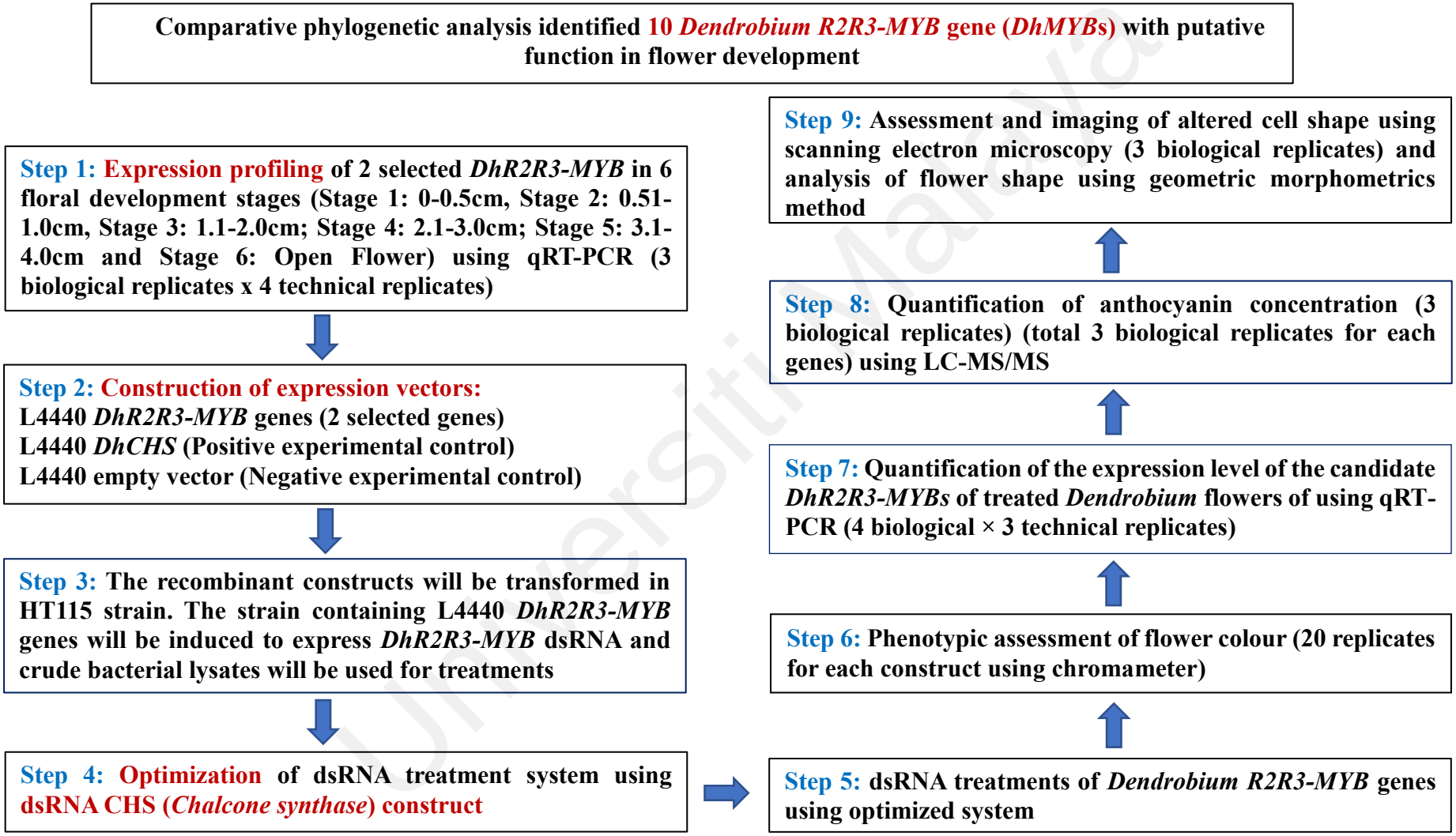

Figure 3-1 : Summary of the experimental workflow of this study

CHAPTER 4: RESULTS

4.1 Identification of *R2R3-MYB* genes in *Dendrobium* orchid related to flower colour and/or shape

BLAST alignments identified a total of 60 putative *R2R3-MYB* gene sequences in the *Dendrobium catenatum* genome sequence (GenBank: GCA_001605985.2) (Zhang et al., 2016) based on homology with the motif sequence and *Arabidopsis R2R3-MYB* genes (Appendix A). The details of motif sequences along with the protein and coding sequence (CDS) of *Dendrobium catenatum* R2R3-MYBs are presented in Appendix A and C. A cross-genera phylogenetic tree was constructed using a set of 225 protein sequences to identify the *Dendrobium* R2R3-MYB associated with flower colour and shape (Figure 4-1). Apart from the *Arabidopsis* and *Dendrobium catenatum* sequences, MYB sequences included in the analysis were chosen for their reported function in flower pigment or shape. The summary of the species name, accession number and validated function of *R2R3-MYB* orthologues used in phylogenetic analysis are shown in Appendix B. Among the several subgroups, four subgroups included genes that have been associated with functions related to flower pigmentation or shape (Table 4-1). These were Group I: transcriptional repressor of anthocyanin, Group II: flavonoid activator; Group III: anthocyanin related MYB, and Group IV: MIXTA-like. A total of ten *DcaMYB* genes were found to cluster within these four subgroups (Table 4-1). Among those, two *MYB* genes with high similarity to MYB from other species are known to have the targeted functions which are *Dca003827/MYB22* (clustered in subgroup III) and *Dca008884/MYB60* (clustered in subgroup IV). These two MYBs were selected to design primers to amplify orthologues from *Dendrobium* hybrid (*Dendrobium* Burmese Ruby × *Dendrobium* Mae-Klong River) for functional characterisation (Table 3-4). The

orthologous sequences from the *Dendrobium* hybrid (*Dendrobium* Burmese Ruby × *Dendrobium* Mae-Klong River) were named "Dh" and using the numbers as assigned by Zhang et al. (2021). Alignment of the sequences of *DhMYB22*, *DhMYB60* and *DhCHS* with their *Dendrobium catenatum* homologs found to have 88.2%, 91.9% and 94.4% nucleotide identity respectively.

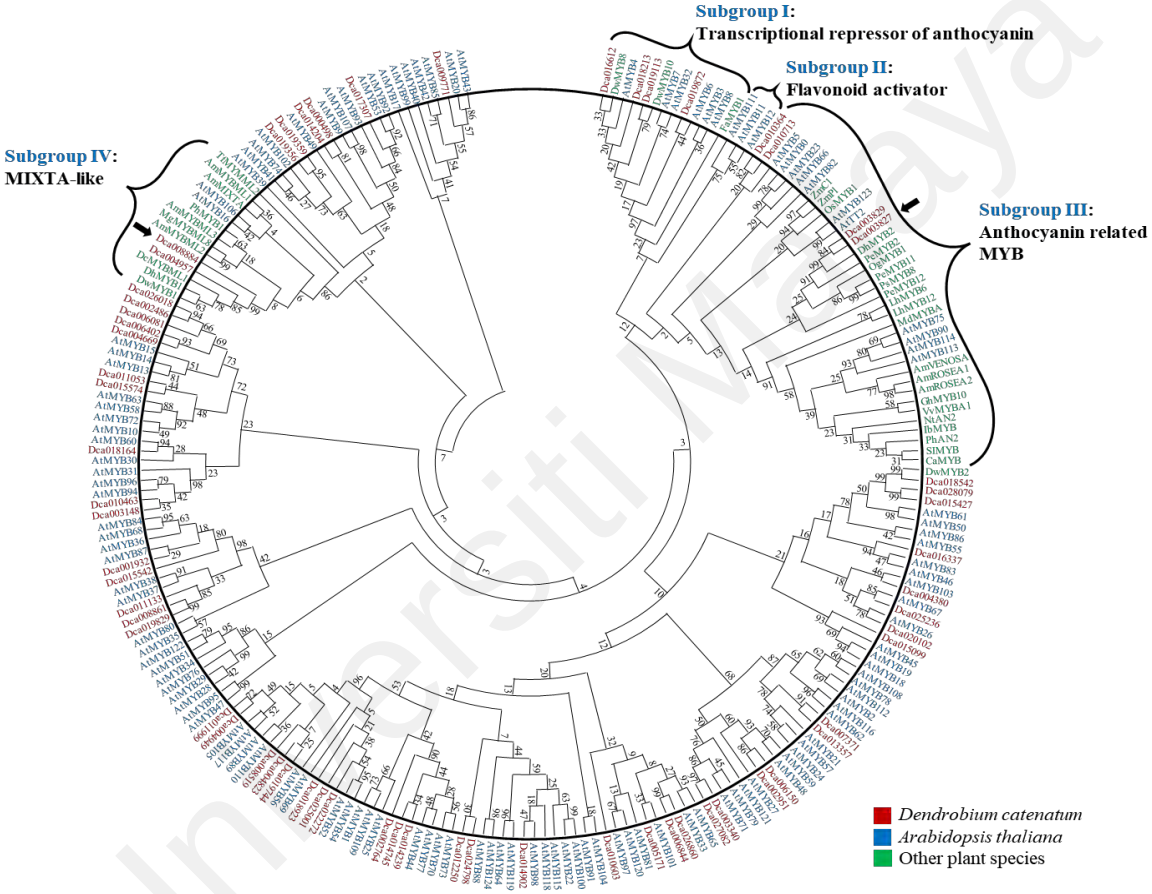

Figure 4-1: A combined phylogenetic tree of full-length R2R3-MYB protein sequences. Red: sequences from *Dendrobium catenatum*; Blue: *Arabidopsis thaliana*; Green: 22 other plant species (detailed in Table S2). Multiple alignments of 221 full-length amino acid sequences of R2R3-MYBs were executed by MUSCLE (version 3.52) and the tree created with MEGA 7.0 using the Maximum-likelihood method with JTT+G+F substitution's model. Support values from a bootstrap analysis with 1000 replicates were used to ensure the statistical reliability of each node.

680

Table 4-1: *Dendrobium catenatum* MYB protein clusters in R2R3 MYB phylogenetic subgroup related to pigmentation and cell shape

Subgroup No	**Predicted function based on group orthologous**	***Dendrobium catenatum* gene clustered in the subgroup**
I	Transcriptional repressor of anthocyanin	*Dca016612* *Dca018213* *Dca019113* *Dca019872*
II	Flavonoid activator	No candidate gene
III	Anthocyanin related MYB	[1]*Dca003827* *Dca003829* *Dca010364* *Dca010713*
IV	MIXTA-like	[2]*Dca008884* *Dca004957*

681 [1]*Dca003827* was used to design primers for amplification of *DhMYB22*
682 [2]*Dca008884* was used to design primers for amplification of *DhMYB60*
683

684

685

686

687

688

4.2 Optimising RNA isolation for *Dendrobium* hybrid

Isolation of high-quality RNA from *Dendrobium* flowers is challenging because of the high levels of pigment, polysaccharides, and polyphenols. In this research four different published methods were tested; three CTAB-based RNA isolation methods (Method 1, Method 2 and Method 4) and one SDS-based method (Method 3) to isolate RNA from the flower of *Dendrobium* hybrid. Method 1 was reported for RNA isolation from tissues including flowers, rich in polyphenols and polysaccharides (Kiefer et al., 2000), and Method 2 was reported for *Phalaenopsis* orchids (Su et al., 2011). Method 3 was a combination of SDS and TRIzol reagent (guanidinium thiocyanate–phenol–chloroform), reported for the buds of the tree peony (*Paeonia suffruticosa* Andr) (Gao et al., 2016) and Method 4 was reported for a pale-yellow orchid *Dendrobium huoshanense* (Liu et al., 2018). A summary of the different isolation methods used for isolation of RNA from *Dendrobium* hybrid flowers is shown in Table 4-3. However, none of the four methods was found to be adequate for the extraction of high-quality RNA from the pigment, polyphenol, and polysaccharide-rich tissue of *Dendrobium* hybrid flowers (Figure 4-2, 4-3, 4-4). Hence, an efficient CTAB method for RNA extraction from the pigment-rich flowers of *Dendrobium* was optimised.

4.2.1 Increasing the sample-buffer ratio improves RNA recovery

The main hurdle while performing the isolation of RNA from mature flowers was the viscous tissue homogenate that arises during the mixing of ground tissue with the extraction buffer. It was found that increasing the sample-buffer ratio to almost double of the other tested methods (Table 4-4), resulted in more efficient mixing of the sample with buffer and better recovery of the supernatant containing the RNA (Table 4-5).

712 **4.2.2 Strong coloured flower tissue resulted in insoluble RNA pellet**

713 Another hurdle was the removal of pigments from the intensely coloured flower
714 tissues. Method 1, Method 2, and Method 4 failed to remove pigment in the extraction
715 step, leaving the aqueous phase dark purple (Figure 4-2). Method 3 that uses a
716 combination of SDS and TRIzol reagent, which includes a phenol:chloroform:isoamyl
717 alcohol extraction step, showed better removal of pigments than other methods. Methods
718 1, 2, and 4 lack the use of phenol in the solvent extraction steps (Figure 4-2 and 4-3).
719 However, the concentration of phenol used in Method 3 was found to be insufficient to
720 obtain a colourless pellet for *Dendrobium* hybrid flower tissue (Figure 4-3). The addition
721 of the P:C:I (125:24:1) extraction step in the improved CTAB method resulted in the
722 comparatively lighter pigmented aqueous phase after P:C:I extraction (Figure 4-2).
723 Samples also showed $A_{260/230}$ ratios within the desired range (Table 4-5) and colourless
724 pellets (Figure 4-5).

725 RNA samples obtained from Method 1 showed $A_{260/230}$ ratios in the range of 1.6–1.7,
726 and samples from Method 2 gave a value of 1.8, which indicated the presence of
727 polyphenol and/or polysaccharide contamination. Similarly, RNA prepared from
728 *Dendrobium* hybrid tissue using Method 3 also showed low absorbance ratios, suggesting
729 contamination with protein (ratio of $A_{260/280}$; 1.6–1.7) and with polyphenol and/or
730 polysaccharides (ratio $A_{260/230}$; 1.6–1.7) (Figure 4-5). To address this, the buffer was
731 modified to have higher concentrations of NaCl (3M), PVP-10 (3% w/v), and ß-
732 mercaptoethanol (3% v/v) (Table 4-3).

4.2.3 Incubation periods in extraction buffer and precipitation of RNA affect the yield of RNA

Different incubation periods in the extraction buffer were tested to maximise RNA yield. The relatively short incubation time of 5–15 min in extraction buffer used in Methods 1–4, resulted in lower RNA recovery along with protein contamination from mature flowers of *Dendrobium* hybrids (Table 4-5). An incubation time of 45 min was found to result in a higher yield and good quality of RNA (Table 4-5).

Another contributing factor that affects the yield of RNA is the low pellet solubility. This might be due to the use of isopropanol in Methods 1 and 3. Method 2, which uses 8 M LiCl (giving a final concentration of 0.37 M in solution with the sample) for nucleic acid precipitation, was the best among the four methods in terms of pellet solubility. Method 4 also used LiCl but at 10 M (giving a much lower final concentration of 0.04 M in solution with the sample due to the used of high volume of reconstitution buffer). In the modified method, precipitation with 8 M LiCl followed by a 75% ethanol wash resulted in soluble pellets that allow for good recovery of RNA in the final aqueous solution (Table 4-5). Overnight precipitation (24 h) improved RNA yield compared to the yield after shorter precipitation time of 3–12 h (Table 4-6).

4.2.4 High-quality RNA isolation from pigment-rich *Dendrobium* flowers

RNA extracted using the improved CTAB method, showed high-quality, intact bands of 28S rRNA and 18S rRNA (Figure 4-5). The concentration of RNA is higher in the improved CTAB method (11.0-12.0 µg/g FW) while Method 1 (1.5-1.7 µg/g FW), Method 2 (1.4-1.5 µg/g FW), Method 3 (0.9 µg/g FW) and Method 4 (0.8-0.9 µg/g FW) gave relatively low concentrations of RNA as shown in Table 4-5.

Figures 4-6 and 4-7 show the suitability of the improved CTAB method in the isolation of RNA based on RNA bands with clear ribosomal peaks and higher RNA Integrity Number (RIN) values (7.9–8.9) compared to Methods 1–4 (RIN: 4.8–6.8). The improved CTAB method was validated using other *Dendrobium* hybrids i.e., *Dendrobium* Burana Jade × [*Dendrobium* Bertha Chong × *Dendrobium* Imelda Romualdez]; *Dendrobium* Trudy Brandt × *Dendrobium* Udom Blue Angel and *Dendrobium* Aridang × *Dendrobium* Burana Sundae produced comparable result/quality thus confirming the suitability of the improved method to isolate RNA from pigment, polyphenol, and polysaccharide-rich tissue (Figure 4-7). A RIN value of ⩾ 7 indicates that the RNA is suitable for high stringency applications (Schroeder et al., 2006) such as cDNA library construction or next-generation sequencing (Deepa et al., 2014).

To determine the reproducibility of the improved CTAB method for isolating RNA from floral tissues of different developmental stages, RNA was extracted from stage 1-5 flower buds of the *Dendrobium* Burmese ruby × *Dendrobium* Mae-klong River in addition to the mature flowers. The integrity of the isolated RNA was evaluated using RT-PCR of an important orchid floral pigment biosynthetic cDNA, *chalcone synthase* (*CHS*). Amplification of a partial coding sequence of *CHS*, produced a band of an expected size of 436 bp, using cDNA synthesised from RNA extracted from flower buds and mature flowers, demonstrating the suitability of this method to isolate RNA suitable for downstream processes across floral development stages (Figure 4-8).

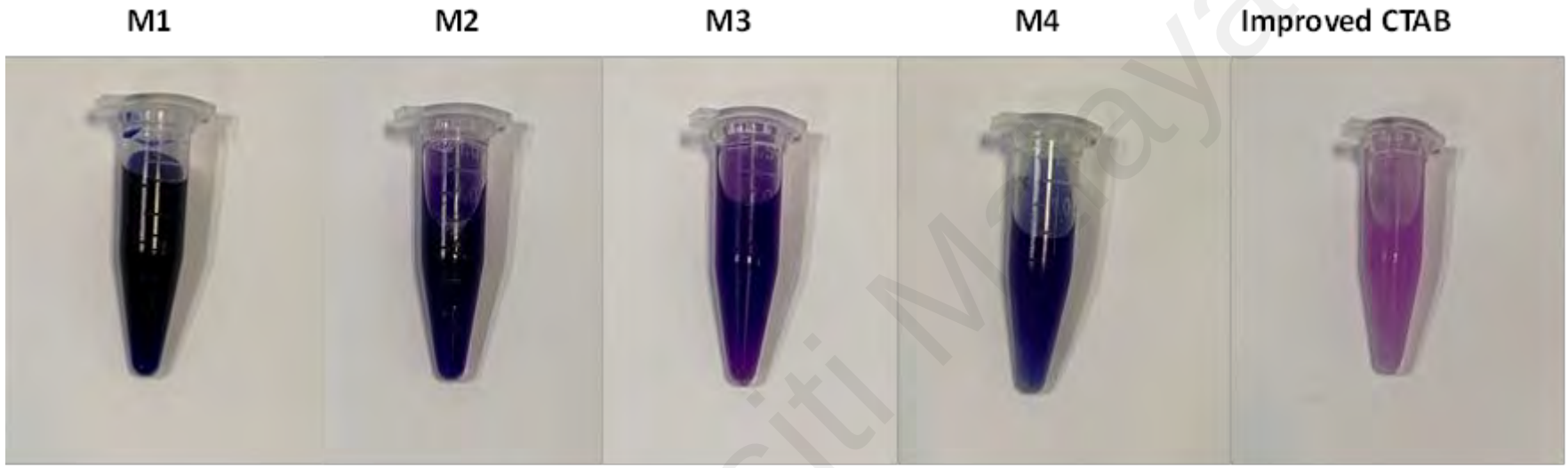

Figure 4-2: The aqueous fraction collected after P:C:I steps of RNA isolation method. **M1**: RNA isolation method of Kiefer et al. (2000), **M2**: RNA isolation method of Su et al. (2011), **M3**: RNA isolation method of Gao et al. (2016), **M4**: RNA isolation method of Liu et al. (2018), **M5**: Improved CTAB method.

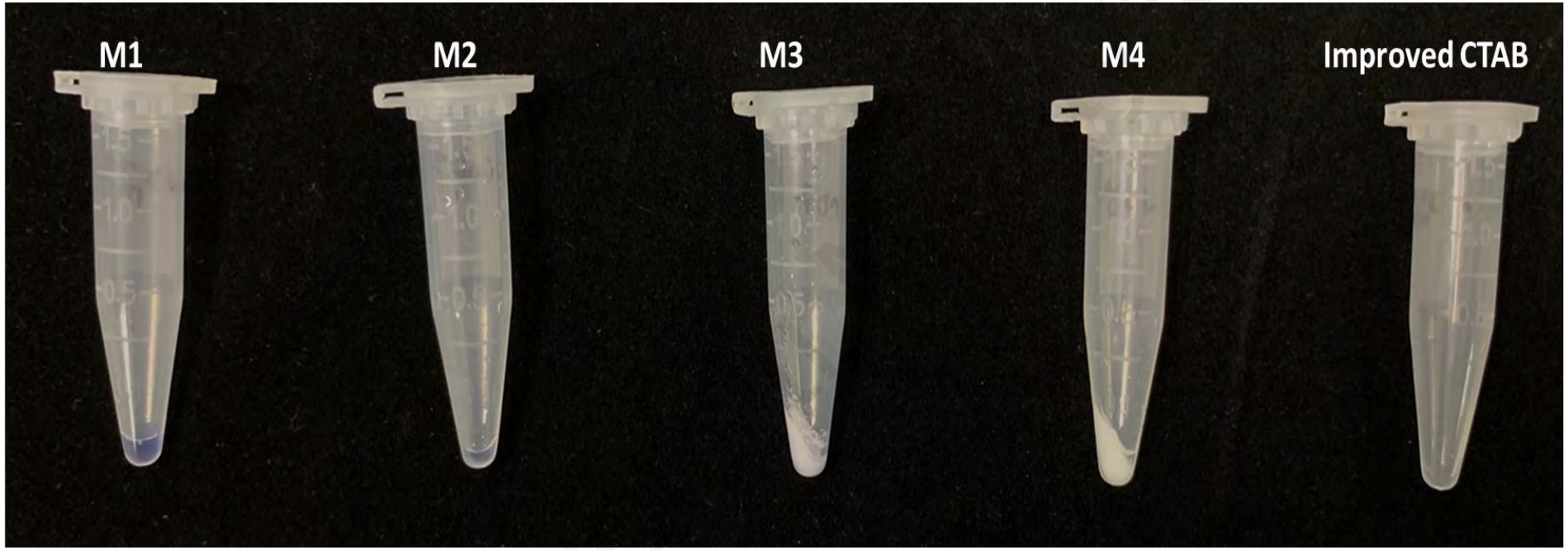

Figure 4-3: RNA pellet obtained from the mature flower of *Dendrobium* hybrid. **M1**: RNA isolation method of Kiefer et al. (2000), **M2**: RNA isolation method of Su et al. (2011), **M3**: RNA isolation method of Gao et al. (2016), **M4**: RNA isolation method of Liu et al. (2018), and **M5**: improved CTAB method.

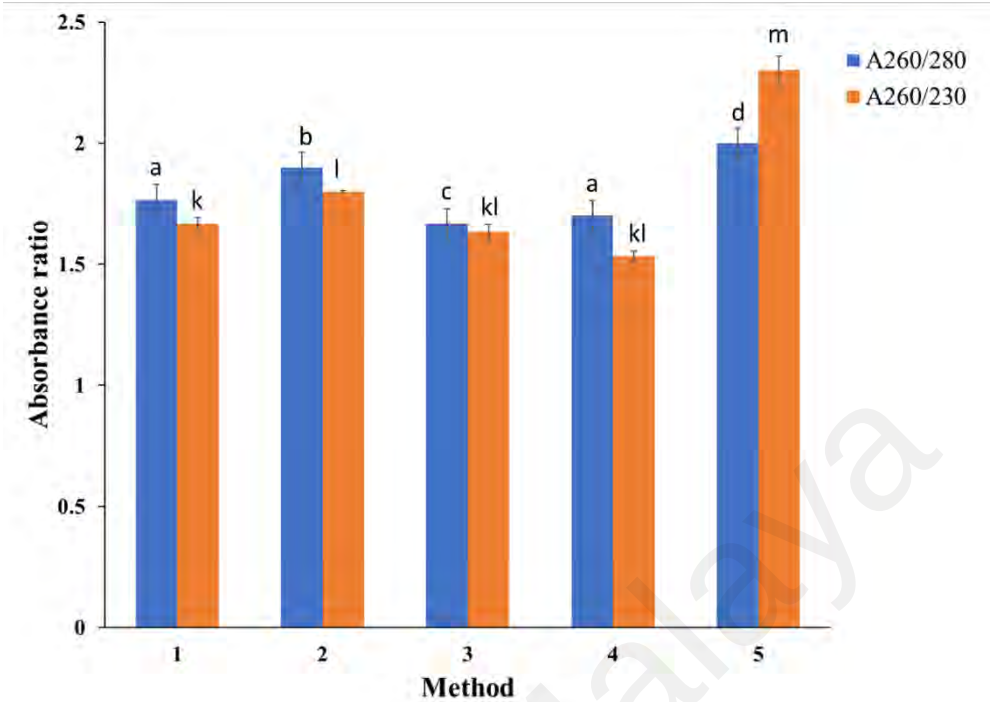

Figure 4-4: Quality of RNA samples isolated from *Dendrobium* hybrid (*Dendrobium* Burmese ruby × *Dendrobium* Mae-klong River) using M1-4 and Improved CTAB method, RNA purity was determined spectrophotometrically using the ratio of absorbance at 260/280 nm and 260/230. Different letters on the top of each bar indicate statistically significant differences (one-way ANOVA, Tukey HSD comparison test, $p < 0.05$)

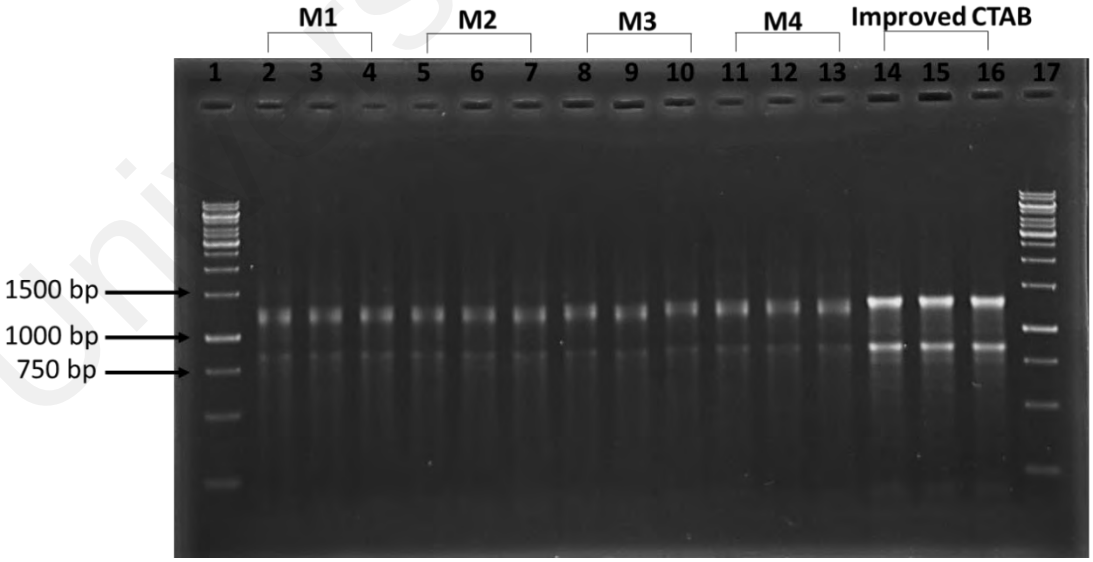

Figure 4-5: Agarose gel electrophoresis of total RNA from *Dendrobium* flower. Lane 1 and 17: 1 kbp (Promega, US). Lane 2-4: Method 1 (M1) (Kiefer et al., 2000). Lane 5-7: Method 2 (M2) (Su et al., 2011). Lane 8-10: Method 3 (M3) (Gao et al., 2016). Lane 11-13: Method 4 (M4) (Liu et al., 2018). Lane 14-16: Method 5 (M5) (Improved CTAB method)

Table 4-2: Summary of different isolation method used for isolation of RNA from *Dendrobium* hybrid (*Dendrobium* Burmese ruby × *Dendrobium* Mae-klong River) flower

	Method 1 (Kiefer et al. 2000)	**Method 2 (Su et al. 2011)**	**Method 3 (Gao et al. 2016)**	**Method 4 (Liu et al. 2018)**	**Improved CTAB method**
Extraction buffer	2 M NaCI, 100 mM Tris-HCI (pH 8), 25 mM EDTA, 2% (w/v) CTAB, 2% (w/v) PVP-10, 0.5% (w/v) spermidine and 2% (v/v) ß-mercaptoethanol added prior to extraction	2 M NaCI, 100 mM Tris-HCI pH 8, 25 mM EDTA, 2% (w/v) CTAB, 2% (w/v) PVP-10 and 2% (v/v) ß-mercaptoethanol added prior to extraction	10 mM Tris-HCl (pH8.0), 1mM EDTA (pH8.0), 20% (w/v) SDS, 1 M NaCl added to SDS extraction buffer: 100 mM Tris-HCl (pH 9.0) and 2% (v/v) ß-mercaptoethanol added prior to extraction	0.25 M NaCl, 50 mM Tris-HCl (pH 7.5), 20 mM EDTA, 1% (w/v) SDS, 4% (w/v) PVP-40	3M NaCl, 100mM Tris-HCl (pH 8.0), 25mM EDTA, 2% (w/v) CTAB, 3% (w/v) PVP-10 and 3 % (v/v) ß-mercaptoethanol added prior to extraction.
Day 1	Grind 500 mg of sample Add 5 ml of prewarmed extraction buffer into powdered tissue Incubate the mixture at 65ºC for 10 min	Grind 500 mg of sample Add 5 ml of extraction buffer into powdered tissue Incubate the mixture at 65ºC for 15 min. Centrifuge the homogenate at 1503 × *g* for 10 min at room temperature	Grind 500 mg of sample Add 1.2 ml of SDS extraction buffer into powdered tissue Incubate the mixture at room temperature for 15 min with occasional inversion	Grind 500 mg of sample Add 375 µl of the mixture buffer, 750 µl C:I and 30 µl of β-mercaptoethanol to the powdered tissue Incubate the mixture at 20ºC for 5 min	Grind 500 mg of sample Add 12 ml of prewarmed (65 ºC for 10 min prior to use) extraction buffer into powdered tissue Incubate the mixture at 65ºC for 45 min and cooled to room temperature and centrifuge at 7000× *g* for 5 min

Add an equal volume of C:I, (24:1) to the sample mixture and vortex about 10 min at room temperature.	Add an equal volume of C:I, (24:1) to the sample mixture	Add 20% SDS into the suspension and invert gently for 5-8 times and following that incubate for 5 min at room temperature		Add an equal volume of P:C:I (125:24:1, pH 4.5) to the sample mixture and vortex about 5 min at room temperature.
Centrifuge for 5 min at 4ºC, at 15871× *g*	Centrifuge for 15 min at 4602 ×*g*	Centrifuge for 10 min at 4ºC, 13523 × *g*	Centrifuge for 5 min at 4ºC, 12 000 x *g*	Centrifuge for 15 min at 4ºC, 17 500 x *g*
Collect the supernatant and add an equal volume of C: I (24:1)	Collect the supernatant and add an equal volume of C: I (24:1)	Collect the supernatant and add 2 volume of TRIzol™ and incubate at room temperature for 10 min	Collect the supernatant and add an equal volume of P:C:I (25:24:1)	Collect the supernatant and add an equal volume of C:I (24:1)
		Add 1/5 volume of chloroform and mix thoroughly		
Vortex and centrifuge for 2 min at 4ºC, 15871 × *g*	Centrifuge for 15 min at 4602 ×*g*	Centrifuge for 10 min at 4ºC, 13523 × *g*	Vortex and centrifuge 5 min 4ºC, 12 000 x *g*	Vortex and centrifuge 15 min at 4ºC, 17500 x *g*
			Collect the supernatant and add an equal volume of P:C:I (25:24:1)	Collect the supernatant and add an equal volume of C:I (24:1)
			Vortex and centrifuge 5 min 4ºC, 12 000 x *g*	Centrifuge 15 min at 4ºC, 17 500 x *g*
Add 2 volume of ice-cold isopropanol to the supernatant	Add $^{1}/_{3}$ volume of 8M LiCl to the supernatant	Add an equal volume of isopropanol to the supernatant	Add $^{1}/_{10}$ volume of 3M sodium acetate, pH 5.2 and 2.5 volume of	Add $^{1}/_{3}$ volume of 8M LiCl to the collected supernatant

			100% ethanol to the supernatant	
Incubate on ice for 5 min and centrifuge for 5 min at 4ºC, 15871 × *g*	Incubate at -20ºC overnight.	Incubate at -20 °C for 20 min.	Incubate at 4ºC for 30 min	Incubate -20 °C overnight.
		Centrifuge for 20 min at 4ºC, 13523 × *g*	Centrifuge 10 min 4ºC, 12 000 x *g*	
Wash the pellet in 1 ml of 70% ethanol and centrifuge 5 min at 4ºC, 15871 × *g*		Add 500 µl of extraction buffer buffer to dissolve the pellet	Add 200 µl of RNase-free water to dissolve the pellet	
Air-dried the pellet for 20 min and dissolved it in 25 µl RNase-free water and stored at -80ºC.		Add an equal volume of P:C:I (25:24:1)		
		Centrifuge for 10 min at 4ºC, 13523 × *g*		
		Add C:I (24:1) to the supernatant		
		Centrifuge for 10 min at 4ºC, 13523 × *g*		
		Add $^{1}/_{10}$ volume of 3M sodium acetate (pH 4.8) and 2 volume ethanol to the supernatant and mix	Add 500 µl of 10M LiCl to the solution and mix gently	
		Incubate at -80 °C for 30 min	Incubate on ice for 60 min	
		Centrifuge for 20 min at 4ºC, 13523 × *g*	Centrifuge 10 min 4ºC, 12 000 x *g*	

			Discard the supernatant and wash the pellet with 500 µl of 70% ethanol. Centrifuge for 5 min at 4ºC, 13523 × *g* Dissolve the air-dry pellet in 25 µl RNase-free water and stored at -80ºC.	Discard the supernatant and wash the pellet with 800 µl of 75% ethanol. Centrifuge 5 min 4ºC, 12 000 x *g* Dissolve the air-dry pellet in 25 µl RNase-free water and stored at -80ºC.	
Day 2	Centrifuge for 30 min at 4ºC, 15871 × *g* Discard the supernatant and wash the pellet with 500 µl of 70% ethanol Centrifuge for 15 min at 4ºC, 15871 × *g* Repeat washing step two times Left to dry the pellet dissolve with 25 µl RNase-free water and stored at -80ºC.	Centrifuge for 30 min at 4ºC, 6010 × *g* Wash the pellet with ice-cold 75% ethanol and resuspended 25 µl RNase-free water and stored at -80ºC.			Centrifuge 30 min at 4ºC, 17 500 x *g* Discard the supernatant and wash the pellet with 500 µl of 70% ethanol Centrifuge 15 min at 4ºC, 17 500 x *g* Repeat washing step two times Dissolve the air-dry pellet in 25 µl RNase-free water and stored at -80ºC.

Table 4-3: The concentration and purity of DNase-treated RNA isolated from mature flower of *Dendrobium* hybrid (*Dendrobium* Burmese ruby × *Dendrobium* Mae-klong River) for different incubation time of extraction buffer.

No	Incubation time (min)	Biological replicate	$A_{260/280}$	$A_{260/230}$	Concentration of RNA (ng/ µl)	RNA yield (µg/g FW)
1	5	S1	1.6	1.5	79.8	4.0
2		S2	1.7	1.4	82.2	4.1
3		S3	1.7	1.6	80.3	4.0
4	10	S1	1.7	1.5	119.0	6.0
5		S2	1.6	1.7	108.0	5.4
6		S3	1.7	1.6	120.0	6.0
7	15	S1	1.7	1.8	137.0	6.9
8		S2	1.7	1.7	135.0	6.8
9		S3	1.6	1.8	129.0	6.5
10	45	S1	2.0	2.2	246	12.3
11		S2	2.0	2.3	258	12.9
12		S3	2.0	2.4	254	12.7

Table 4-4: The concentration and quality of DNase-treated RNA isolated from mature flower of *Dendrobium* hybrid (*Dendrobium* Burmese ruby × *Dendrobium* Mae-klong River) using different RNA extraction methods

No	Method	Biological replicate	$A_{260/280}$	$A_{260/230}$	Concentration of RNA (ng/ µl)	RNA yield (µg/g FW)	RIN	Reference
1	Method 1	S1	1.7	1.7	30.2	1.5	4.80	Kiefer et al. 2000
		S2	1.8	1.6	32.7	1.6	4.90	
		S3	1.8	1.6	33.9	1.7	5.10	
2	Method 2	S1	1.9	1.8	27.3	1.4	5.10	Su et al. 2011
		S2	1.9	1.8	28.5	1.4	5.80	
		S3	1.9	1.8	29.0	1.5	5.90	
3	Method 3	S1	1.7	1.7	18.6	0.9	6.30	Gao Y et al. 2011
		S2	1.7	1.6	17.3	0.9	6.30	
		S3	1.6	1.6	16.9	0.9	6.80	
4	Method 4	S1	1.7	1.6	17.8	0.9	6.30	Liu et al. 2018
		S2	1.7	1.5	16.5	0.8	6.80	
		S3	1.7	1.5	14.9	0.8	6.70	
5	Improved CTAB method	S1	2.0	2.2	225.0	11.3	8.70	
		S2	2.0	2.3	220.0	11.0	8.90	
		S3	2.0	2.4	239.0	12.0	8.80	

Table 4-5: The concentration and purity of DNase-treated RNA isolated from mature flower of *Dendrobium* hybrid (*Dendrobium* Burmese ruby × *Dendrobium* Mae-klong River) for different incubation time during precipitation using 8M LiCl.

No	Incubation time (h)	Biological replicate	$A_{260/280}$	$A_{260/230}$	Concentration of RNA (ng/ µl)	RNA yield (µg/g FW)
1	3	S1	1.9	2.0	45.7	2.3
2		S2	2.0	1.9	46.0	2.3
3		S3	1.9	1.8	47.3	2.4
4	6	S1	2.0	1.9	71.0	3.6
5		S2	2.1	2.0	70.6	3.5
6		S3	2.0	2.1	69.9	3.5
7	8	S1	2.0	1.9	96.4	4.8
8		S2	2.0	2.0	96.0	4.8
9		S3	2.1	2.2	95.6	4.8
10	10	S1	2.0	2.1	126	6.3
11		S2	2.0	2.0	127	6.4
12		S3	2.0	2.2	126	6.3
13	12	S1	2.1	2.3	162	8.1
14		S2	2.1	2.2	170	8.5
15		S3	2.0	2.1	176	8.8
16	24	S1	2.0	2.2	256	12.8
17		S2	2.0	2.3	252	12.6
18		S3	2.0	2.4	244	12.2

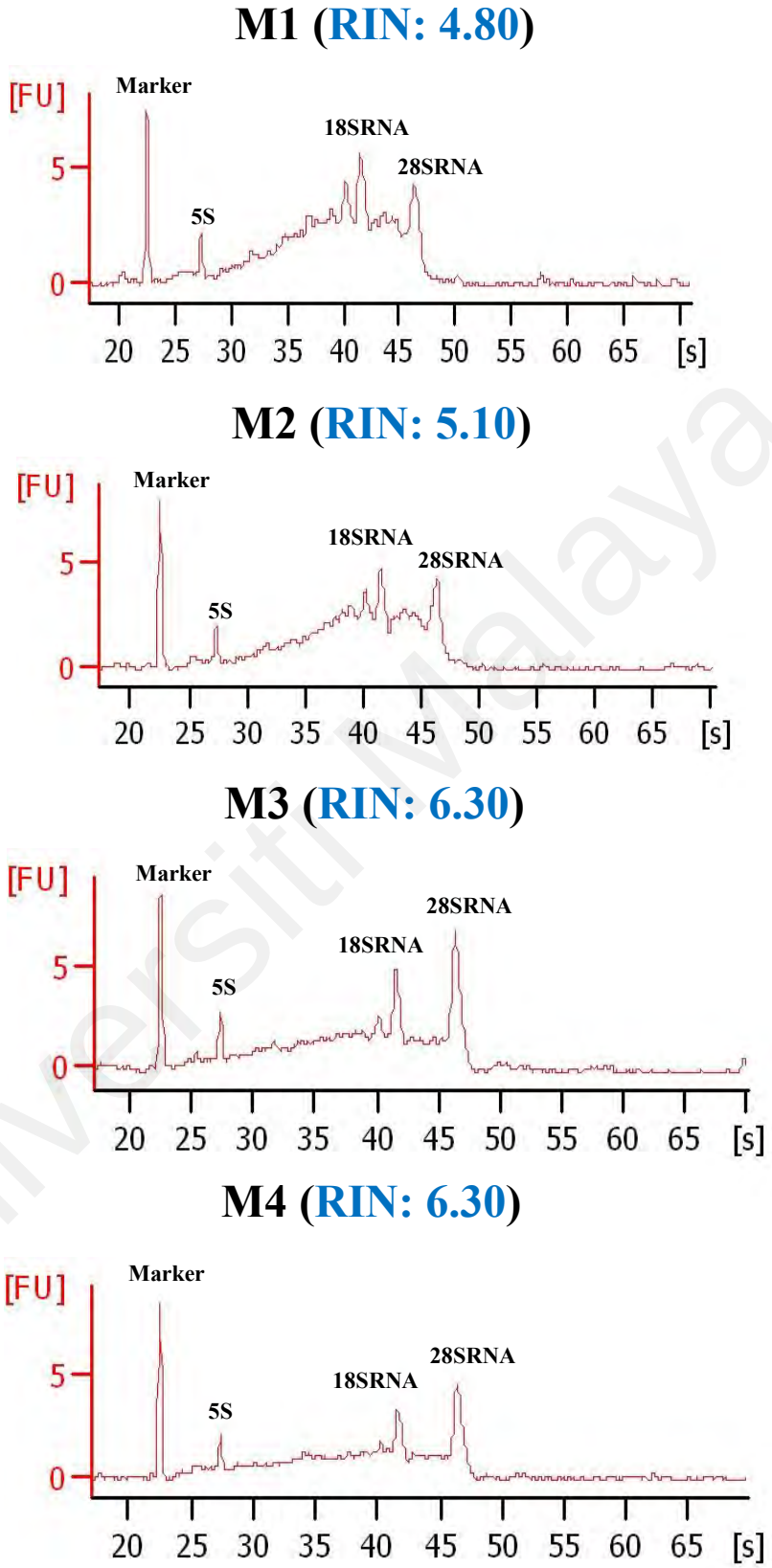

Figure 4-6 : RNA Integrity Number (RIN) values for M1: Method 1, M2: Method 2, M3: Method 3 and M4: Method 4. RNA isolated from mature flower of *Dendrobium* hybrid (*Dendrobium* Burmese ruby × *Dendrobium* Mae-klong River)

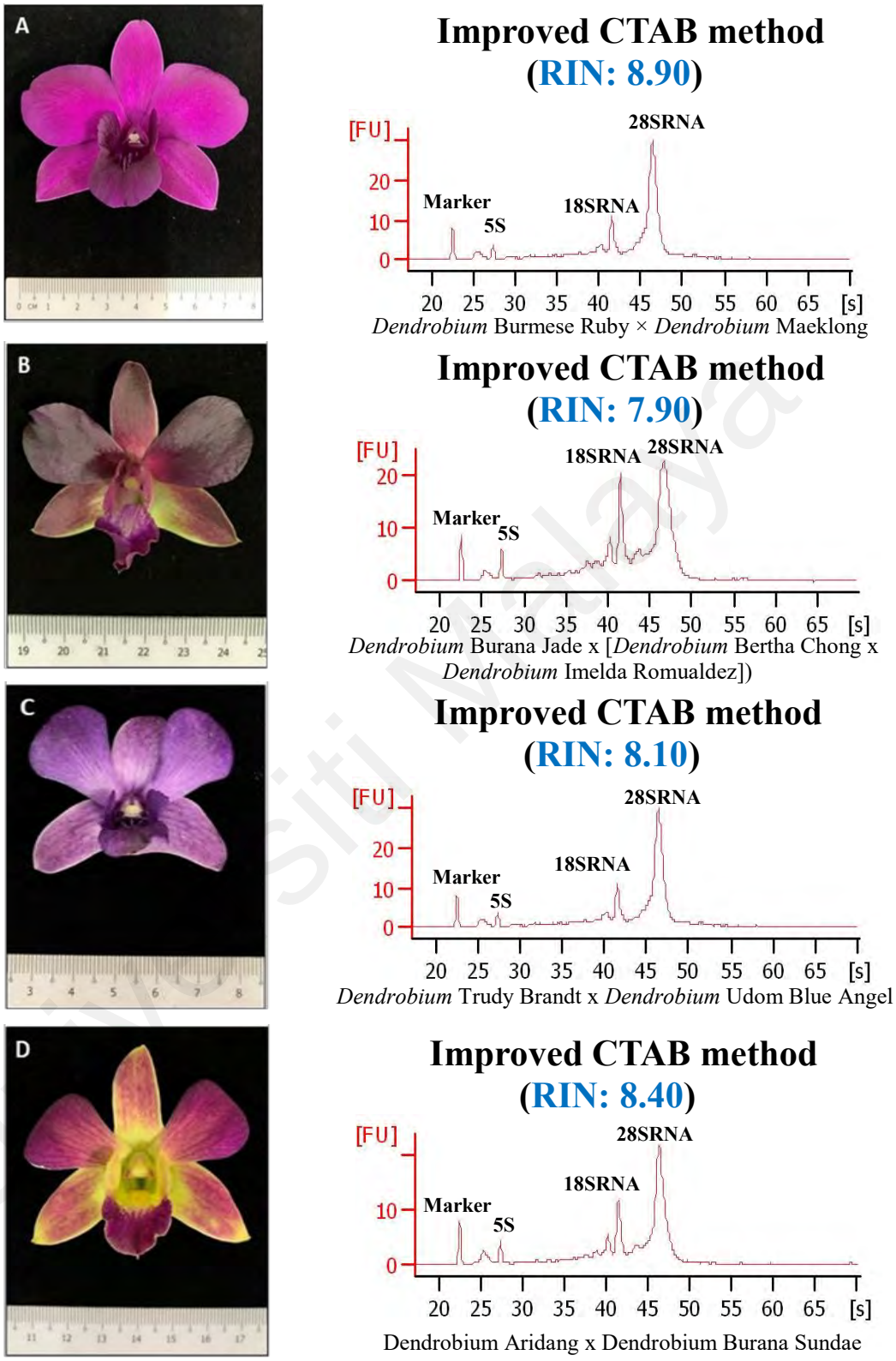

Figure 4-7 : RNA Integrity Number (RIN) values for flowers of *Dendrobium* hybrids using Improved CTAB method for RNA isolation. **A:** *Dendrobium* Burmese ruby × *Dendrobium* Mae-klong River; **B:** *Dendrobium* Burana Jade × [*Dendrobium* Bertha Chong × *Dendrobium* Imelda Romualdez]; **C:** *Dendrobium* Trudy Brandt × *Dendrobium* Udom Blue Angel and **D:** *Dendrobium* Aridang × *Dendrobium* Burana Sundae

Figure 4-8: RT-PCR amplification of *DhCHS* cDNA from *Dendrobium* hybrid. Lane 1 and 9: 100 bp HyperLadder™ (Bioline, UK); Lanes 2 – 8 are PCR products after cDNA synthesis from RNA isolated from flower buds of six different developmental stages of *Dendrobium* hybrid flowers. Lane 2: RNA isolated from stage 1 flower bud; Lane 3: RNA isolated from stage 2; Lane 4: RNA isolated from stage 3; Lane 5: RNA isolated from stage 4; Lane 6: RNA isolated from stage 5; Lane 7: RNA isolated from stage 6 sepals; Lane 8: RNA isolated from stage 6 petals; Lane 10: negative control (no template).

4.3 Construction and expression of *R2R3-MYB* and *DhCHS* dsRNA

DhMYB22 and *DhMYB60* were selected to construct dsRNA expression vectors for gene silencing. *DhMYB22* (the homolog of *Dca003827*) and *DhMYB60* (the homolog of *Dca008884*) were chosen because they clustered together with homologs that had been confirmed in other plants to function for flower colour and shape (Figure 4-1 and Table 4-1). The selected DNA sequences based on primer designed (Table 3-1) from *DhMYB22*, *DhMYB60* and *DhCHS* were PCR amplified from cDNA of *Dendrobium* hybrid and the products showed the expected band sizes (Figure 4-9). The amplified products were ligated into pGEM®-T Easy Vector, and desired constructs confirmed using DNA sequencing. To form the recombinant plasmids of expression vector L4440 with a fragment of interest for each of the genes *DhMYB22*, *DhMYB60* and *DhCHS,* each construct of pGEM®-T Easy was digested to produce a band of the expected size (Figure 4-10). Colony PCR of *Escherichia coli* DH5α and RNase III-deficient *Escherichia coli* strain HT115 (DE3) was confirmed by looking into the amplicon product for each of the three gene sequences i.e., *DhMYB22* (501 bp), *DhMYB60* (530 bp) and *DhCHS* (436 bp) (Figure 4-11).

Each constructed plasmid (L4440_*DhMYB22*, L4440_*DhMYB60* and L4440_*DhCHS* (shown in the top panel of Figure 4-12) was tested to ensure the RNA of the crude lysate produced bands of the expected sizes. The agarose gel result shown in Figure 4-12 shows a single band with the expected size for each of the three dsRNAs (*DhCHS*: 640 bp, *DhMYB22*: 705 bp and *DhMYB60*: 734 bp) and showed no contamination of DNA and ssRNA.

800

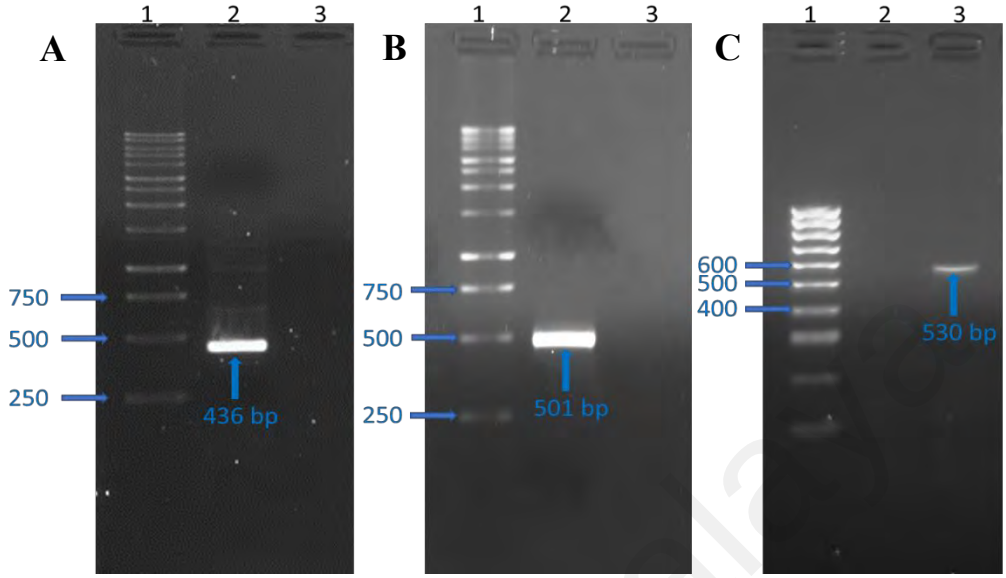

Figure 4-9: PCR amplification of *CHS* and *R2R3-MYB* genes sequences **A**. PCR amplification of *DhCHS* gene sequence Lane 1: 1 Kbp ladder (Promega, USA); Lane 2: *DhCHS* amplicon and Lane 3: -ve control, **B**. PCR amplification of *DhMYB22* gene by using *TransTaq* DNA Polymerase High Fidelity (HiFi). Lane 1: 1 Kbp ladder (Promega, USA); Lane 2: *DhMYB22* amplicon and Lane 3: -ve control, **C.** PCR amplification of *DhMYB60* by using *TransTaq* DNA Polymerase High Fidelity (HiFi). Lane 1: 100 bp ladder HyperLadder™ (Bioline, UK); Lane 2: -ve control and Lane 3: *DhMYB60* amplicon.

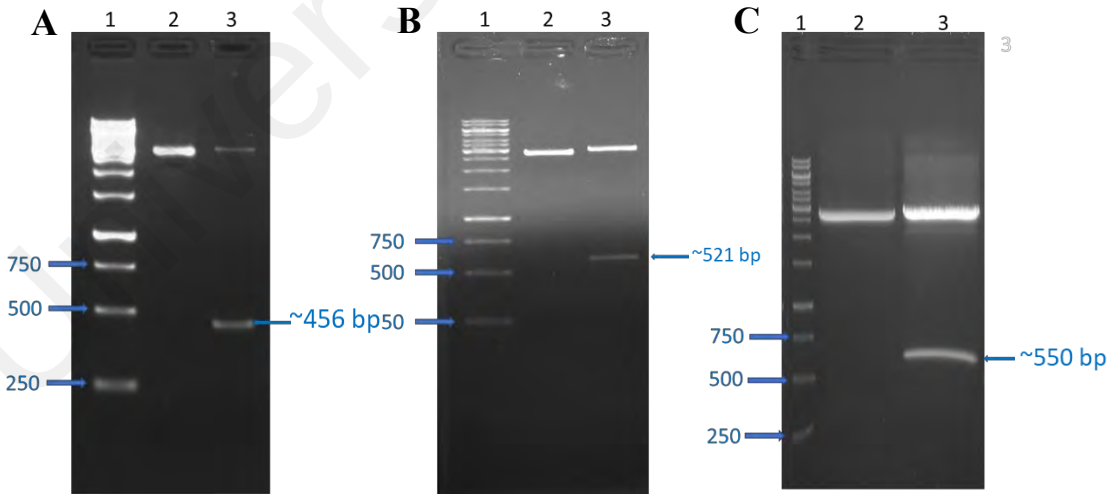

Figure 4-10: Plasmid digestion of *CHS* and *R2R3-MYB* genes sequences **A**. Plasmid digestion of *DhCHS* gene. Lane 1: 1 Kbp ladder (Promega, USA); Lane 2: undigested pGEM®-T Easy and Lane 3: digested pGEM®-T Easy *DhCHS*, **B**. Plasmid digestion of *DhMYB22* gene. Lane 1: 1 Kbp ladder (Promega, USA); Lane 2: undigested pGEM®-T Easy and Lane 3: digested pGEM®-T Easy *DhMYB22*, **C.** Plasmid digestion of *DhMYB60* gene. Lane 1: 1 Kbp ladder (Promega, USA); Lane 2: undigested pGEM®-T Easy and Lane 3: digested pGEM®-T Easy *DhMYB60* amplicon

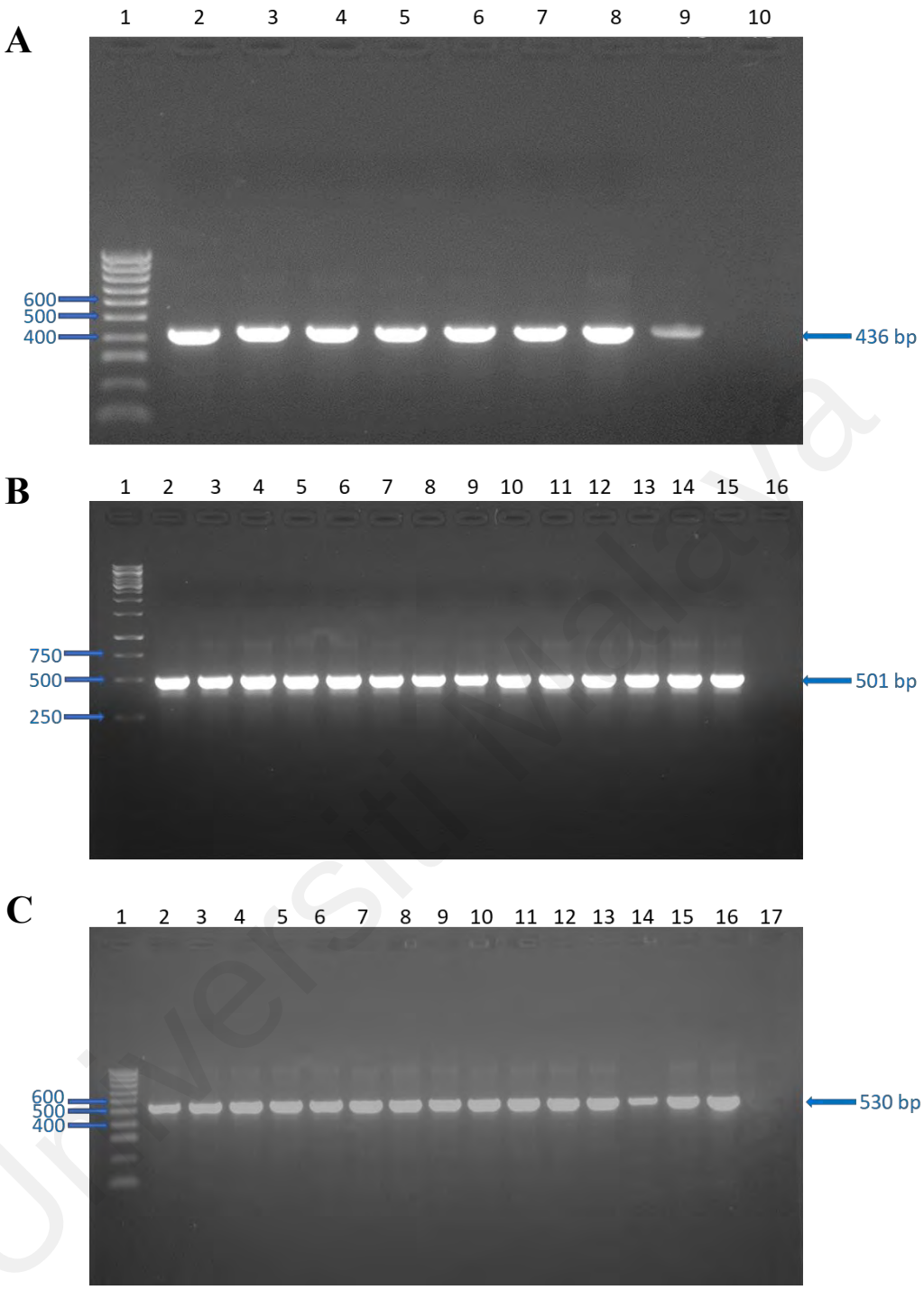

Figure 4-11: Colony PCR of transformed HT115_L4440_*DhCHS* and *DhMYB22* and *DhMYB60*. **A**. Colony PCR of transformed HT115_L4440_*DhCHS*. Lane 1: 100 bp ladder HyperLadder™ (Bioline, UK); Lane 2-8: *DhCHS* amplicon; Lane 9: *DhCHS* +ve control and Lane 10: -ve control, **B**. Colony PCR of transformed HT115_L4440_*DhMYB22*. Lane 1: 1 Kbp ladder (Promega, USA); Lane 2-14: *DhMYB22* amplicon; Lane 15: *DhMYB22* +ve control and Lane 16: -ve control, **C.** Colony PCR of transformed HT115_L4440_*DhMYB60*. Lane 1: 100 bp ladder HyperLadder™ (Bioline, UK); Lane 2-15: *DhMYB60* amplicon; Lane 16: *DhMYB60* +ve control and Lane 17: -ve control.

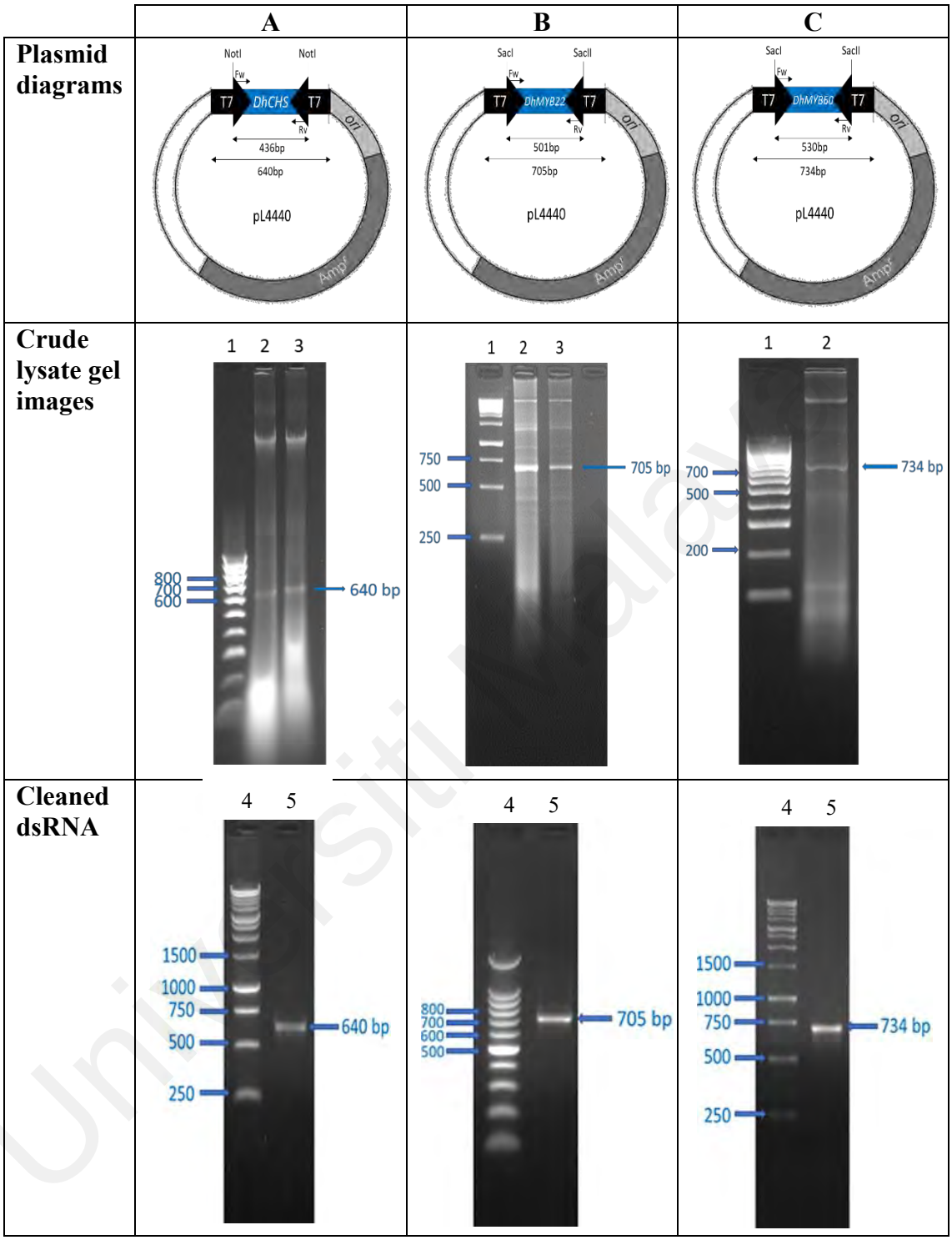

Figure 4-12: Plasmid diagrams, crude lysate gel images and cleaned dsRNA of *R2R3-MYB* genes and *DhCHS* **A**. *DhCHS*: Lane 1: 100 bp ladder HyperLadder™ (Bioline, UK), Lane 2 and 3: *DhCHS* amplicon; Lane 4: 1 Kbp ladder (Promega, USA) and Lane 5: *DhCHS* product. **B**. *DhMYB22*: Lane 1: 1 Kbp ladder (Promega, USA); Lane 2 and 3: *DhMYB22* amplicon; Lane 4: 100 bp ladder HyperLadder™ (Bioline, UK) and Lane 5: *DhMYB22* product. **C.** *DhMYB60***:** Lane 1: 100 bp ladder HyperLadder™ (Bioline, UK); Lane 2: *DhMYB60* amplicon; Lane 4: 1 Kbp ladder (Promega, USA) and Lane 5: *DhMYB60* product.

4.4 Off-target gene prediction for dsRNA constructs

As RNA silencing experiments have the potential for unintended silencing of non-targeted gene transcripts (off-target silencing), potential genes that could be unintended targets of dsRNA constructs of *DhMYB22*, *DhMYB60* and *DhCHS* were explored using si-Fi21 software (Lück et al., 2019). Off-target prediction analysis showed siRNA identical or reverse complementary regions of 16-25 nt of the dsRNA sequences was conducted and found that the only strong matches were with the genes being targeted. The sequence of *DhMYB22* dsRNA mainly targeted *Dca003827* (the *D. catenatum* homologue of DhMYB22) followed by *Dca003829* (25–66 hits) (Table 4-7). According to the BLAST result, *Dca003827* is 88.2%, similar to *DhMYB22* while *Dca008884* is 91.9%, similar to *DhMYB60*. Other than that, 6 other *MYB* genes (*Dca028226*, *Dca022534*, *Dca020624*, *Dca016337*, *Dca012246* and *Dca009933*) (Table 4-7) showed 12 or fewer hits. Similarly, *DhMYB60* dsRNA was shown to target *Dca008884* (the *Dendrobium catenatum* homolog of DhMYB60) with 131-182 total hits and low siRNA hits for other 7 genes (*Dca004957*, *Dca023230*, *Dca011059*, *Dca006402*, *Dca019358*, *Dca020822* and *Dca017917*) (Table 4-8). It was found that *DhCHS* dsRNA only strongly targets *Dca003406*, (the *Dendrobium catenatum* homolog used for primer design and amplification of the *Dendrobium* hybrid *CHS* used to make the dsRNA) with some, but much poorer, matches to two of the other seven *CHS* loci in the *Dendrobium catenatum* genome sequence (Table 4-9).

Table 4-6: Alignment of coding sequence (CDS) of *Dendrobium catenatum* with double-stranded RNA *DhMYB22* of *Dendrobium* hybrid and off-target prediction by using si-Fi21 software

Query Sequence:
>DhMYB22
CATGGACTACTTCGGAAGACAAGCTCTTGAAGGCTTTCGTCAATATTCATGGAGAAGGCAGATGGACGACGATGCCACACGAAGCA
GGGCTGAGAAGGTCTGGGAAGAGCTGTCGACTCCGATGGCTAAATTACCTGAGGCCCAACGTTAAACGTGGAAACTTTTCTGAGGAA
GAGGACGACCTCATCATCAGGCTTCATAAACTCCTTGGCAATAGATGGTCTCTGATTGCTGGAAGGCTACCCGGTCGGACAGATAAT
GAAATAAAAAACTATTGGAACACAATCTTATGTAAGAAAGCAAGCTTTCAACATCAAATGCATCAGCCAAGCCGCCCAAGCATCAT
ACAAAGACCTCCAACTTCTAATCTTGGATTTCCAACATCATCATCCACAACACAATCACAAGCTGCCACAAATGATA

		Alignment	**Off-Target Prediction (si-Fi21)**		
CDS Sequence	**Length of sequence**	**Similarity**	**Regions with at least 16 nt perfect match**	**Regions with at least 21 nt perfect match**	**Regions with at least 25 nt with only 1 mismatch**
Dca003827	759 bp	88.2%	66	27	0
Dca003829	873 bp	87.2%	62	25	0
Dca028226	315 bp	56.2%	12	5	0
Dca022534	588 bp	29.7%	9	4	0
Dca020624	1665 bp	19.4%	5	0	0
Dca016337	984 bp	30.7%	4	0	0
Dca012246	222 bp	39.1%	3	0	0
Dca009933	1323 bp	21.7%	2	0	0

Table 4-7: Alignment of coding sequence (CDS) of *Dendrobium catenatum* with double-stranded RNA *DhMYB60* of *Dendrobium* hybrid and off-target prediction by using si-Fi21 software

Query Sequence:
>*DhMYB60*
GGGAAGTTTAGTATGCAGGAAGAACAGACCATCATCCAGCTTCATGCTCTCCTTGGTAACAGATGGTCTGCAATTGCAACGC
ACCTACCCAAGAGAACTGATAATGAGATCAAGAATTACTGGAACACACATCTGAAGAAACAGCTAGCAAAGATGGGGATTG
ACCCAGTGACACATAAACCCAAGAGTGTCACCCTTGCCTCTGCCGACGGCCATGTAAGAAGCACTGCAAATCTCAACCACAT
GGCACAATGGGAGAGTGCTCGCCTTGAAGCTGAGGCTCGCCTTGTACGTGAGTCCAAGCTCCGCAGCAGTGCTCCTCCCGCC
AACTTCCCTTCACAGCATCCACCTTCACCACCACCTCTTGTCGCCATGCCAACAGTAGTGTATCCCTCTCTCGACGTGCTGCA
AGCTTGGAAAGGTGTGTGGCCCAAGCCTGCAGCCAATAGCCAAG

		Alignment	**Off-Target Prediction (si-Fi21)**		
CDS Sequence	**Length of sequence**	**Similarity**	**Regions with at least 16 nt perfect match**	**Regions with at least 21 nt perfect match**	**Regions with at least 25 nt with only 1 mismatch**
Dca008884	1086 bp	91.9%	131	86	182
Dca004957	1044 bp	78.8%	22	3	38
Dca023230	765 bp	34.2%	20	15	13
Dca011059	1005 bp	28.5%	14	9	11
Dca006402	708 bp	37.5%	11	4	2
Dca019358	1068 bp	31.9%	8	3	15
Dca020822	969 bp	27.3%	8	3	8
Dca017917	969 bp	31.5%	8	3	12

Table 4-8: Alignment of coding sequence (CDS) of *Dendrobium catenatum* with double-stranded RNA *Chalcone synthase* (*DhCHS*) of *Dendrobium* hybrid and off-target prediction by using si-Fi21 software.

Query Sequence:
> *DhCHS*
GATGGTCTGGGAAGCTGAGACGAGTTGGAAAAGCGGTCGCTCAGTAGTCAAGTCAGGGTCAGATCCAACTATAACAG
CTGCAGCCCCATCGCCAAACAGCGCCTGCCCGACAAGAGAATCGAGATGGGATTCCGACGGCCCGCGGAACGTAACTG
CTGTGATTTCTGAACAAACGACGAGAACTCGCGCGCCGGCGTTGTTCTCGGCGAGGTCTTTGGCAAGGCGAAGGACGGT
GCCGCCGGCGAAGCAGCCTTGTTGGTAAAGCATGATTCGATTGACGGATGGACGGAGACCGAGGAGACGAGTGAGTTG
GTAGTCGGCACCGGGCATGTCTACGCCG

		Alignment	Off-Target Prediction (si-Fi21)		
CDS Sequence	**Length of sequence**	**Similarity**	**Regions with at least 16 nt perfect match**	**Regions with at least 21 nt perfect match**	**Regions with at least 25 nt with only 1 mismatch**
Dca003406	1188 bp	94.4%	128	93	203
Dca014503	1173 bp	39.4%	16	3	16
Dca016721	1173 bp	33.0%	2	0	0
Dca007368	1173 bp	29.5%	0	0	0
Dca007369	1173 bp	29.1%	0	0	0
Dca012323	1173 bp	31.1%	0	0	0
Dca012324	1167 bp	21.3%	0	0	0
Dca004217	1149 bp	20.1%	0	0	0

4.5 Degradation study for dsRNA stability

A degradation study was used to determine the stability of dsRNA kept at 4 °C and at room temperature (23 °C) before exogenous treatment onto flower buds (Table 4-10 and Figure 4-13). The quality of dsRNA was in the high range (1.8-2.2) and there was no significant reduction in RNA over the 6-day observation.

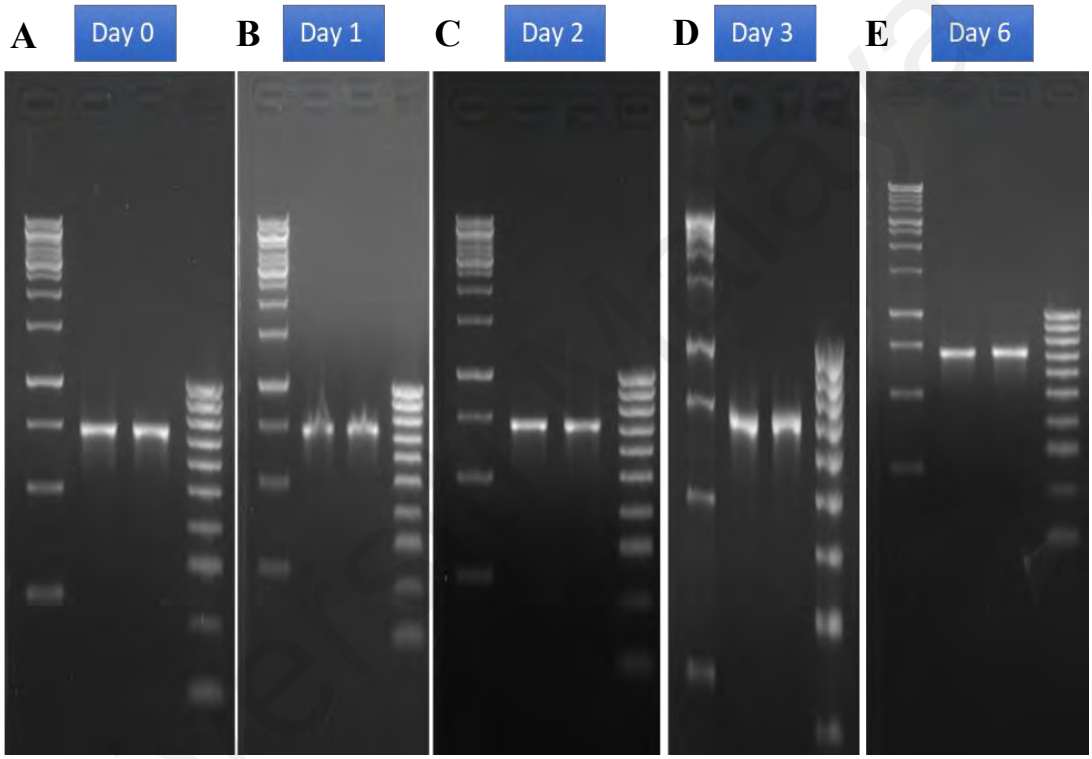

Figure 4-13: Visualisation of *DhMYB60* dsRNA on agarose gel for 6-day. **A.** Visualisation of *DhMYB60* dsRNA on agarose gel for day 0. **B.** Visualisation of *DhMYB60* dsRNA on agarose gel for day 1. **C.** Visualisation of *DhMYB60* dsRNA on agarose gel for day 2. **D**. Visualisation of *DhMYB60* dsRNA on agarose gel for day 3. **e.** Visualisation of *DhMYB60* dsRNA on agarose gel for day 6.

Table 4-9: The RNA concentration at different temperatures for *DhMYB60* dsRNA

Days	Temperature	Concentration (ng/µl)	A260/A280	A260/A230
0	4 °C	40.33	2.049	1.759
	RT	38.50	2.026	2.136
1	4 °C	40.33	2.049	1.739
	RT	38.50	2.026	2.136
2	4 °C	39.50	2.059	1.455
	RT	39.83	2.059	1.400
3	4 °C	39.00	2.069	1.690
	RT	39.50	2.060	1.519
6	4 °C	39.50	1.976	1.528
	RT	39.00	1.951	1.569

RT: room temperature

4.6 Phenotypes of silencing experiment of *DhMYB22*, *DhMYB60*, *DhCHS*, Empty Vector and control *Dendrobium* hybrid floral buds

Dendrobium hybrid floral buds were treated separately in different plants with dsRNA from *DhMYB22*, *DhMYB60*, *DhCHS* (positive control) and empty vector (negative control) as shown in the experimental design in Figure 4-14. All dsRNA treated floral buds showed less pigmentation than the floral bud of the control plant at stage 6. *DhMYB22* dsRNA treated floral buds showed less pigmentation (compared to control) at all developmental stages and even compared with *DhCHS* dsRNA treated floral buds. In addition to less pigmentation, *DhMYB60* dsRNA treated floral buds also showed marked differences in floral shape compared to the flowers of the control group (Figure 4-14).

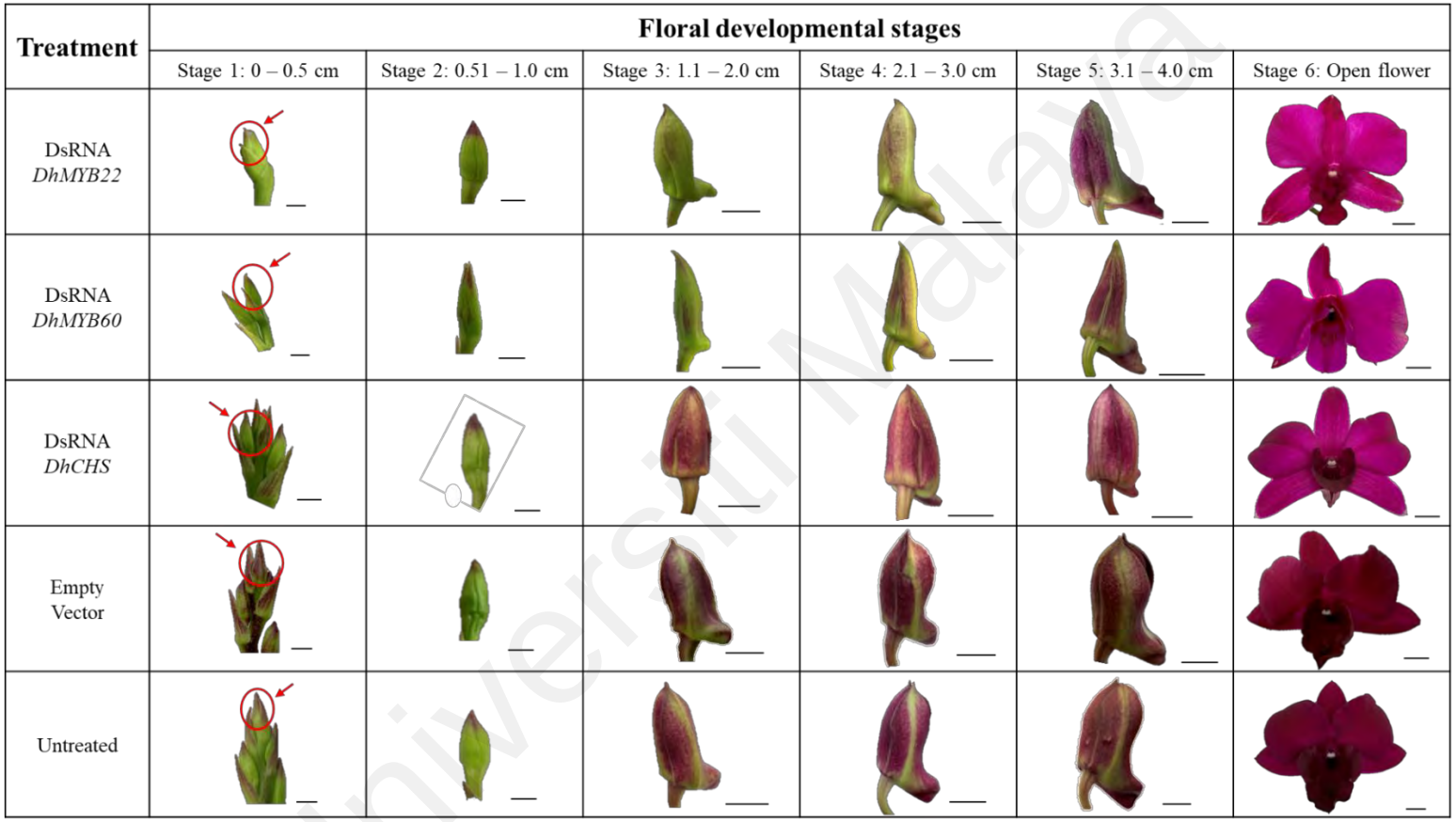

Figure 4-14: Floral buds and open flower from plants treated with dsRNA of *DhMYB22*, *DhMYB60* or *DhCHS*, empty vector and untreated *Dendrobium* hybrid. Images of floral buds were captured at stages 1 to 6, with samples harvested at the same stages for phenotypic measurements. Times of sampling from the start of treatments (or the start of the experiment for untreated) were 5 days (stage 1), 10 days (stage 2), 15 days (stage 3), 20 days (stage 4), 25 days (stage 5) and 30 days (stage 6). For stage 1, multiple buds on each raceme are shown before dissection of single buds for sampling. Bars for stage 1 and stage 2 = 0.5 cm. Bars for stage 3, stage 4, stage 5 and stage 6 = 1 cm.

845 **4.7 Treatment of flower buds with dsRNA reduces transcript levels of the**
846 **targeted RNAs**

847 To determine the effect of dsRNA treatment on gene expression during flower
848 development, transcripts were quantified from dsRNA treated, empty vector treated and
849 from untreated floral buds at stages 1 to 5 and from the floral organs of open flowers at
850 stage 6 (sepals, petals and lips) using qRT-PCR with gene specific primers (Figure 4-15).
851 The qRT-PCR profiles of untreated plants for each target RNA give an indication of the
852 expression profile during normal flower development, with *DhMYB22* (Figure 4-15)
853 showing highest expression at stages 1 and 6 in contrast to *DhMYB60* and *DhCHS* (Figure
854 4-15), which peak at stages 5 and 4 respectively. In addition to the two *MYB* genes
855 investigated here, treatments with dsRNA of *DhCHS*, a structural gene in the early part
856 of the anthocyanin biosynthesis pathway, were included to allow direct comparison of the
857 effect of exogenous dsRNA treatments on a gene with a known role in flower colour
858 development. After treatment with dsRNA of *DhCHS*, the transcript accumulation was
859 1.28 to 10.08-fold lower than those of untreated or empty vector treated flowers of the
860 same stage. On the other hand, after treatment with dsRNA of *DhMYB22*, the transcript
861 accumulation was 1.87 to 64-fold lower and after treatment with dsRNA of *DhMYB60*
862 (Figure 4-15), the transcript accumulation was 1.66 to 10.08-fold lower compared to the
863 untreated and empty vector treated flower. Flowers treated with empty vector did not
864 show any significant difference in expression of genes compared to untreated flower,
865 which indicated that bacterial lysate background does not affect expression of *R2R3-MYB*
866 gene in flowers (Figure 4-15).

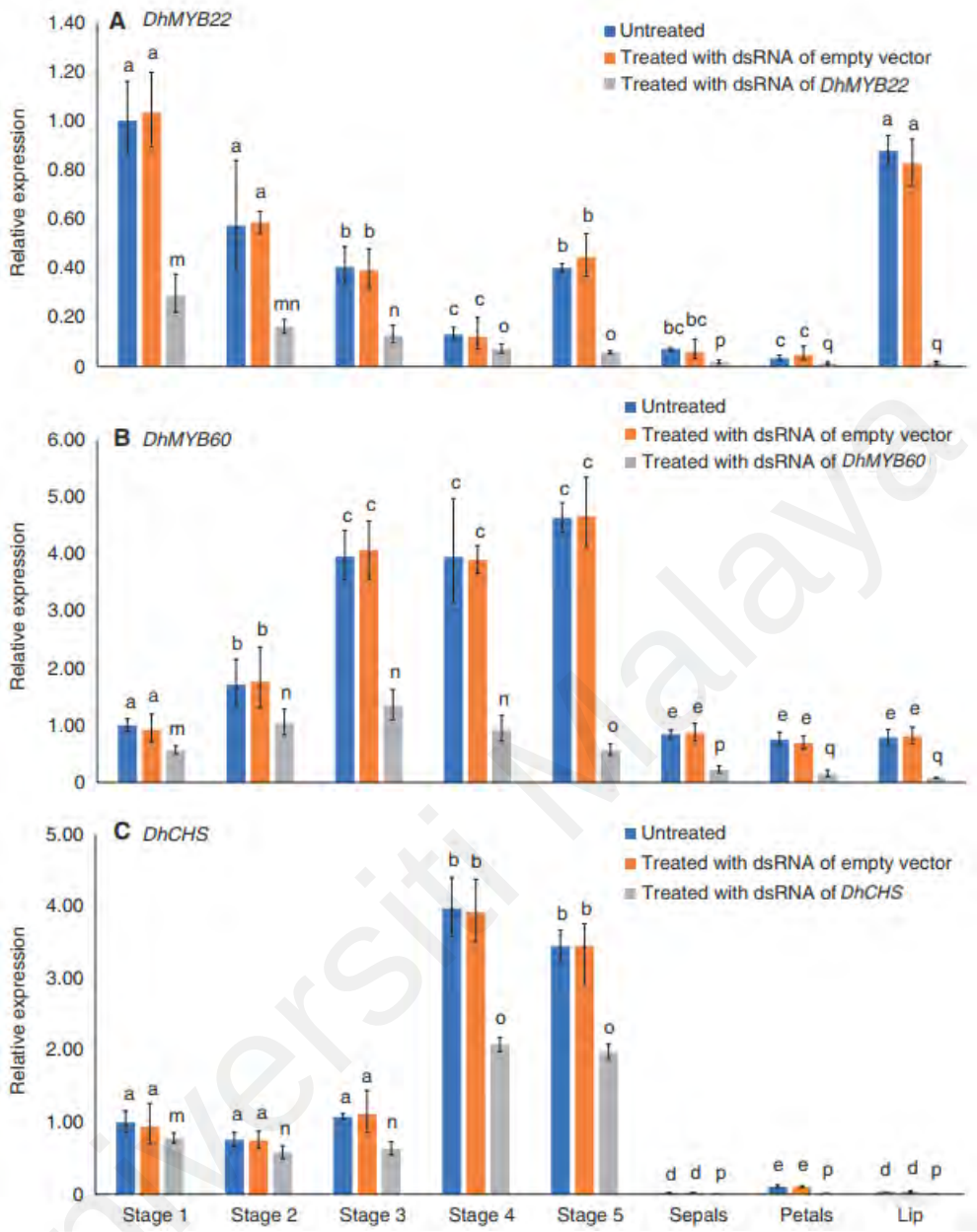

Figure 4-15: Expression of *DhMYB22*, *DhMYB60* and *DhCHS* in untreated and dsRNA-treated *Dendrobium* floral buds and open flower parts using qRT–PCR. Error bars indicate standard deviations from three biological replicates. Different letters on the top of each bar indicate statistically significant differences in expression level (one-way ANOVA, Tukey HSD comparison test, $P < 0.05$). **A.** Expression of *DhMYB22* in untreated flowers and flowers treated with dsRNA of *DhMYB22* or empty vector. The relative mRNA abundance of *DhMYB22* was normalized with respect to the reference gene, β-actin. The expression value for the untreated bud (*DhMYB22* cDNA) at stage 1 was set to a value of 1.0 and subsequently expression levels for the other stages of untreated (stage 2–5 buds and organs of open flower) and treated samples (stage 1–5 buds and organs of open flower) with dsRNA of *DhMYB22* are reported relative to this number. **B.** Expression of *DhMYB60* in untreated flowers and flowers treated with dsRNA of *DhMYB60* or empty vector.

The relative mRNA abundance of *DhMYB60* was normalized with respect to the reference gene, β-actin. The expression value for the untreated bud (*DhMYB60* cDNA) at stage 1 was set to a value of 1.0 and subsequently expression levels for the other stages of untreated (stage 2–5 buds and organs of open flower) and treated samples (stage 1–5 buds and organs of open flower) with dsRNA of *DhMYB60* are reported relative to this number. **C.** Expression of *DhCHS* in untreated flowers and flowers treated with dsRNA of *DhCHS* or empty vector. The relative mRNA abundance of *DhCHS* was normalized with respect to the reference gene, β-actin. The expression value for the untreated bud (*DhCHS* cDNA) at stage 1 was set to a value of 1.0 and subsequently expression levels for the other stages of untreated (stage 2–5 buds and organs of open flower) and treated samples (stage 1–5 buds and organs of open flower) with dsRNA of *DhCHS* are reported relative to this number.

867

4.8 Silencing of *DhMYB22* and *DhMYB60* in *Dendrobium* hybrid

4.8.1 Reduced pigmentation and anthocyanin content in flowers

Analysis of *DhMYB22* and *DhMYB60* dsRNA treated buds showed them to have significantly lower pigmentation than untreated controls, particularly from stage 3 of flower development onwards (Figure 4-14). The quantification of colour difference (ΔE) measured by colorimeter in open flower (Figure 4-16 and Table 4-10) showed that sepals of *DhMYB22* and *DhMYB60* dsRNA treated flowers were around 20-fold less intensely coloured than untreated flowers. Petals and lips of *DhMYB22* and *DhMYB60* dsRNA treated flowers similarly showed a reduction in colour intensity (Figure 4-18 and Table 4-10). The sepals, petals and lips of *DhCHS* dsRNA treated flowers were around 15-fold less intensely coloured compared to untreated flowers. Among the flower parts, the lightest magenta colour was observed for sepals of flowers treated with *DhMYB60* followed by petals of flowers treated with *DhMYB22* (Figure 4-14), which is also noticeable in ColorHexa data (Table 4-10 and Appendix H).

As colour in *Dendrobium* flowers is mainly a result of anthocyanin pigments, the total anthocyanin concentration from stage 1 to open flower (stage 6) was quantified. A gradual increase in concentration was observed with the stage of development (Figure 4-17). However, *DhMYB22* and *DhMYB60* followed by *DhCHS* dsRNA treated flowers showed significantly lower total anthocyanin concentrations compared to untreated flowers at the same stages. At stage 6, petals of *DhMYB22* dsRNA treated flower, and the lips and sepals of *DhMYB60* dsRNA treated flowers had lower total anthocyanin concentrations than other floral organs (Figure 4-17).

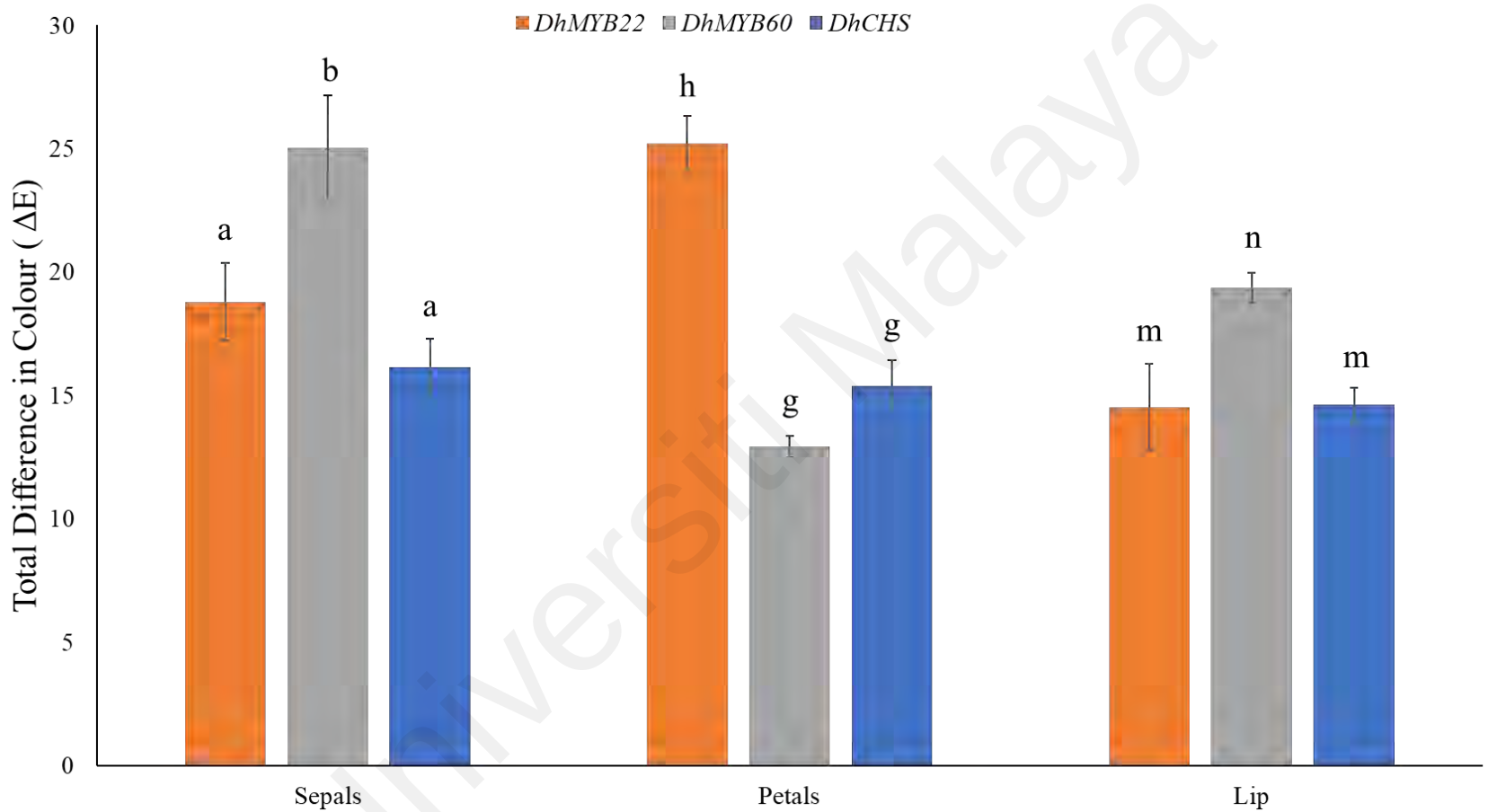

Figure 4-16: Total colour difference (ΔE) between untreated and dsRNA treated sepals, petals and lips. Treatments were either with dsRNA to *DhMYB22*, dsRNA to *DhMYB60* or dsRNA to *DhCHS* with untreated control used as the comparator for all three treatments. Error bars indicate standard deviations from three biological replicates. Different letters on the top of each bar indicate statistically significant differences (One-way ANOVA, Tukey HSD comparison test $p < 0.05$).

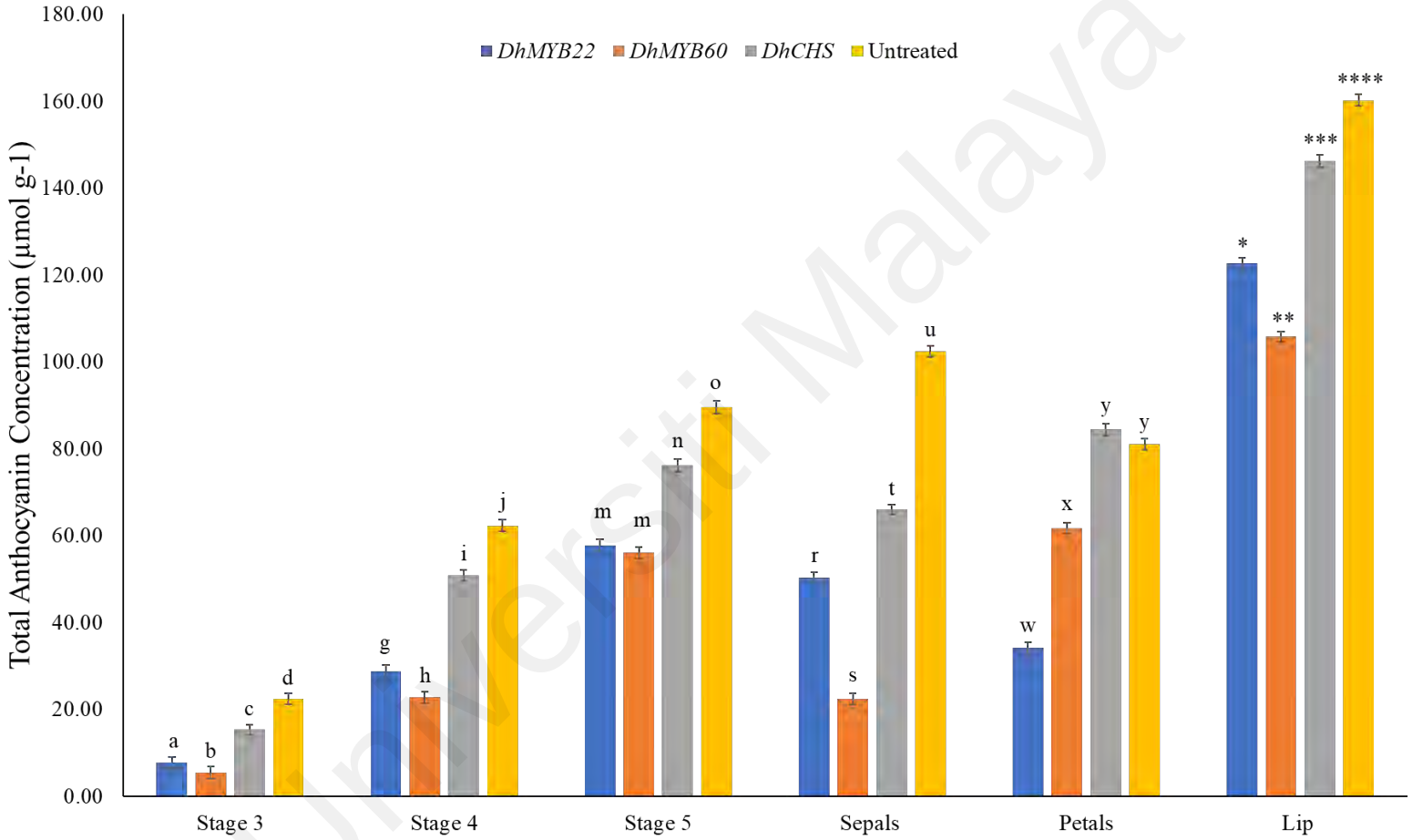

Figure 4-17: Total anthocyanin concentration of untreated and dsRNA treated floral buds and open flowers. Treatment were with dsRNA of *DhMYB22*, *DhMYB60* or *DhCHS*. Error bars indicate standard deviations from three biological replicates. Different letters or stars on the top of each bar indicate statistically significant differences (One-way ANOVA, Tukey HSD comparison test $p < 0.05$).

Table 4-10: Colorimetric parameter (L*, a*, b*. C*, h and ΔE) for Sepals, Petals and Lip treated with dsRNA of *DhMYB22*, *DhMYB60*, *DhCHS* and untreated flower. Different letters indicate statistically significant difference according to One-way ANOVA, Tukey HSD comparison test ($p < 0.05$)

Treatment	Sample	L*	a*	b*	C*	h	ΔE
DhMYB22	Sepals	27.11 ± 1.08^{bc}	44.10 ± 1.10^{ab}	-21.20 ± 1.38^{de}	48.99 ± 1.48^{b}	334.44 ± 1.10^{def}	18.80 ± 1.57^{c}
	Petals	26.19 ± 0.79^{bc}	47.01 ± 0.45^{a}	-27.23 ± 0.93^{f}	54.35 ± 0.78^{a}	330.00 ± 0.73^{ef}	25.23 ± 1.10^{a}
	Lip	11.20 ± 1.03^{g}	21.30 ± 1.59^{e}	-7.56 ± 1.13^{b}	22.70 ± 1.77^{e}	340.86 ± 2.16^{bcd}	14.53 ± 1.75^{cd}
DhMYB60	Sepals	38.60 ± 2.57^{a}	40.05 ± 1.05^{bc}	-24.57 ± 0.76^{ef}	47.05 ± 0.92^{bc}	328.43 ± 1.12^{f}	25.04 ± 2.11^{ab}
	Petals	23.65 ± 0.17^{cd}	38.20 ± 0.49^{c}	-18.75 ± 0.62^{d}	42.60 ± 0.35^{c}	333.85 ± 0.96^{def}	12.91 ± 0.43^{d}
	Lip	16.81 ± 0.43^{f}	23.77 ± 0.83^{e}	-12.36 ± 0.22^{c}	26.80 ± 0.80^{e}	332.41 ± 0.61^{ef}	19.36 ± 0.62^{bc}
DhCHS	Sepals	28.19 ± 0.37^{b}	41.54 ± 1.05^{bc}	-19.36 ± 1.10^{d}	45.9 ± 1.16^{bc}	335.04 ± 1.24^{cdef}	16.14 ± 1.17^{cd}
	Petals	25.25 ± 0.24^{bcd}	41.38 ± 0.71^{bc}	-18.16 ± 1.23^{d}	45.27 ± 0.96^{bc}	336.41 ± 1.33^{bcde}	15.37 ± 1.05^{cd}
	Lip	17.34 ± 0.66^{f}	21.19 ± 0.59^{e}	-6.25 ± 0.80^{b}	22.2 ± 0.53^{e}	343.54 ± 2.17^{ab}	14.63 ± 0.69^{cd}
Untreated	Sepals	21.69 ± 0.30^{de}	31.15 ± 1.11^{d}	-9.22 ± 0.57^{bc}	32.49 ± 1.19^{d}	343.60 ± 0.68^{ab}	0.00
	Petals	19.03 ± 0.37^{ef}	30.51 ± 1.11^{d}	-9.63 ± 0.57^{bc}	32.00 ± 1.19^{d}	342.57 ± 0.63^{abc}	0.00
	Lip	12.12 ± 0.70^{g}	8.73 ± 0.41^{f}	-1.28 ± 0.28^{a}	8.92 ± 0.37^{f}	349.16 ± 2.95^{a}	0.00

Means ± SD (n = 3), different letters indicate statistically significant according to One-way ANOVA, Tukey HSD comparison test ($p < 0.05$)

4.8.2 Reduced anthocyanin compounds

Cyanidin-3-glucoside and cyanidin-3-rutinoside are reported as main anthocyanin compounds in magenta or crimson flowers (Gilbert, 1971). Hence, the quantification of these two anthocyanins concentration in the untreated flowers showed a gradual increase in concentration from stage 3 to 6 (Table 4-11).

At stage 6 the lips of open flowers had 1.4-1.5-fold higher concentrations than petals and sepals (Table 4-11). For dsRNA *DhMYB22* treated flowers, cyanidin-3-glucoside was only detected in the lips of flowers at stage 6 and this was at levels 14.2-fold lower than that of lips of untreated flowers. No cyanidin-3-rutinoside was detected in any flower stages after treatment with dsRNA for *DhMYB22* (Table 4-11). *DhMYB60* dsRNA treated flowers also showed negligible to undetectable cyanidin-3-rutinoside at all stages and a 2.0 to 10.9-fold lower cyanidin-3-glucoside concentration compared to untreated flowers (Table 4-11). The dsRNA *DhCHS* treated flowers showed a 2.0-2.5-fold reduction in cyanidin-3-glucoside and 2.4-8.0-fold reduction in cyanidin-3-rutinoside concentration.

Table 4-11: Quantification of two anthocyanin compounds; cyanidin-3-glucoside (C3G) and cyanidin-3-rutinoside (C3R) using LC-MS/MS. Data are mean ± standard deviation (n = 3). Different letters indicate statistical significance according to one-way ANOVA, Tukey HSD comparison test ($p < 0.05$).

Stages	Untreated (Area, counts)	Untreated (µg/ml)	*DhCHS* (Area, counts)	*DhCHS* (µg/ml)	*DhMYB60* (Area, counts)	*DhMYB60* (µg/ml)	*DhMYB22* (Area, counts)	*DhMYB22* (µg/ml)
Cyanidin-3-glucoside (C3G)								
Stage 3	782 ± 1.03 [a]	143 ± 0.57[a]	548 ± 0.95 [a]	67 ± 0.32[a]	421 ± 0.73 [a]	27 ± 0.35[a]	143 ± 0.99 [a]	0 ± 0.00 [a]
Stage 4	823 ± 1.06 [a]	156 ± 0.89[a]	576 ± 1.01 [b]	77 ± 0.64[b]	473 ± 0.49 [b]	43 ± 0.19[b]	212 ± 0.89 [b]	0 ± 0.00 [a]
Stage 5	1010 ± 0.93 [b]	216 ± 0.56[b]	635 ± 0.60 [c]	96 ± 0.47[c]	500 ± 0.38 [c]	52 ± 0.29[c]	226 ± 1.04 [a]	0 ± 0.00 [a]
Sepals	1020 ± 0.89 [b]	218 ± 0.45[b]	670 ± 1.02 [e]	107 ± 0.78[e]	400 ± 0.85 [e]	20 ± 0.45[e]	338 ± 0.93 [a]	0 ± 0.00 [a]
Petals	1060 ± 1.08 [c]	230 ± 0.91[c]	744 ± 0.84 [d]	131 ± 0.52[d]	529 ± 1.10 [d]	61 ± 0.29[d]	309 ± 0.75 [a]	0 ± 0.00 [a]
Lip	1390 ± 0.76 [d]	340 ± 0.67[d]	761 ± 0.58 [d]	136 ± 0.43[d]	542 ± 0.24 [g]	66 ± 0.34[g]	414 ± 1.02 [b]	24 ± 0.19 [b]
Cyanidin-3-rutinoside (C3R)								
Stage 3	578 ± 0.78 [a]	56 ± 0.83[a]	309 ± 1.02 [a]	7 ± 0.25[a]	210 ± 0.87 [a]	0 ± 0.00 [a]	50 ± 1.12 [a]	0 ± 0.00 [a]
Stage 4	588 ± 0.64 [a]	58 ± 0.75[a]	343 ± 0.94 [b]	13 ± 0.21[b]	235 ± 0.59 [a]	0 ± 0.00 [a]	155 ± 1.06 [a]	0 ± 0.00 [a]
Stage 5	698 ± 0.93 [b]	78 ± 0.59[b]	355 ± 0.86 [b]	15 ± 0.32[b]	238 ± 0.79 [a]	0 ± 0.00 [a]	162 ± 0.73 [a]	0 ± 0.00 [a]

Table 4-11 (Continue)

Sepals	718 ± 0.89 [d]	82 ± 0.51[d]	459 ± 1.01 [c]	34 ± 0.29[c]	260 ± 0.96 [a]	0 ± 0.00 [a]	196 ± 0.80 [a]	0 ± 0.00 [a]
Petals	1070 ± 1.02 [c]	147 ± 0.49[c]	445 ± 0.68 [c]	32 ± 0.41[c]	270 ± 1.02 [a]	0 ± 0.00 [a]	183 ± 0.79 [a]	0 ± 0.00 [a]
Lip	1760 ± 0.83 [e]	274 ± 1.09[e]	536 ± 0.95 [a]	49 ± 0.39[a]	282 ± 0.59 [b]	2 ± 0.10[b]	204 ± 0.62 [a]	0 ± 0.00 [a]

4.9 Anthocyanin biosynthesis pathway

To gain insight into the pigment production in *Dendrobium*, the anthocyanin biosynthesis pathway for *Dendrobium* hybrid was reconstructed using the KEGG pathway (map00941: Flavonoid biosynthesis and map00942: Anthocyanin biosynthesis) as a framework (Figure 4-18). The anthocyanin pathway predicted for *Dendrobium catenatum* showed three variants of protein sequence for Phenylalanine ammonia-lyase (PAL), 12 variants of protein sequence of 4-coumarate-CoA ligase (4CL), three variants of protein sequence of Trans-cinnamate 4-monooxygenase (CYP73A), eight variants of protein sequence of Chalcone synthase (CHS), three variants of protein sequence of Chalcone isomerase (CHI), three variants of protein sequence of Flavanone 3-dioxygenase (F3'H), two variants of protein sequence of Flavone 4-reductase (DFR) and one protein sequence for Flavonoid 3',5'-hydroxylase (F3'5'H), Anthocyanidin synthase (ANS) and Anthocyanidin 3-o glucosyltransferase (BZ1) as shown in Table 4-12.

Table 4-12: List of enzymes predicted for anthocyanin pathway in *Dendrobium catenatum* with protein ID and gene name.

Enzymes	Protein ID	Gene name
PAL	PKU66031.1	*Dca009106*
	PKU67212.1	*Dca018706*
	PKU83924.1	*Dca006399*
4CL	PKU59257.1	*Dca021679*
	PKU60627.1	*Dca028287*
	PKU61702.1	*Dca028179*
	PKU69277.1	*Dca002547*
	PKU70137.1	*Dca020627*
	PKU76975.1	*Dca001581*
	PKU76982.1	*Dca001588*
	PKU78544.1	*Dca011101*
	PKU78981.1	*Dca000325*
	PKU79693.1	*Dca010921*
	PKU85016.1	*Dca017185*
	PKU87815.1	*Dca021161*
CYP73A	PKU65157.1	*Dca004773*
	PKU71536.1	*Dca004378*
	PKU81518.1	*Dca007625*
CHS	PKU63580.1	*Dca016721*
	PKU64649.1	*Dca014503*
	PKU71375.1	*Dca004217*
	PKU72004.1	*Dca007368*
	PKU72005.1	*Dca007369*
	PKU78203.1	*Dca012323*
	PKU78204.1	*Dca012324*
	PKU85665.1	*Dca003406*
CHI	PKU61563.1	*Dca015002*
	PKU62518.1	*Dca022190*
	PKU82843.1	*Dca006141*

Table 4-12 (Continue)

F3'H	PKU63605.1	*Dca016746*
	PKU71892.1	*Dca026619*
	PKU79966.1	*Dca025966*
DFR	PKU66109.1	*Dca026354*
	PKU75314.1	*Dca022117*
CYP75A	PKU76391.1	*Dca000994*
ANS	PKU73584.1	*Dca026251*
BZ1	PKU83017.1	*Dca009489*

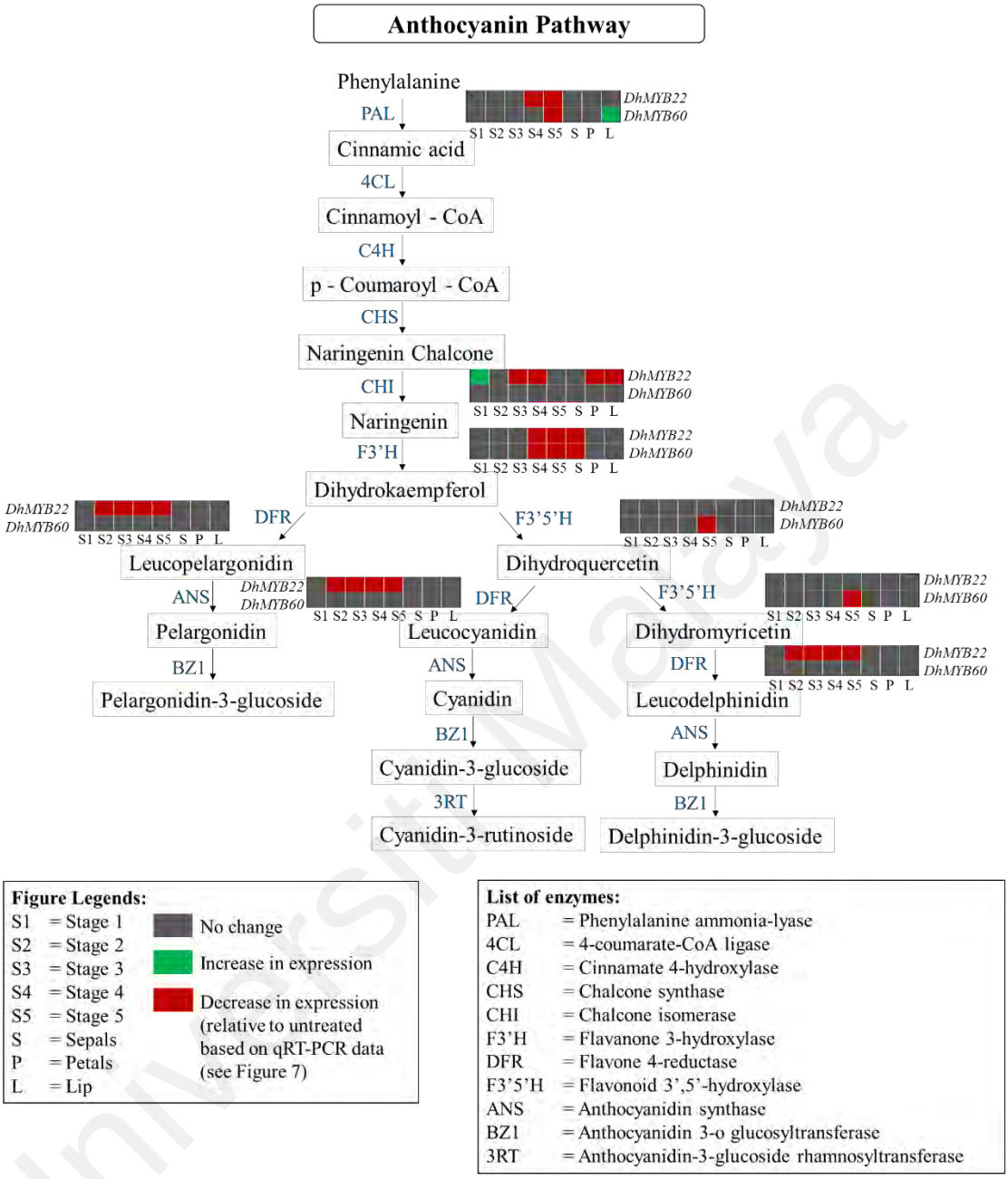

Figure 4-18: Schematic diagram showing relative changes in gene expression in the anthocyanin biosynthesis pathway genes in plants treated with dsRNA of *DhMYB22* and *DhMYB60*. Heat maps on the figure show relative differences in gene expression based on qRT-PCR data between treated and untreated samples.

928

929 **4.10 Silencing of *DhMYB22* resulted in constricted lips, while silencing of**
930 ***DhMYB60* resulted in narrow floral buds and narrow sepals**

931 The flower buds treated with dsRNA of *DhMYB60* showed visible differences in floral
932 organ shape from stage 3 onwards with a distinctly narrow and pointed bud (Figure 4-
933 14). To quantify the shape deviation resulting from the treatments with dsRNA,
934 wireframe graphs (Figure 4-19 and 4-20) were generated from TPS output images from
935 images of flowers at stages 3 to 6. Images from stages 3 to 5 had 11 landmarks, while
936 stage 6 images had 9-15 landmarks (Appendix G). Quantification of Procrustes distance
937 using these landmarks showed that the greatest shape distance was between buds and
938 flowers treated with dsRNA of *DhMYB60*, while the shape distance in those of other
939 treatment, empty vector untreated flowers, most markedly observed at stages 3 and 6
940 (Figure 4-21 and 4-22).

941 Flowers treated with dsRNA of *DhMYB22* and *DhMYB60* showed differences in the
942 lip and sepal shape compared to untreated flowers or empty vector treated flowers (Figure
943 4-21 and 4-22). Flowers treated with empty vector showed no differences in floral organ
944 shape compared to untreated flowers. Other than that, significant differences in floral
945 organ shape were observed between flower treated with *DhMYB22* and *DhMYB60*
946 dsRNA.). Narrow and constricted lips were observed in *DhMYB22* dsRNA treated open
947 flowers with constriction at landmarks 4 and 7 (Figure 4-19 and 4-20). Based on this
948 result, *DhMYB22*, primarily identified as anthocyanin biosynthesis related group
949 (subgroup III), was associated with altered organ shape, which is a function specific to
950 MYB from the MIXTA group (subgroup IV). Hence, a motif analysis was performed,
951 which showed DhMYB22 does not contain a typical MIXTA motif

(AQWESARxxAExRLxRES) but did show the presence of a common motif (H[Q/K]PX4I[I/L]) seen in MIXTA-like MYBs (Appendix I).

The *DhMYB60* dsRNA treated open flowers had relatively narrow sepals, visible at landmarks 1-3, 5-7, 9-11, 14. While the difference in floral organ shape was observed, no significant changes in epidermal cell shape were observed for flowers treated with dsRNA of *DhMYB22* and *DhMYB60* (Figure 4-23). However, cell density of *DhMYB60* dsRNA treated petal and *DhMYB22* dsRNA treated lips were found to be higher compared to untreated flower (Figure 4-23).

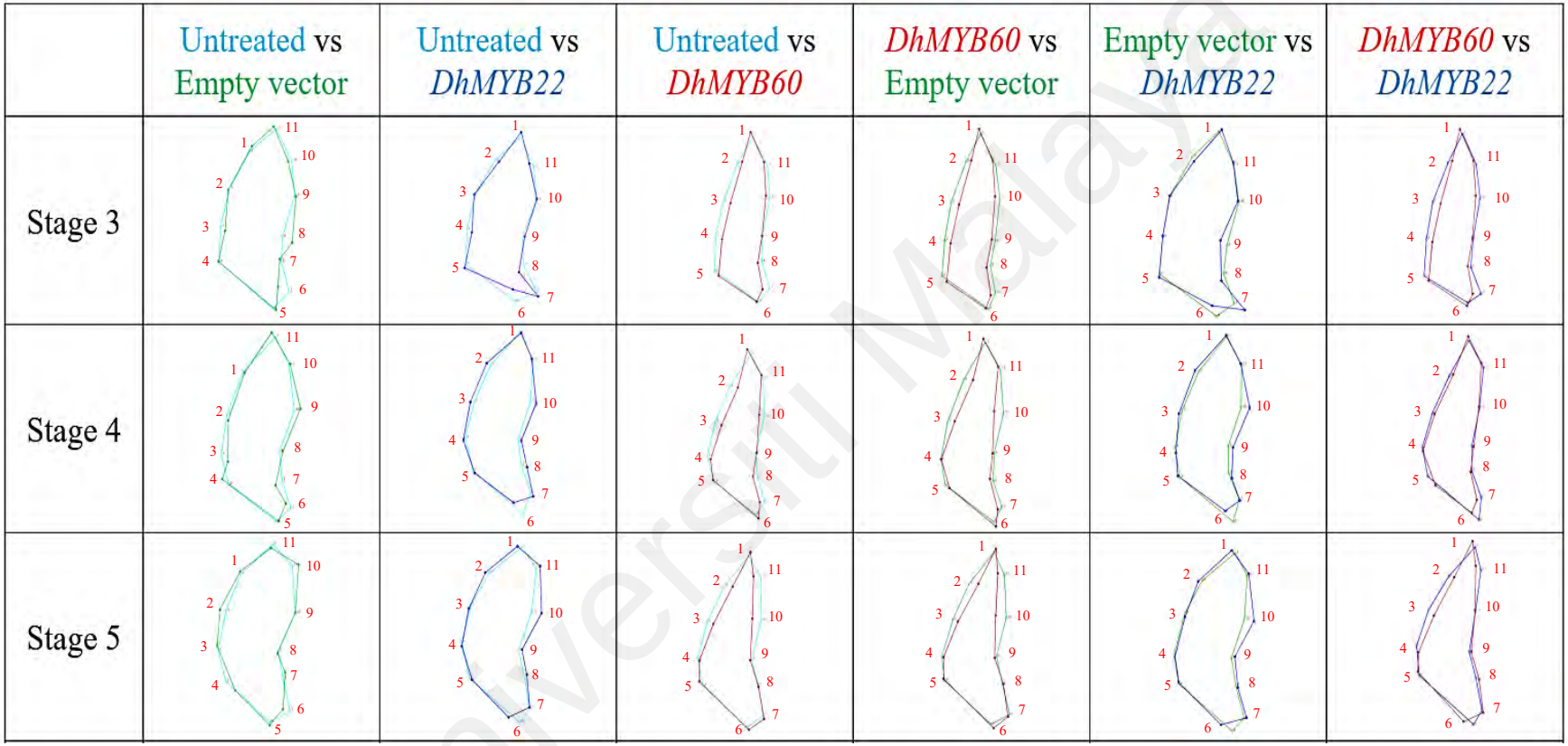

Figure 4-19: Procrustes analysis of changes in floral organ shape between untreated and dsRNA treated flower buds. Images of floral buds at each bud stage from 3 - 5 were pairwise compared: Untreated vs treatment with dsRNA of empty vector; Untreated vs treatment with dsRNA of *DhMYB22*; Untreated vs treatment with dsRNA of *DhMYB60*; Treatment with dsRNA of empty vector vs treatment with dsRNA of *DhMYB60* vs*;* Treatment with dsRNA of empty vector vs treatment with dsRNA of *DhMYB22;* and treatment with dsRNA of *DhMYB60* vs treatment with dsRNA of *DhMYB22* using MorphoJ tool (Klingenberg, 2011). Wireframe graphs where dots indicate the landmarks points and lines indicate the frame of each organ shape.

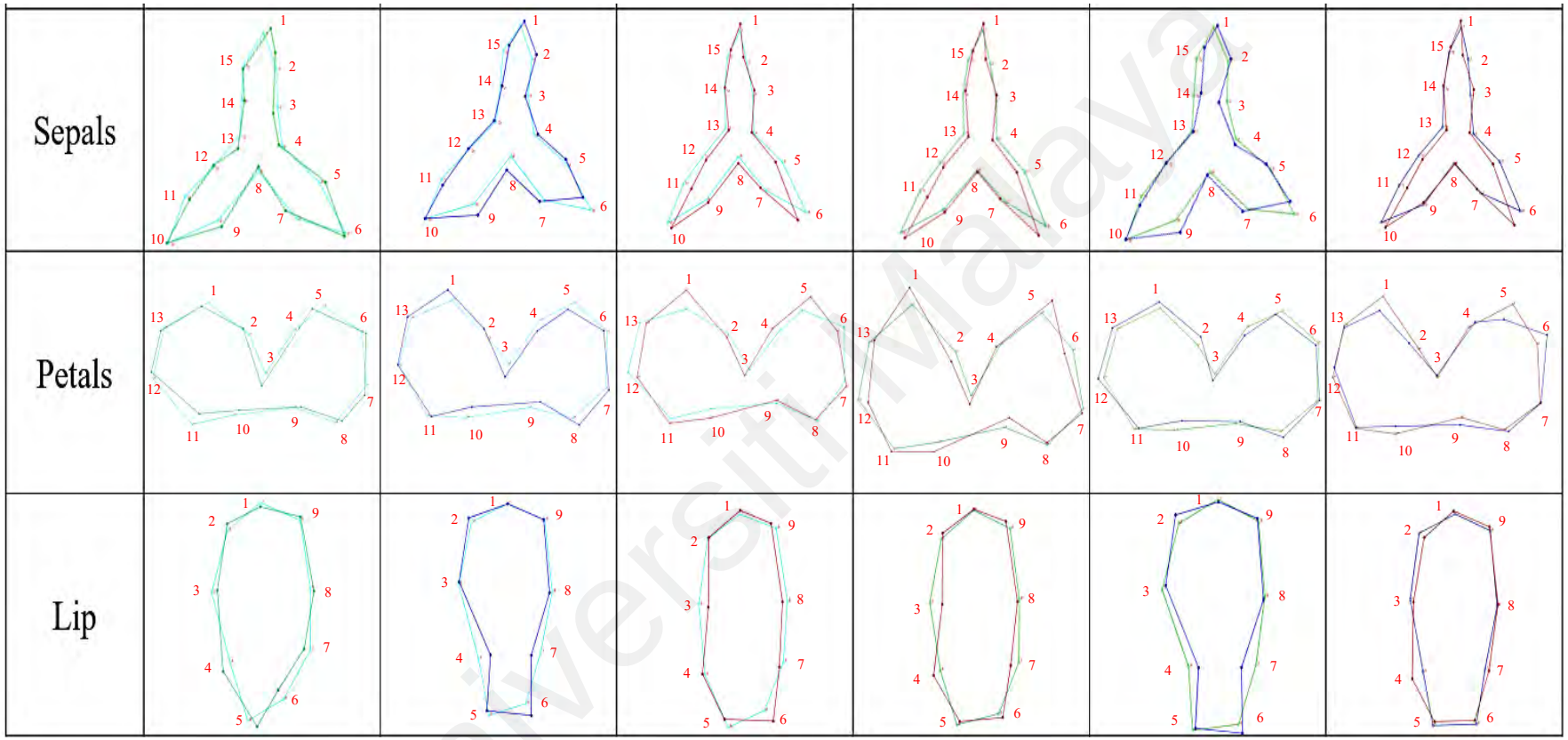

Figure 4-20: Procrustes analysis of changes in floral organ shape between untreated and dsRNA treated flower buds. Images of open flowers (Sepals, Petals and Lip) were pairwise compared: Untreated vs treatment with dsRNA of empty vector; Untreated vs treatment with dsRNA of *DhMYB22*; Untreated vs treatment with dsRNA of *DhMYB60*; Treatment with dsRNA of empty vector vs treatment with dsRNA of *DhMYB60* vs*;* Treatment with dsRNA of empty vector vs treatment with dsRNA of *DhMYB22;* and treatment with dsRNA of *DhMYB60* vs treatment with dsRNA of *DhMYB22* using MorphoJ tool (Klingenberg, 2011). Wireframe graphs where dots indicate the landmarks points and lines indicate the frame of each organ shape.

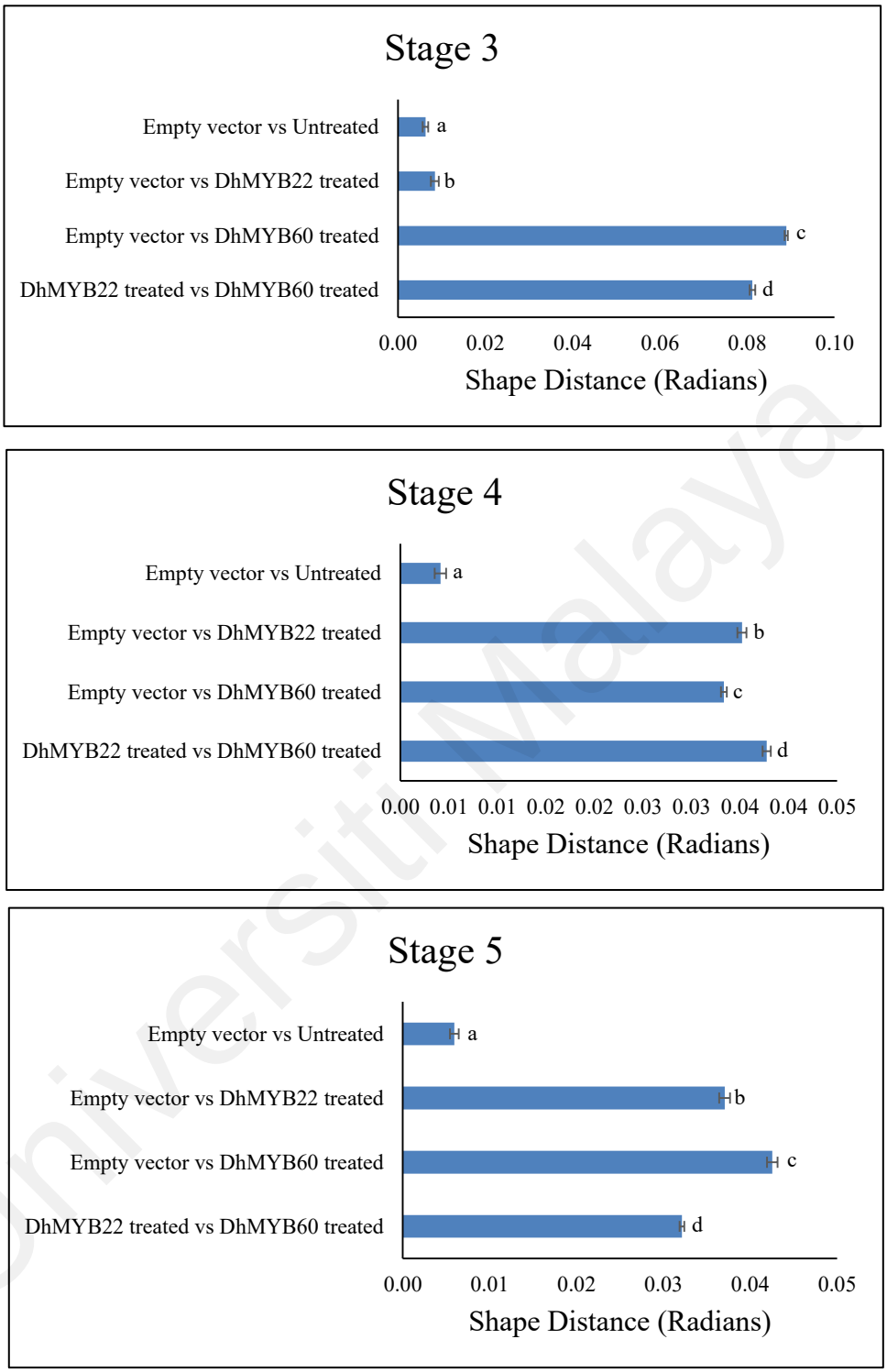

Figure 4-21: Shape distance between untreated and dsRNA treated flower buds. Comparison of floral buds at stages 3- 5 for: Treatment with dsRNA of empty vector vs untreated; Treatment with dsRNA of empty vector vs treatment with dsRNA of *DhMYB22*; Treatment with dsRNA of empty vector vs treatment with dsRNA of *DhMYB60*; and treatment with dsRNA of *DhMYB22* vs treatment with dsRNA of *DhMYB60*. Error bars indicate standard deviations from three biological replicates. Different letters on the top of each bar indicate statistically significant differences (One-way ANOVA, Tukey HSD comparison test $p < 0.05$).

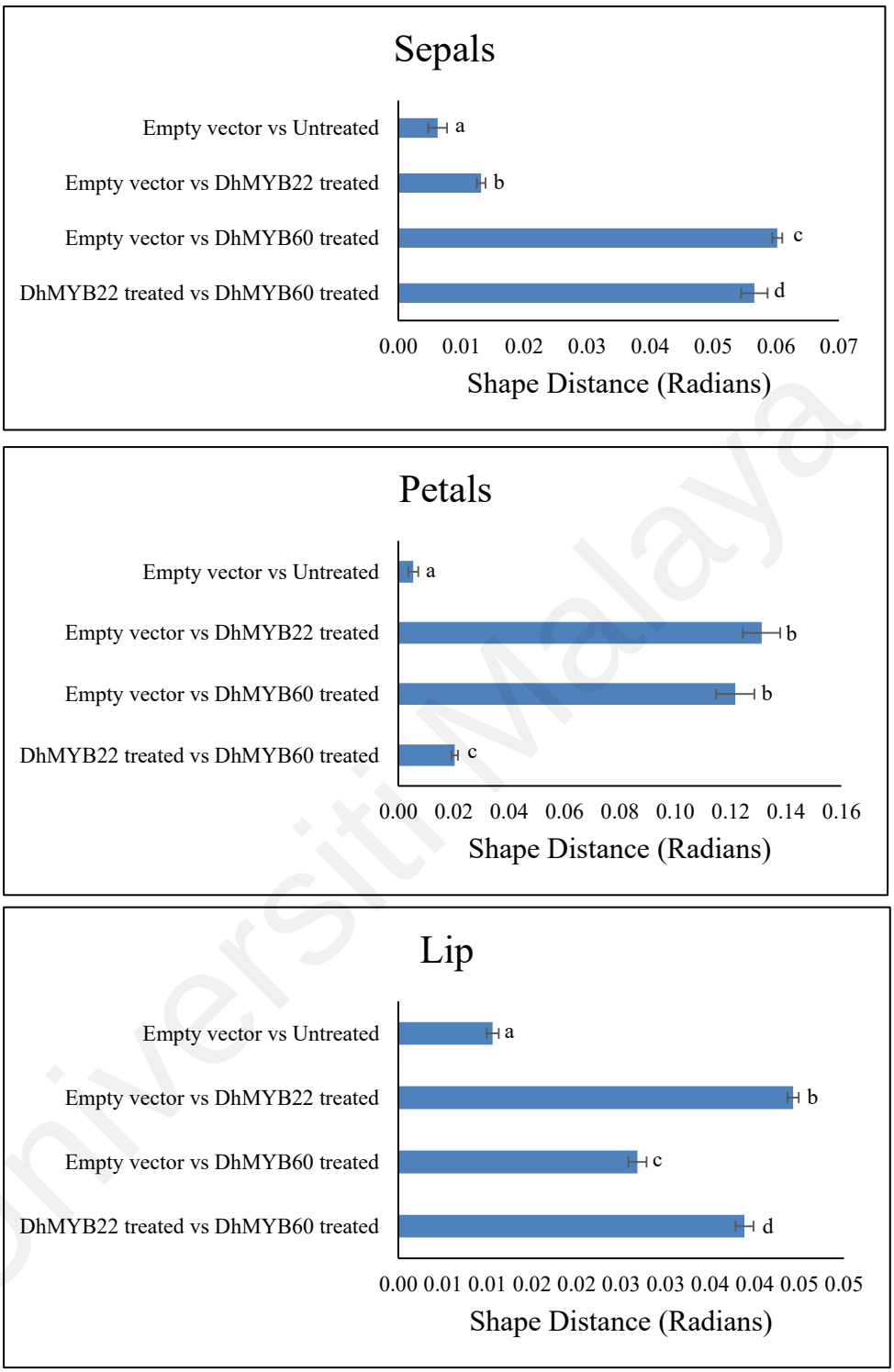

Figure 4-22: Shape distance between untreated and dsRNA treated flower buds. Comparison of open flowers (Sepals, Petals and Lip) for: Treatment with dsRNA of empty vector vs untreayed; Treatment with dsRNA of empty vector vs treatment with dsRNA of *DhMYB22*; Treatment with dsRNA of empty vector vs treatment with dsRNA of *DhMYB60*; and treatment with dsRNA of *DhMYB22* vs treatment with dsRNA of *DhMYB60*. Error bars indicate standard deviations from three biological replicates. Different letters on the top of each bar indicate statistically significant differences (One-way ANOVA, Tukey HSD comparison test $p < 0.05$).

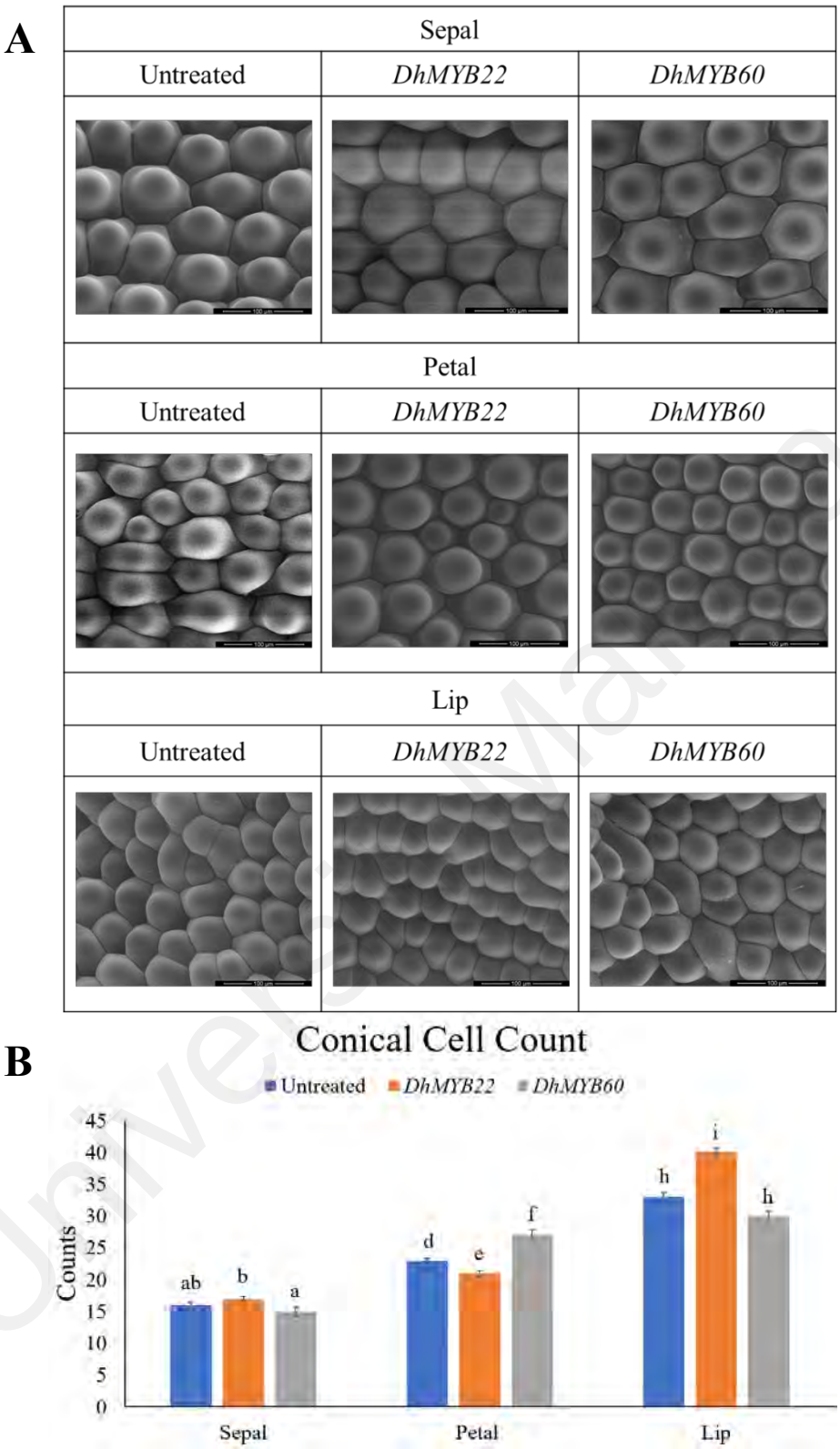

Figure 4-23: A. Field Emission Scanning Electron Microscope images of adaxial epidermal cell shape in sepal, petal, and lip of untreated, *DhMYB22* and *DhMYB60* treated *Dendrobium* hybrid. **B.** Density of conical cells in sepal, petal, and lip of untreated, *DhMYB22* and *DhMYB60* treated *Dendrobium* hybrid. Different letters indicate statistical significance according to one-way ANOVA, Tukey HSD comparison test ($p < 0.05$).

4.11 Expression of anthocyanin biosynthesis pathway genes of *DhMYB22* and *DhMYB60* treated *Dendrobium* hybrid

To investigate the effect of *DhMYB22* and *DhMYB60* dsRNA treatment on expression of anthocyanin biosynthesis pathway genes (Figure 4-20), transcript accumulation was quantified using qRT-PCR (Figure 4-21, 4-22, 4-23, 4-24, 4-25). At stage 1, there was no reduction in gene expression for either treatment, however there was a 1.09-fold increase in expression of *Chalcone isomerase* (*CHI*) for the *DhMYB22*-treated flower bud (Figure 4-24). At stages 2 to 5, *DhMYB22* dsRNA treatment resulted in significantly lower expression of the *Dihydroflavonol 4-reductase* (*DFR*) gene (Stage 2: 1.8-fold; Stage 3: 1.6-fold, Stage 4 and 5: 2.0-fold); *Chalcone isomerase* (*CHI*) gene (Stage 3: 1.3-fold and Stage 4: 1.3-fold) (Figure 4-24). *Phenylalanine ammonia-lyase* (*PAL)* gene (Stage 4: 1.3-fold and stage 5: 1.8-fold) and *Flavanone 3-hydroxylase* (*F3'H*) gene (Stage 4: 1.7-fold; Stage 5: 1.4-fold) (Figure 4-24). Treatment with dsRNA of *DhMYB22* dsRNA also resulted in significantly lower expression of *CHI* in flower petals (2.0-fold) and lip (2.2-fold) and of *Flavanone 3-hydroxylase* (*F3'H*) gene in sepals (1.2-fold) (Figure 4-24). Treatment with dsRNA of *DhMYB60* dsRNA resulted in significantly lower expression in flowers only at stages 4 and later, including *F3'H* gene (Stage 4: 1.3-fold; Stage 5: 2.2-fold and sepals 2.3-fold) ; *PAL* gene (Stage 5: 1.3- fold) and *Flavonoid 3',5'-hydroxylase* (*F3'5'H*) gene (Stage 5: 1.9-fold) (Figure 4-24).

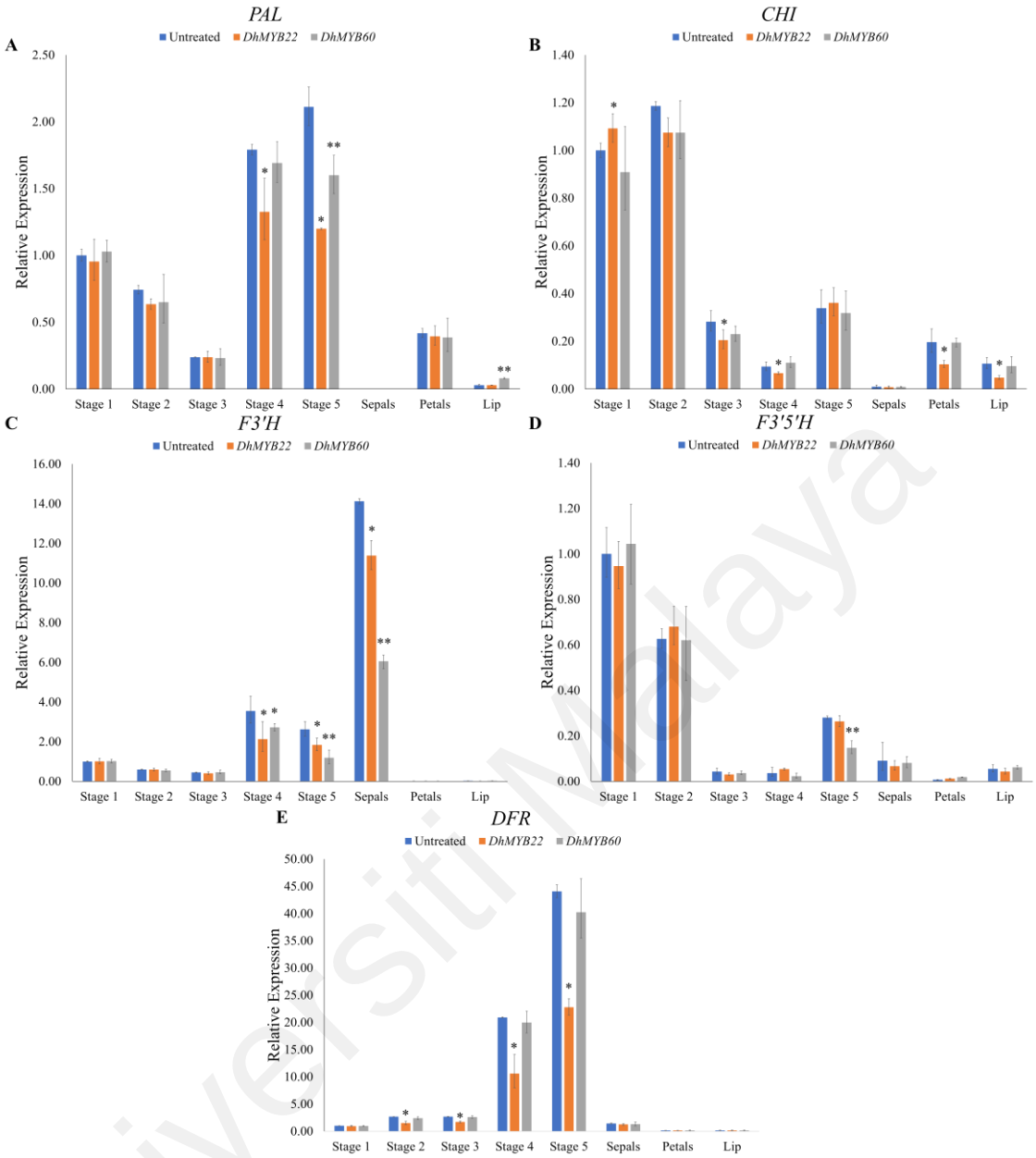

Figure 4-24: Expression of *PAL*, *CHI*, *F3'H*, *F3'5'H* and *DFR* in untreated, *DhMYB22* dsRNA-treated and *DhMYB60* dsRNA-treated *Dendrobium* floral buds and open flower parts using qRT–PCR. Error bars indicate standard deviations from three biological replicates. Different numbers of asterisks indicate statistically significant differences (oneway ANOVA, Tukey HSD comparison test, $P < 0.05$). **A.** Expression of *PAL* in untreated flowers and flowers treated with dsRNA of *DhMYB22* and *DhMYB60*. Relative mRNA abundance of *PAL* was normalized with respect to the reference gene, β-actin. Expression of untreated bud cDNA at stage 1 was set to a value of 1.0 and subsequently expression levels for the other stages of untreated samples (stage 2–5 buds and organs of open flower) and samples treated with dsRNA of *DhMYB22* or *DhMYB60* (stage 1–5 buds and organs of open flower) are reported relative to this number. **B.** Expression of *CHI* in untreated flowers and flowers treated with dsRNA of *DhMYB22* and *DhMYB60*. Relative mRNA abundance of *CHI* was normalized with respect to the reference gene, β-actin. Expression of untreated bud cDNA at stage 1 was set to a value of 1.0 and subsequently expression levels for the other stages of untreated samples (stage 2–5 buds and organs of open flower) and samples treated with dsRNA of

DhMYB22 or *DhMYB60* (stage 1–5 buds and organs of open flower) are reported relative to this number. **C.** Expression of *F3'H* in untreated flowers and flowers treated with dsRNA of *DhMYB22* and *DhMYB60.* Relative mRNA abundance of *F3'H* was normalized with respect to the reference gene, β-actin. Expression of untreated bud cDNA at stage 1 was set to a value of 1.0 and subsequently expression levels for the other stages of untreated samples (stage 2–5 buds and organs of open flower) and samples treated with dsRNA of *DhMYB22* or *DhMYB60* (stage 1–5 buds and organs of open flower) are reported relative to this number. **D.** Expression of *F3'5'H* in untreated flowers and flowers treated with dsRNA of *DhMYB22* and *DhMYB60.* Relative mRNA abundance of *F3'5'H* was normalized with respect to the reference gene, β-actin. Expression of untreated bud cDNA at stage 1 was set to a value of 1.0 and subsequently expression levels for the other stages of untreated samples (stage 2–5 buds and organs of open flower) and samples treated with dsRNA of *DhMYB22* and *DhMYB60* (stage 1–5 buds and organs of open flower) are reported relative to this number. **E.** Expression of *DFR* in untreated flowers and flowers treated with dsRNA of *DhMYB22* and *DhMYB60.* Relative mRNA abundance of *DFR* was normalized with respect to the reference gene, β-actin. Expression of untreated bud cDNA at stage 1 was set to a value of 1.0 and subsequently expression levels for the other stages of untreated samples (stage 2–5 buds and organs of open flower) and samples treated with dsRNA of *DhMYB22* or *DhMYB60* (stage 1–5 buds and organs of open flower) are reported relative to this number.

979

CHAPTER 5: DISCUSSION

Orchids have a great commercial value as cut flowers and potted plants, but there is a market demand for novel flower colours and shapes. The processes involved in breeding orchids are quite time consuming. Biotechnology methods *via* transformation are also slow, and there is a lack of information over which genes affect flowers most. The specific objectives are; to optimise the isolation of RNA from *Dendrobium* hybrid floral tissue, to identify and select two candidate *R2R3-MYB* genes related to flower colour and/or shape, to investigate the temporal and stage-specific expression of two selected *R2R3-MYB* genes related to flower colour and/or shape in different development stages of *Dendrobium* flower buds, to prepare dsRNA expression constructs for the knockdown of two selected *R2R3-MYB* genes, to determine the role of the two selected *R2R3-MYB* genes on flower development *via* quantification of phenotypic changes, biochemical assays and expression analysis (qRT-PCR assay) of plants with knocked-down expression.

5.1 High-quality RNA isolation from pigment-rich *Dendrobium* flowers

Dendrobium flowers contain high levels of protein, carbohydrates and secondary metabolites, including flavonoids, pigments, and polyphenols (Moretti et al., 2013). Obtaining pure RNA with high yield from such tissues is a cumbersome process as polysaccharides and polyphenols have similar chemical properties to RNA and tend to co-precipitate with RNA (Asif et al., 2006; Shu et al., 2014). The co-precipitation of these compounds with RNA reduces yield and increases the possibility of rapid degradation, making the sample unsuitable for further downstream processing. The current study has optimised an efficient RNA isolation method for mature flowers of *Dendrobium* hybrids.

Four previously published methods for secondary metabolite-rich tissues; three CTAB-based RNA isolation methods (Methods 1, 2, and 4) and one SDS-based method

(Method 3) were tested and found to be inadequate to produce high-quality RNA from the pigment, polyphenol, and polysaccharide-rich tissue of *Dendrobium* hybrid flowers. The main challenge in extracting RNA from mature flowers is the viscous tissue homogenate that results from mixing ground tissue with extraction buffer. When the sample was ground and mixed with buffer was inefficient, centrifugation of the RNA-containing supernatant could be recovered by centrifugation. The optimal sample-to-buffer ratio for nucleic acid extraction varies by species and tissue type, resulting in a viscous but well-dispersed homogenate (Murray and Thompson 1980). It is observed that increasing the sample–buffer ratio used in the early step of extraction (Table 4-3 and Table 4-4) almost increase the efficiency of mixing the sample with buffer and recovering the RNA containing supernatant.

Another obstacle that needed to be overcome was extracting the pigments from the intensely coloured flower tissues. Method 1, Method 2, and Method 4 did not successfully remove pigment during the extraction process, resulting in the aqueous phase being a deep purple colour (Figure 4-2 and Figure 4-3). Method 3, which uses a mixture of SDS and TRIzol reagent that includes an extraction stage using phenol, chloroform, and isoamyl alcohol was shown to remove pigments more effectively than the previous methods. The improved removal of pigment was likely because of the presence of phenol in the TRIzol reagent which have ability to denature proteins (Chomczynski and Sacchi 1987), in addition to the high phenol proportion in the P:C:I extraction included in this method. To further improve the separation of RNA from pigments and other superfluous cell materials, a P:C:I (125:24:1) solution was added for the purification step prior to the two rounds of C:I extraction in which the proportion of phenol was relatively high. Phenol and chloroform are widely reported to extract high-quality RNA (Li 2015; Lee et al., 2015; Toni et al., 2018).

It was difficult to recover high-quality RNA from flower tissues using Methods 1, 3, and 4. The insoluble gel-like pellets (Figure 4-3) indicated inefficient contaminant separation from RNA (Muoki et al., 2012). To address this, the buffer's concentrations of NaCl (3 M), PVP-10 (3 %), and ß-mercaptoethanol (3 %) were increased based on Method 1, Method 2, Method 3 and Method 4. The higher NaCl concentration in the extraction buffer promotes the salting-out of the protein while keeping RNA in solution (El-Ashram et al., 2016). A higher NaCl content also helps avoid polysaccharide-RNA co-precipitation (Fang et al., 1992). Precipitation from aqueous solution was improved by increasing the PVP-10 concentration to 3%. (Carpenter et al., 1976). The relatively high concentration of β-mercaptoethanol in the modified extraction buffer (compared to Method 1, Method 2 and Method 3) removed polyphenol compounds more effectively (Wong et al., 2014) and inactivated ribonucleases released during cell lysis (Lehninger et al., 2005).

In order to maximise RNA yield, several incubation periods were tested in the extraction buffer. Lower RNA recovery and protein contamination occurred with short incubation durations from mature flowers of *Dendrobium* hybrids. An incubation time of 45 min resulted in a higher yield and good quality of RNA. The use of isopropanol in Methods 1 and 3 may contribute for low pellet solubility because isopropanol promotes the co-precipitation of salts (Choi et al., 2018). It is also difficult to completely remove isopropanol from samples because of its low volatility, compared to ethanol, which further deteriorates the quality of RNA (Surzycki 2012). The optimised CTAB method produced a soluble pellet that enabled significant RNA recovery in the final aqueous solution after precipitation with LiCl. An advantage of using LiCl for RNA recovery is that it does not efficiently co-precipitate protein, DNA, polysaccharide, or salts (Barman et al., 2017). Extraction of RNA from mature flowers of four different *Dendrobium*

hybrids with the optimised method resulted in high yields and significantly higher RNA quality, demonstrating the improved method's efficiency and reproducibility (Figure 4-7). Floral bud (Stage 1: 0-0.5 cm; Stage 2: 0.51-1.0 cm; Stage 3: 1.1-2.0 cm; Stage 4: 2.1-3.0 cm and Stage 5: 3.1-4.0 cm) does not contain high amount in polysaccharides and phenolic compounds compared with mature flower (Stage 6), thus the optimised method able to isolate high-quality RNA.

5.2 Functional prediction of *DhMYB22* and *DhMYB60* in flower development in *Dendrobium* hybrid

Dendrobiums belong to a genus of tropical orchids bearing flowers with diverse pigmentation patterns and shapes (Li et al., 2017). The *Dendrobium* hybrid (*Dendrobium* Burmese Ruby × *Dendrobium* Mae-Klong River) used in this study is a popular hybrid with dark magenta flowers (Figure 4-14). Although some data on structural genes involved in pigment synthesis in *Dendrobium* orchids are available, there is not much is known about the genes that regulate flower colour and shape development. Among MYB family transcription factors, *DhMYB2* has been shown to work in tandem with *DhbHLH1* to regulate anthocyanin synthesis during floral development (Petroni & Tonelli, 2011; Xu et al., 2015) and *DhMYB1* influences the development of conical cell shape in floral epidermal cells (Lau et al., 2015).

In this investigation, 60 *R2R3-MYB* genes with the consensus sequence of ppspW*p-EcpbLbphlppaG.....ppWspItppls.....sR*sppscp+appb bpp were identified within the only published genome for this genus, that of *Dendrobium catenatum* (Appendix A). With 60 genes, the *R2R3-MYB* gene family in *Dendrobium catenatum* is smaller than those reported for *Phalaenopsis equestris* (115), *Dendrobium officinale* (117) (He et al., 2019) and *Cattleya* hybrid 'KOVA' (65) (Li et al., 2020) but is larger than that of *Dendrobium* hybrid Woo Leng (21 R2R3-MYB genes) (Wu et al., 2003). From the ten R2R3-MYB

were associated with the regulation of flower pigmentation pattern and shape, based on homology with orthologues reported for other flower species (Figure 4-1, Table 4-1), *DhMYB22* was chosen for further functional characterisation as this gene clustered with orthologues associated with anthocyanin-related MYB. At the same time, *DhMYB60* was selected as this gene clustered with orthologues associated with MIXTA-like functions which are involved in cell and organ shape development (Noda et al., 1994).

5.3 Validation of function of *DhMYB22* and *DhMYB60* in *Dendrobium* hybrid

The expression of *DhMYB22* and *DhMYB60* during flower development were found to be stage- and organ-specific (Section 4.9, Figure 4-15). *DhMYB1* is expressed throughout flower bud development and is involved in the development of the conical cell shape of the epidermal cells of the *Dendrobium* hybrida (*Dendrobium* 'Bobby Messina' × *Dendrobium* 'Chao Phraya') flower labellum (Lau et al., 2015). Chiou & Yeh (2008) revealed that *OgMYB1* was actively expressed during floral development but not expressed in yellow lip tissue of *Oncidium* Gower Ramsey flowers. Both *DhMYB1* and *OgMYB1* show the temporal and spatial specific expression and an association with flower phenotype, further strengthening the reliability of the orthologous predicted function of *DhMYB22* and *DhMYB60* in *Dendrobium* hybrid (Figure 4-1).

Validation of the predicted floral regulatory functions of *DhMYB22* and *DhMYB60* was based on the direct application of sequence-specific exogenous dsRNA to reduce the expression of these genes. The use of exogenously applied dsRNA for RNA silencing is faster than transgenic or gene editing approaches and has been successfully applied to protect against viral infection in a *Brassolaeliocattleya* hybrid (Lau et al., 2014) and for a loss of gene function study in *Dendrobium* (Lau et al., 2015). The direct application of dsRNA of *DhMYB22* and *DhMYB60* on flower buds was associated with a significant reduction in the targeted transcripts compared to their expression in untreated buds and

open flowers (Figure 4-15), indicating successful gene knockdown using this direct application approach. It was notable that while the knockdown of expression of *DhCHS*, an essential gene for flower pigment synthesis, was evident in altered colour phenotype (Figure 4-14), the reduction in flower colour was much less than previously reported for co-suppressed gene silencing by transient transgenic expression of *chalcone synthase* in *Petunia* (Napoli et al., 1990) but was however similar to the moderate levels of suppression seen by expression of a hairpin RNA to silence *Chalcone synthase* in *Dendrobium* Sonia 'Earsakul' (Ratanasut et al., 2015). The moderate level of suppression is mainly because, based on bioinformatic prediction, the dsRNA sequence used in these experiments likely only silences a minor proportion of the total *CHS* mRNA, having a strong sequence match to only one of the eight predicted *CHS* loci in the *Dendrobium catenatum* genome (Section 4.4, Table 4-9). However, it is still unclear whether the other *CHS* loci are expressed in flowers. Watanabe et al. (2017) previously targeted the *dihydroflavonol-4-reductase-B* (*DFR-B*) gene, which encodes an anthocyanin biosynthetic enzyme, and found variations in stem colour during the early phase of plant tissue culture. About 75 percent of transgenic plants produced anthocyanin-free white flowers due to the biallelic alterations in the Cas9 cleavage site in *DFR-B* by a single base insertion or deletion of more than two bases. Thus, for future studies, and with better genome annotation for *Dendrobium* species and hybrids, structural genes with low or single gene copy number in the genome, such as homologues of *DFR* and *anthocyanidin synthase* (*ANS*), maybe more robust controls for gene silencing towards producing paler, or even white flowers.

5.4 Roles of *DhMYB22* and *DhMYB60* in anthocyanin production

The roles of *DhMYB22* and *DhMYB60* in anthocyanin production in *Dendrobium* was supported by the less intense colour (lower pigment levels) of dsRNA *DhMYB22* and

DhMYB60 treated flowers (Figure 4-14 and 4-16), suppression of anthocyanin biosynthesis genes, (Figure 4-24), and lower total anthocyanin contents (Figure 4-17, Table 4-12) when compared with untreated flowers. While floral organ specific expression was not apparent for *DhMYB22*, expression of *DhMYB60* was lowest in petals and highest in lips, which coincided with the anthocyanin levels (Figure 4-17, Table 4-12) and colour intensities of these floral organs (Table 4-11, Appendix H).

Such distinct regulation in pigmentation patterns between flower parts was also reported for *PeMYBs* in *Phalaenopsis* spp (Hsu et al., 2015) and *LhMYB* in Asiatic hybrid lily (Yamagishi et al., 2010) and indicated a role for *DhMYB22* in regulating floral organ-specific pigmentation. Based on the expression of anthocyanin biosynthesis genes, it can be suggested that the knockdown of *DhMYB22* led to the reduction of DFR levels at stages 2-5, lower F3'H levels at stages 4 and 5 and in sepals, and lower levels of PAL, CHI and F3'H (Figure 4-24). Similarly, the gene expression data supports the idea that knockdown of *DhMYB60* could result in reduced levels of PAL, F3'H, F3'5'H at stage 5 and F3'H in sepals (Figure 4-24).

Although *DhMYB60* encodes a MIXTA-like MYB, which is reported to have a function in regulating cell and organ shape development (Noda et al., 1994), its knockdown was associated with a reduction in anthocyanin levels. A reduction in the expression of related genes (F3′H and F3′5′H) (Figure 4-24) and a visible difference in the intensity of the flower colour (Figure 4-16 and 4-17, Table 4-12). A combination of phylogenetic and bioinformatics tools has previously been used to identify a flower colour-associated MYB (Gates et al., 2018), and this approach showed that, based on local alignment using BLAST, *MYB* genes might be most similar to those from different functional groups. This is likely a consequence of rapid evolution resulting in multiple gene duplications and the neofunctionalization that is characteristic of this large gene

family (Jiang and Rao, 2020; Wheeler et al., 2022). Examples of MIXTA-like R2R3-MYBs (*PaMYB9A1* and *PaMYB9A2*, also known as *PaMYB9A1/2*) evolving additional functions have also been reported recently in *Phalaenopsis* orchid (Lu et al., 2022). They showed that *PaMYB9A1/2* functions to coordinate conical epidermal cell development and cuticular wax biosynthesis (Lu et al., 2022). In the case of *Dendrobium*, the results suggest that *DhMYB22* and *DhMYB60* have functions characteristic of both the anthocyanin-related and MIXTA-like R2R3-MYB, but also it is likely that their influence on flower shape and colour are related, but possibly not the major regulators for these anthocyanin biosynthesis pathways.

5.5 Roles of *DhMYB22* and *DhMYB60* in flower bud and floral organ shape

In addition to regulating flower colour development, changes in flower bud and floral organ shapes after gene silencing with dsRNA of *DhMYB22* and dsRNA of *DhMYB60* (Figure 4-14, 4-15) provide an additional role for each of these transcription factors in flower shape development. In the case of DhMYB22, the difference in colour in the lip (Figure 4-16) was not as marked as the reduction in gene expression (Figure 4-15), which suggests that other factors are in play in the regulation of the anthocyanin biosynthetic pathway in this floral organ. Interestingly, DhMYB22 knockdown showed an association with altered organ shape, with notable constriction of the lip (Figure 4-14), the organ showing the greatest reduction in *DhMYB22* RNA. Generally, MIXTA-like MYBs are known for their role in cell and organ shape development (Noda et al., 1994). Although analysis of the DhMYB22 amino acid sequence did not show the presence of a typical MIXTA motif, the motif H[Q/K]PX4I[I/L], seen in MIXTA-like MYBs (subgroup IV), was present in DhMYB22 and DhMYB2. Hence, further study by swapping or deletion of this motif may be useful to further explore its role in influencing organ shape.

Based on sequence homology (Figure 4-1, Table 4-1), *DhMYB60* is an orthologue of MIXTA-like group R2R3-MYB transcription factors that have previously been reported to influence cell shape, but not floral organ shape in *Dendrobium* (*DhMYB1*, Lau et al., 2015) and both cell and floral organ shape in *Petunia* (*PhMYB1*, Baumann et al., 2007). In *Petunia* (Baumann et al., 2007) and more recently in *Arabidopsis* (Hong et al., 2016), differences in floral organ shape were associated with changes in cell shape and cell numbers. Baumann et al. (2007) describe the phenotypic analysis of a *phmyb1* mutant and confirm the role of *PhMYB1* in controlling cell morphogenesis in the petal epidermis. Hong et al. (2016) used a genetic screen to find mutants that have irregular sepal shapes. They found that a mutation in the *variable organ size and shape 1* (*vos1*) gene causes the sepals to have variable sizes and shapes. They found that the mutation reduces the variability of cell growth among neighbouring cells and disrupts the spatiotemporal averaging of cell growth. Besides, Hong et al. (2016) showed that reactive oxygen species (ROS) play a role in regulating the spatiotemporal averaging of cell growth. ROS levels increase during sepal maturation, which coincides with the decrease of cellular variability and the increase of sepal uniformity.

The change in floral organ shape (Figure 4-14) but not epidermal shape resulting from dsRNA treatments with *DhMYB22* and *DhMYB60* (Figure 4-23), show that regulation of floral epidermal cell shape and floral organ shape may be independent of one another, or that at least this is the case in *Dendrobium*. The narrowed lips resulting from the silencing of *DhMYB22* and the narrowed petals resulting from the silencing of *DhMYB60* may be due to changes in cell number or in other cell layers of the floral organ tissue. Indeed, these tissues showed comparatively higher conical cell density in the epidermis of dsRNA-treated organs compared with those of untreated flowers (Figure 4-23). A possible way to further study this topic is to examine the relationship between reactive

oxygen species (ROS) and the silencing effect of DhMYB60 on cell growth. Hong et al. (2016) demonstrated that ROS are involved in regulating the spatiotemporal pattern of cell growth. They found that ROS levels increased during sepal maturation, which corresponded to the decrease of cell variability and the increase of sepal uniformity. However, to support this hypothesis, more robust data would be required from a comprehensive analysis of cross-sectioned samples.

CHAPTER 6: CONCLUSION

DhMYB22 and *DhMYB60* are differentially expressed at different stages of flower bud development in *Dendrobium* hybrid (*Dendrobium* Burmese Ruby × *Dendrobium* Mae-Klong River). Silencing of *DhMYB22* with dsRNA showed this R2R3-MYB to have roles in anthocyanin production and pigmentation of petals. *DhMYB22*, despite not showing typical MIXTA-like MYB motifs, was also associated with shape development of the floral labellum, though without an apparent influence on epidermal cell shape. The role of the MIXTA-like *DhMYB60* in *Dendrobium* flowers is regulation of shape development of sepals, likely by modifying cell number. However, the silencing of *DhMYB60* was also associated with lower anthocyanin production and flower pigmentation. Reduction of the total anthocyanin content and of *PAL* and *F3'H* gene expression in *DhMYB22* and *DhMYB60* treated flowers, indicate that both *DhMYB22* and *DhMYB60* regulate anthocyanin production.

Future study

Identification of *DhMYB22* and *DhMYB60* in regulating pigment intensity and floral organ shape in *Dendrobium* hybrid would be an interesting topic for further study and determining the gene targets of these R2R3-MYB transcription factors and by manipulation using exogenously dsRNA could be useful for altered floral shapes and colours of *Dendrobium* in the future. In addition, experimental validation of other MYBs (Anthocyanin-related MYBs: *Dca003829*, *Dca010364* and *Dca010713*; MIXTA-like: *Dca004957*) predicted in this study to have a role in floral colour and shape (Figure 4-1 and Table 4-1) can help to establish a deep understanding on the functions of different groups and members of this rapidly evolved transcription factor family. It is also interesting to observe the effect of silencing the transcriptional repressor of anthocyanin, which has been functionally predicted based on orthologous R2R3-MYB's (*Dca016612*,

Dca018213, *Dca019113* and *Dca019872*). Conducting an expansion or detailed study into the investigation of regulatory factors associated with flower colour in *Dendrobium* would be the one of the ways to gain a comprehensive understanding of the flower colour. It is acknowledged that while a phylogenetic approach has helped us to identify specific family members with essential roles in floral colour and shape regulation, due to possible duplication events and switches in functional roles are seen in plant MYB family evolution (Gates et al., 2018), there are very likely additional candidates not identified by this analysis. Bulk transcriptome sequencing from the phenotypic pool and association mapping provides an alternative strategy for systematically isolating genes controlling relative complex traits by association analysis which can further establish a broader view of the genetic basis of specific floral shapes and colour traits.

REFERENCES

Abu Dardak, R., Ahmad, A. A., Nik Mohamad Masdek, N., Muhammad, R. M., Ahmad, H. (2020). Producer's Perspective on the Potential of Malaysia's Floriculture Industry. Retrieved August 26, 2020, from https://ap.fftc.org.tw/article/1924

Aharoni, A., De Vos, C. R., Wein, M., Sun, Z., Greco, R., Kroon, A., ... & O'Connell, A. P. (2001). The strawberry FaMYB1 transcription factor suppresses anthocyanin and flavonol accumulation in transgenic tobacco. *The Plant Journal*, *28*(3), 319-332.

An, C., Saha, S., Jenkins, J. N., Ma, D.-P., Scheffler, B. E., Kohel, R. J., . . . Stelly, D. M. (2008). Cotton (*Gossypium* spp.) R2R3-MYB transcription factors SNP identification, phylogenomic characterization, chromosome localization, and linkage mapping. *Theoretical and Applied Genetics, 116*(7), 1015-1026. doi:10.1007/s00122-008-0732-4

Andrade, E. D., & Hunter, W. B. (2016). RNA interference–natural gene-based technology for highly specific pest control (HiSPeC). *RNA interference*, 391-409.

Asif, M., Trivedi, P., Solomos, T., & Tucker, M. (2006). Isolation of high-quality RNA from apple (*Malus domestica*) fruit. *Journal of agricultural and food chemistry*, *54*(15), 5227-5229.

Avila, J., Nieto, C., Cañas, L., Benito, M. J., & Paz- Ares, J. (1993). *Petunia hybrida* genes related to the maize regulatory *C1* gene and to animal myb proto-oncogenes. *The Plant Journal*, *3*(4), 553-562.

Azuma, A., Kobayashi, S., Yakushui, H., Yamada, M., Mitani, N., & Sato, A. (2007). *VvmybA1* genotype determines grape skin color. *VITIS-GEILWEILERHOF-*, *46*(3), 154.

Ban, Y., Honda, C., Hatsuyama, Y., Igarashi, M., Bessho, H., & Moriguchi, T. (2007). Isolation and functional analysis of a MYB transcription factor gene that is a key regulator for the development of red coloration in apple skin. *Plant and cell physiology*, *48*(7), 958-970.

Barman, P., Choudhary, A. K., & Geeta, R. J. B. (2017). A modified protocol yields high-quality RNA from highly mucilaginous *Dioscorea* tubers. *3 Biotech*, 7(2), 150.

Baulcombe, D. (2004). RNA silencing in plants. *Nature, 431*(7006), 356-363. doi:10.1038/nature02874

Baumann, K., Perez-Rodriguez, M., Bradley, D., Venail, J., Bailey, P., Jin, H., . . . Martin, C. (2007). Control of cell and petal morphogenesis by R2R3 MYB transcription factors. *Development, 134*(9), 1691. doi:10.1242/dev.02836

Berger, B. A., Ricigliano, V. A., Savriama, Y., Lim, A., Thompson, V., & Howarth, D. G. (2017). Geometric morphometrics reveals shifts in flower shape symmetry and size following gene knockdown of *CYCLOIDEA* and *ANTHOCYANIDIN SYNTHASE*. *BMC plant biology*, *17*(1), 1-14.

Bernstein, E., Caudy, A. A., Hammond, S. M., & Hannon, G. J. (2001). Role for a bidentate ribonuclease in the initiation step of RNA interference. *Nature, 409*(6818), 363-366. doi:10.1038/35053110

Broecker, F., & Moelling, K. (2019). Evolution of immune systems from viruses and transposable elements. *Frontiers in microbiology, 10*, 51.

Carpenter, A., Siggia, S., & Carter, S. (1976). Separation and/or concentration of phenolic materials from dilute aqueous solutions. *Analytical chemistry, 48*(1), 225-228.

Chen, Y., Zhang, X., Wu, W., Chen, Z., Gu, H., & Qu, L. J. (2006). Overexpression of the wounding- responsive gene *AtMYB15* activates the shikimate pathway in *Arabidopsis*. *Journal of Integrative Plant Biology*, *48*(9), 1084-1095.

Chiou, C.-Y., & Yeh, K.-W. (2008). Differential expression of MYB gene (*OgMYB1*) determines color patterning in floral tissue of *Oncidium* Gower Ramsey. *Plant Molecular Biology, 66*(4), 379-388.

Chiou, C. Y., & Yeh, K. W. (2011). Coloration and Color Patterning in Floral Tissues of *Oncidium* Gower Ramsey. In *Orchid Biotechnology II* (pp. 101-115).

Choi, C., Yoon, S., Moon, H., Bae, Y.-U., Kim, C.-B., Diskul-Na-Ayudthaya, P., . . . Ryu, S. (2018). mirRICH, a simple method to enrich the small RNA fraction from over-dried RNA pellets. *RNA Biology, 15*(6), 763-772. doi:10.1080/15476286.2018.1451723

Chomczynski, P., & Sacchi, N. (1987). Single-step method of RNA isolation by acid guanidinium thiocyanate-phenol-chloroform extraction. *Analytical biochemistry*, *162*(1), 156-159.

Christenhusz, M. J. M., & Byng, J. W. (2016). The number of known plants species in the world and its annual increase. *Phytotaxa, 261*(3), 201. doi:10.11646/phytotaxa.261.3.1

Cone, K. C., Cocciolone, S. M., Moehlenkamp, C. A., Weber, T., Drummond, B. J., Tagliani, L. A., ... & Perrot, G. H. (1993). Role of the regulatory gene *pl* in the photocontrol of maize anthocyanin pigmentation. *The Plant Cell*, *5*(12), 1807-1816.

Dalakouras, A., Jarausch, W., Buchholz, G., Bassler, A., Braun, M., Manthey, T., . . . Wassenegger, M. (2018). Delivery of Hairpin RNAs and Small RNAs Into Woody and Herbaceous Plants by Trunk Injection and Petiole Absorption. *Frontiers in Plant Science, 9*, 1253.

Dalakouras, A., Wassenegger, M., Dadami, E., Ganopoulos, I., Pappas, M. L., & Papadopoulou, K. (2020). Genetically modified organism-free RNA interference: exogenous. *Plant Physiology, 182*, 38-50.

Davies, K. M., & Schwinn, K. E. (2003). Transcriptional regulation of secondary metabolism. *Functional Plant Biology, 30*(9), 913-925.

De, L. C., Rao, A. N., Rajeevan, P. K., & Pathak, P. (2014). Orchid improvement—An overview. *Journal Orchid Society India*, *28*, 35-45.

Deepa, K., Sheeja, T. E., Santhi, R., Sasikumar, B., Cyriac, A., Deepesh, P. V., & Prasath, D. (2014). A simple and efficient protocol for isolation of high-quality functional RNA from different tissues of turmeric (*Curcuma longa* L.). *Physiology and Molecular Biology of Plants, 20*(2), 263-271. doi:10.1007/s12298-013-0218-y

Deluc, L., Barrieu, F., Marchive, C., Lauvergeat, V., Decendit, A., Richard, T., . . . Hamdi, S. (2006). Characterization of a Grapevine R2R3-MYB Transcription Factor That Regulates the Phenylpropanoid Pathway. *Plant Physiology, 140*(2), 499. doi:10.1104/pp.105.067231

Deng, J., Wu, D., Shi, J., Balfour, K., Wang, H., Zhu, G., ... & Zhu, Z. (2020). Multiple MYB Activators and Repressors Collaboratively Regulate the Juvenile Red Fading in Leaves of Sweetpotato. *Frontiers in plant science*, *11*, 941.

Di Stilio, V. S., Martin, C., Schulfer, A. F., & Connelly, C. F. (2009). An ortholog of MIXTA-like2 controls epidermal cell shape in flowers of *Thalictrum*. *New Phytol, 183*(3), 718-728. doi:10.1111/j.1469-8137.2009.02945.x

Ding, J.-T., Tu, H.-Y., Zang, Z.-L., Huang, M., & Zhou, S.-J. (2018). Precise control and prediction of the greenhouse growth environment of *Dendrobium candidum*. *Computers and Electronics in Agriculture, 151*, 453-459. doi: 10.1016/j.compag.2018.06.037

Dryden, I. L., & Mardia, K. V. (1998). Statistical shape analysis: Wiley series in probability and statistics. *New York, NY: John Wiley & Sons, Ltd*.

Dubos, C., Stracke, R., Grotewold, E., Weisshaar, B., Martin, C., & Lepiniec, L. (2010). MYB transcription factors in *Arabidopsis*. *Trends in Plant Science, 15*(10), 573-581. doi: 10.1016/j.tplants.2010.06.005

Dubrovina, A. S., & Kiselev, K. V. (2019). Exogenous RNAs for Gene Regulation and Plant Resistance. *International Journal of Molecular Sciences, 20*(9). doi:10.3390/ijms20092282

Edgar, R. C. (2004). MUSCLE: multiple sequence alignment with high accuracy and high throughput. *Nucleic acids research*, *32*(5), 1792-1797.

El-Ashram, S., Al Nasr, I., & Suo, X. (2016). Nucleic acid protocols: Extraction and optimization. *Biotechnology Reports, 12*, 33-39. doi: 10.1016/j.btre.2016.10.001

Elomaa, P., Uimari, A., Mehto, M., Albert, V. A., Laitinen, R. A., & Teeri, T. H. (2003). Activation of anthocyanin biosynthesis in *Gerbera hybrida* (Asteraceae) suggests conserved protein-protein and protein-promoter interactions between the anciently diverged monocots and eudicots. *Plant Physiology*, *133*(4), 1831-1842.

Fang, G., Hammar, S., & Grumet, R. (1992). A quick and inexpensive method for removing polysaccharides from plant genomic DNA. *Biotechniques*, *13*(1), 52-4.

Fellmann, C., & Lowe, S. W. (2014). Stable RNA interference rules for silencing. *Nature cell biology, 16*(1), 10-18.

Fire, A., Xu, S., Montgomery, M. K., Kostas, S. A., Driver, S. E., & Mello, C. C. (1998). Potent and specific genetic interference by double-stranded RNA in *Caenorhabditis elegans*. *Nature, 391*(6669), 806-811. doi:10.1038/35888

Fitch, C. M. (2004). *The best orchids for indoors*: Brooklyn Botanic Garden.

Gao, Y., Zhao, G., Jiang, C., Song, Y., Ye, K., & Feng, S. (2016). Comparison of Different Methods for RNA Extraction from Floral Buds of Tree Peony (*Paeonia suffruticosa* Andr.). *Notulae Botanicae Horti Agrobotanici Cluj-Napoca*, *44*(2), 418–422. https://doi.org/10.15835/nbha44210402

Gao, D., He, B., Zhou, Y., & Sun, L. (2011). Genetic and molecular analysis of a purple sheath somaclonal mutant in japonica rice. *Plant cell reports*, *30*(5), 901-911.

Gates, D. J., Olson, B. J., Clemente, T. E., & Smith, S. D. (2018). A novel R3 MYB transcriptional repressor associated with the loss of floral pigmentation in *Iochroma*. *New Phytologist*, *217*(3), 1346-1356.

Gilbert, R. I. (1971). An unusual anthocyanin in Antirrhinum majus. *Phytochemistry*, *10*(11), 2848-2849.

Gilding, E. K., & Marks, M. D. (2010). Analysis of purified glabra3- shapeshifter trichomes reveals a role for NOECK in regulating early trichome morphogenic events. *The Plant Journal*, *64*(2), 304-317.

Glover, B. J., & Martin, C. (1998). The role of petal cell shape and pigmentation in pollination success in *Antirrhinum majus*. *Heredity, 80*(6), 778-784. doi:10.1046/j.1365-2540.1998.00345.x

Goodall, C. (1991). Procrustes methods in the statistical analysis of shape. *Journal of the Royal Statistical Society: Series B (Methodological)*, *53*(2), 285-321.

Hamilton, A. J., & Baulcombe, D. C. (1999). A species of small antisense RNA in posttranscriptional gene silencing in plants. *Science*, *286*(5441), 950-952.

Hassanin, A. A., Soliman, S. S. A., Ismail, T. A., & Amin, M. K. A. (2017). The Role of *Slmyb* Gene In Tomato Fruit Development. *Zagazig Journal of Agricultural Research*, *44*(3), 969-988.

He, C., Teixeira da Silva, J. A., Wang, H., Si, C., Zhang, M., Zhang, X., . . . Duan, J. (2019). Mining MYB transcription factors from the genomes of orchids (*Phalaenopsis* and *Dendrobium*) and characterization of an orchid *R2R3-MYB* gene involved in water-soluble polysaccharide biosynthesis. *Scientific Reports, 9*(1), 13818. doi:10.1038/s41598-019-49812-8

Hew, C. S., & Yong, J. W. H. (2004). *The physiology of tropical orchids in relation to the industry*: World Scientific Publishing Company.

Higashi, Y., & Saito, K. (2013). Network analysis for gene discovery in plant-specialized metabolism. *Plant, Cell & Environment, 36*(9), 1597-1606. doi:10.1111/pce.12069

Hoffer, P., Ivashuta, S., Pontes, O., Vitins, A., Pikaard, C., Mroczka, A., ... & Voelker, T. (2011). Posttranscriptional gene silencing in nuclei. *Proceedings of the National Academy of Sciences, 108*(1), 409-414.

Holton, T. A., & Cornish, E. C. (1995). Genetics and Biochemistry of Anthocyanin Biosynthesis. *The Plant Cell, 7*(7), 1071-1083. doi:10.1105/tpc.7.7.1071

Hong, L., Dumond, M., Tsugawa, S., Sapala, A., Routier-Kierzkowska, A. L., Zhou, Y., ... & Roeder, A. H. (2016). Variable cell growth yields reproducible organ

development through spatiotemporal averaging. *Developmental cell*, *38*(1), 15-32.

Hongmei, M., Margaret, P., & Robert, G. (2009). Anthocyanin Regulatory/Structural Gene Expression in *Phalaenopsis*. *Journal of the American Society for Horticultural Science, 134*(1), 88-96. doi:10.21273/JASHS.134.1.88

Hsiao, Y. Y., Pan, Z. J., Hsu, C. C., Yang, Y. P., Hsu, Y. C., Chuang, Y. C., . . . Chen, H. H. (2011). Research on Orchid Biology and Biotechnology. *Plant and Cell Physiology, 52*(9), 1467-1486. doi:10.1093/pcp/pcr100

Hsu, C.-C., Chen, Y.-Y., Tsai, W.-C., Chen, W.-H., & Chen, H.-H. (2015). Three R2R3-MYB Transcription Factors Regulate Distinct Floral Pigmentation Patterning in *Phalaenopsis* spp. *Plant Physiology, 168*(1), 175. doi:10.1104/pp.114.254599

Ibrahim, U. K., Muhammad, I. I., & Salleh, R. M. (2011). The effect of pH on color behavior of *Brassica oleracea* anthocyanin. *Journal Applied Science, 11*(13), 2406-2410.

Jaffé, F. W., Tattersall, A., & Glover, B. J. (2007). A truncated MYB transcription factor from *Antirrhinum majus* regulates epidermal cell outgrowth. *Journal of Experimental Botany, 58*(6), 1515-1524. doi:10.1093/jxb/erm020

Jalal, J. S., & Singh, P. (2015). Threatened orchids of Maharashtra: A preliminary assessment based on IUCN regional guidelines and conservation prioritisation. *Journal Orchid Society India*, *29*, 1-14.

Jay, F., Vitel, M., Brioudes, F., Louis, M., Knobloch, T., & Voinnet, O. (2019). Chemical enhancers of posttranscriptional gene silencing in *Arabidopsis*. *RNA, 25*(9), 1078-1090.

Jia, L., Clegg, M. T., & Jiang, T. (2004). Evolutionary dynamics of the DNA-binding domains in putative R2R3-MYB genes identified from rice subspecies indica and japonica genomes. *Plant Physiology*, *134*(2), 575-585.

Jiang, C. K., & Rao, G. Y. (2020). Insights into the diversification and evolution of R2R3-MYB transcription factors in plants. *Plant physiology*, *183*(2), 637-655.

Jin, H., & Martin, C. (1999). Multifunctionality and diversity within the plant MYB-gene family. *Plant Molecular Biology, 41*(5), 577-585. doi:10.1023/A:1006319732410

Kanehisa, M., Sato, Y., & Morishima, K. (2016). BlastKOALA and GhostKOALA: KEGG Tools for Functional Characterization of Genome and Metagenome Sequences. *J Mol Biol, 428*(4), 726-731. doi: 10.1016/j.jmb.2015.11.006

Kiefer, E., Heller, W., & Ernst, D. J. P. M. B. R. (2000). A simple and efficient protocol for isolation of functional RNA from plant tissues rich in secondary metabolites. *18*(1), 33-39.

Kim, S., Hwang, G., Lee, S., Zhu, J.-Y., Paik, I., Nguyen, T. T., . . . Oh, E. (2017). High Ambient Temperature Represses Anthocyanin Biosynthesis through Degradation of HY5. *Frontiers in Plant Science, 8*(1787). doi:10.3389/fpls.2017.01787

Klingenberg, C. P., & Marugán-Lobón, J. (2013). Evolutionary covariation in geometric morphometric data: analyzing integration, modularity, and allometry in a phylogenetic context. *Systematic biology*, *62*(4), 591-610.

Klingenberg, C. P. (2020). Walking on Kendall's shape space: Understanding shape spaces and their coordinate systems. *Evolutionary Biology*, *47*(4), 334-352.

Koes, R., Verweij, W., & Quattrocchio, F. (2005). Flavonoids: a colorful model for the regulation and evolution of biochemical pathways. *Trends in Plant Science, 10*(5), 236-242. doi: 10.1016/j.tplants.2005.03.002

Kumar, S., Stecher, G., & Tamura, K. (2016). MEGA7: Molecular Evolutionary Genetics Analysis Version 7.0 for Bigger Datasets. *Molecular Biology and Evolution, 33*(7), 1870-1874. doi:10.1093/molbev/msw054

Langmead, B., Trapnell, C., Pop, M., & Salzberg, S. L. (2009). Ultrafast and memory-efficient alignment of short DNA sequences to the human genome. *Genome biology*, *10*(3), 1-10.

Lau, S. E., Mazumdar, P., Hee, T. W., Song, A. L. A., Othman, R. Y., & Harikrishna, J. A. (2014). Crude extracts of bacterially-expressed dsRNA protect orchid plants against *Cymbidium* mosaic virus during transplantation from in vitro culture. *The Journal of Horticultural Science and Biotechnology*, *89*(5), 569-576.

Lau, S.-E., Schwarzacher, T., Othman, R. Y., & Harikrishna, J. A. (2015). dsRNA silencing of an R2R3-MYB transcription factor affects flower cell shape in a *Dendrobium* hybrid. *BMC Plant Biology, 15*(1), 194. doi:10.1186/s12870-015-0577-3

Lee, H. S., & Wicker, L. (1991). Anthocyanin pigments in the skin of lychee fruit. *Journal of Food Science*, *56*(2), 466-468.

Lee, W. S., Gudimella, R., Wong, G. R., Tammi, M. T., Khalid, N., & Harikrishna, J. A. (2015). Transcripts and microRNAs responding to salt stress in *Musa acuminata* Colla (AAA Group) cv. Berangan roots. *PLoS One*, *10*(5), e0127526.

Lehninger, A. L., Nelson, D. L., & Cox, M. M. (2005). Lehninger principles of biochemistry New York. In: WH Freeman.

Letunic, I., Khedkar, S., & Bork, P. (2021). SMART: recent updates, new developments and status in 2020. *Nucleic acids research*, *49*(D1), D458-D460.

Li R (2015) Forensic biology. CRC Press, Boca Raton

Li, B.-J., Zheng, B.-Q., Wang, J.-Y., Tsai, W.-C., Lu, H.-C., Zou, L.-H., . . . Wang, Y. (2020). New insight into the molecular mechanism of colour differentiation among floral segments in orchids. *Communications Biology, 3*(1), 89. doi:10.1038/s42003-020-0821-8

Li, C., Qiu, J., Ding, L., Huang, M., Huang, S., Yang, G., & Yin, J. (2017). Anthocyanin biosynthesis regulation of *DhMYB2* and *DhbHLH1* in *Dendrobium* hybrids petals. *Plant Physiology and Biochemistry, 112*, 335-345. doi: 10.1016/j.plaphy.2017.01.019

Liu, L., Han, R., Yu, N., Zhang, W., Xing, L., Xie, D., & Peng, D. J. P. o. (2018). A method for extracting high-quality total RNA from plant rich in polysaccharides and polyphenols using *Dendrobium huoshanense*. *13*(5), e0196592.

Livak, K. J., & Schmittgen, T. D. (2001). Analysis of relative gene expression data using real-time quantitative PCR and the 2− ΔΔCT method. *Methods*, *25*(4), 402-408.

Lück, S., Kreszies, T., Strickert, M., Schweizer, P., Kuhlmann, M., & Douchkov, D. (2019). siRNA-Finder (si-Fi) Software for RNAi-Target Design and Off-Target Prediction. *Frontiers in Plant Science, 10*(1023). doi:10.3389/fpls.2019.01023

Lu, H. C., Lam, S. H., Zhang, D., Hsiao, Y. Y., Li, B. J., Niu, S. C., ... & Liu, Z. J. (2022). *R2R3-MYB* genes coordinate conical cell development and cuticular wax biosynthesis in *Phalaenopsis aphrodite*. *Plant physiology*, *188*(1), 318-331.

Luo, M. R. (Ed.). (2016). *Encyclopedia of color science and technology*. Springer Reference.

Luo, D., Xiong, C., Lin, A., Zhang, C., Sun, W., Zhang, J., ... & Wang, T. (2021). *SlBBX20* interacts with the COP9 signalosome subunit SlCSN5-2 to regulate anthocyanin biosynthesis by activating *SlDFR* expression in tomato. *Horticulture research*, *8*.

Mahmood, W. J. W. (2006). Developing Malaysian seed industry: Prospects and challenges. *Economic Technology Management Review*, *1*, 51-59.

Mehrtens, F., Kranz, H., Bednarek, P., & Weisshaar, B. (2005). The Arabidopsis transcription factor MYB12 is a flavonol-specific regulator of phenylpropanoid biosynthesis. *Plant Physiology, 138*(2), 1083-1096. doi:10.1104/pp.104.058032

Miller, R., Owens, S. J., & Rørslett, B. (2011). Plants and colour: Flowers and pollination. *Optics & Laser Technology, 43*(2), 282-294. doi: 10.1016/j.optlastec.2008.12.018

Moretti, M., Cossignani, L., Messina, F., Dominici, L., Villarini, M., Curini, M., & Marcotullio, M. C. (2013). Antigenotoxic effect, composition and antioxidant activity of *Dendrobium speciosum*. *Food chemistry*, *140*(4), 660-665.

Mount, D. W. (2007). Using the basic local alignment search tool (BLAST). *Cold Spring Harbor Protocols, 2007*(7), pdb-top17.

Muoki, R. C., Paul, A., Kumari, A., Singh, K., & Kumar, S. (2012). An improved protocol for the isolation of RNA from roots of tea (*Camellia sinensis* (L.) O. Kuntze). *Molecular biotechnology*, *52*(1), 82-88.

Murray, M. G., & Thompson, W. F. (1980). Rapid isolation of high molecular weight plant DNA. *Nucleic acids research*, *8*(19), 4321-4326.

Napoli, C., Lemieux, C., & Jorgensen, R. (1990). Introduction of a Chimeric *Chalcone Synthase* Gene into *Petunia* Results in Reversible Co-Suppression of Homologous Genes in trans. *The Plant Cell, 2*(4), 279. doi:10.1105/tpc.2.4.279

Nik Rozana, N. M. M., & Noorlidawati, A. H. (2016). Malaysian Floriculture Industry Development Policy. *Malaysian Agricultural Research and Development Institute*.

Noda, K.-i., Glover, B. J., Linstead, P., & Martin, C. (1994). Flower colour intensity depends on specialized cell shape controlled by a Myb-related transcription factor. *Nature, 369*(6482), 661-664.

Obbard, D. J., Gordon, K. H. J., Buck, A. H., & Jiggins, F. M. (2009). The evolution of RNAi as a defence against viruses and transposable elements. *Philosophical Transactions of the Royal Society B: Biological Sciences, 364*(1513), 99-115.

Ogata, K., Kanei-Ishii, C., Sasaki, M., Hatanaka, H., Nagadoi, A., Enari, M., ... & Sarai, A. (1996). The cavity in the hydrophobic core of Myb DNA-binding domain is reserved for DNA recognition and trans-activation. *Nature structural biology*, *3*(2), 178-187.

Oh, I. H., & Reddy, E. P. (1999). The myb gene family in cell growth, differentiation and apoptosis. *Oncogene*, *18*(19), 3017-3033.

Pan, Z.-J., Chen, Y.-Y., Du, J.-S., Chen, Y.-Y., Chung, M.-C., Tsai, W.-C., . . . Chen, H.-H. (2014). Flower development of *Phalaenopsis* orchid involves functionally divergent SEPALLATA-like genes. *New Phytologist, 202*(3), 1024-1042. doi:10.1111/nph.12723

Pattanaik, S., Kong, Q., Zaitlin, D., Werkman, J. R., Xie, C. H., Patra, B., & Yuan, L. (2010). Isolation and functional characterization of a floral tissue-specific R2R3 MYB regulator from tobacco. *Planta*, *231*(5), 1061-1076.

Paz- Ares, J., Wienand, U., Peterson, P. A., & Saedler, H. (1986). Molecular cloning of the c locus of *Zea mays*: a locus regulating the anthocyanin pathway. *The EMBO Journal*, *5*(5), 829-833.

Perez-Rodriguez, M., Jaffe, F. W., Butelli, E., Glover, B. J., & Martin, C. (2005). Development of three different cell types is associated with the activity of a specific MYB transcription factor in the ventral petal of *Antirrhinum majus* flowers. *Development, 132*(2), 359. doi:10.1242/dev.01584

Petroni, K., & Tonelli, C. (2011). Recent advances on the regulation of anthocyanin synthesis in reproductive organs. *Plant science*, *181*(3), 219-229.

Pridgeon, A. M., Schuiteman, A., Chase, M. W., Cameron, K. M., Freudenstein, J. V., Salazar, G., & van den Berg, C. (2015). An updated classification of Orchidaceae. *Botanical Journal of the Linnean Society, 177*(2), 151-174. doi:10.1111/boj.12234

Quattrocchio, F., Wing, J. F., Leppen, H. T., Mol, J. N., & Koes, R. E. (1993). Regulatory genes controlling anthocyanin pigmentation are functionally conserved among plant species and have distinct sets of target genes. *The Plant Cell*, *5*(11), 1497-1512.

Rasika, G. M., Adelheid, R. K., & Teresita, D. A. (2003). Pigment Distribution and Epidermal Cell Shape in *Dendrobium* Species and Hybrids. *HortScience, 38*(4), 573-577. doi:10.21273/HORTSCI.38.4.573

Ratanasut, K., Monmai, C., & Piluk, P. (2015). Transient hairpin RNAi-induced silencing in floral tissues of *Dendrobium* Sonia 'Earsakul'by agroinfiltration for rapid assay of flower colour modification. *Plant Cell, Tissue and Organ Culture (PCTOC)*, *120*(2), 643-654.

Riaz, B., Chen, H., Wang, J., Du, L., Wang, K., & Ye, X. (2019). Overexpression of Maize *ZmC1* and *ZmR* Transcription Factors in Wheat Regulates Anthocyanin Biosynthesis in a Tissue-Specific Manner. *International Journal of Molecular Sciences, 20*(22), 5806.

Rohlf, F. J., & Slice, D. (1990). Extensions of the Procrustes method for the optimal superimposition of landmarks. *Systematic biology*, *39*(1), 40-59.

Ruiz-Ferrer, V., & Voinnet, O. (2009). Roles of plant small RNAs in biotic stress responses. *Annual review of plant biology, 60*, 485-510.

Sambrook, J., & Russell, D. W. (2006). *The condensed protocols from molecular cloning: a laboratory manual*.

Saurabh, S., Vidyarthi, A. S., & Prasad, D. (2014). RNA interference: concept to reality in crop improvement. *Planta, 239*(3), 543-564.

Schroeder, A., Mueller, O., Stocker, S., Salowsky, R., Leiber, M., Gassmann, M., . . . Ragg, T. (2006). The RIN: an RNA integrity number for assigning integrity values to RNA measurements. *BMC Molecular Biology, 7*(1), 3. doi:10.1186/1471-2199-7-3

Schwinn, K., Venail, J., Shang, Y., Mackay, S., Alm, V., Butelli, E., . . . Martin, C. (2006). A Small Family of MYB Regulatory Genes Controls Floral Pigmentation Intensity and Patterning in the Genus *Antirrhinum*. *The Plant Cell, 18*(4), 831-851. doi:10.1105/tpc.105.039255

Scoville, A. G., Barnett, L. L., Bodbyl-Roels, S., Kelly, J. K., & Hileman, L. C. (2011). Differential regulation of a MYB transcription factor is correlated with transgenerational epigenetic inheritance of trichome density in *Mimulus guttatus*. *New Phytologist, 191*(1), 251-263. doi:10.1111/j.1469-8137.2011.03656.x

Sheehan, T. J. (1992). 5 - Orchids. In R. A. Larson (Ed.), *Introduction to Floriculture (Second Edition)* (pp. 113-142). New York: Academic Press.

Shimada, S., Otsuki, H., & Sakuta, M. (2006). Transcriptional control of anthocyanin biosynthetic genes in the *Caryophyllales*. *Journal of Experimental Botany, 58*(5), 957-967. doi:10.1093/jxb/erl256

Shu, C., Sun, S., Chen, J., Chen, J., & Zhou, E. (2014). Comparison of different methods for total RNA extraction from sclerotia of *Rhizoctonia solani*. *Electronic Journal of Biotechnology*, *17*(1), 50-54.

Slice, D. E. (2001). Landmark coordinates aligned by Procrustes analysis do not lie in Kendall's shape space. *Systematic biology*, *50*(1), 141-149.

Song, M. S., & Rossi, J. J. (2017). Molecular mechanisms of Dicer: endonuclease and enzymatic activity. *Biochemical Journal, 474*(10), 1603-1618.

Stracke, R., Ishihara, H., Huep, G., Barsch, A., Mehrtens, F., Niehaus, K., & Weisshaar, B. (2007). Differential regulation of closely related R2R3-MYB transcription factors controls flavonol accumulation in different parts of the *Arabidopsis thaliana* seedling. *The Plant Journal, 50*(4), 660-677. doi:10.1111/j.1365-313X.2007.03078.x

Stracke, R., Werber, M., & Weisshaar, B. (2001). The R2R3-MYB gene family in *Arabidopsis thaliana*. *Current Opinion in Plant Biology, 4*(5), 447-456.

Su, C.-l., Chao, Y.-T., Alex Chang, Y.-C., Chen, W.-C., Chen, C.-Y., Lee, A.-Y., . . . physiology, c. (2011). De novo assembly of expressed transcripts and global analysis of the *Phalaenopsis aphrodite* transcriptome. *52*(9), 1501-1514.

Surzycki, S. (2012). *Basic techniques in molecular biology*: Springer Science & Business Media.

Suzuki, A., Suzuki, T., Tanabe, F., Toki, S., Washida, H., Wu, C. Y., & Takaiwa, F. (1997). Cloning and expression of five myb-related genes from rice seed. *Gene, 198*(1-2), 393-398. doi:10.1016/s0378-1119(97)00344-2

Takos, A. M., Jaffé, F. W., Jacob, S. R., Bogs, J., Robinson, S. P., & Walker, A. R. (2006). Light-induced expression of a MYB gene regulates anthocyanin biosynthesis in red apples. *Plant physiology*, *142*(3), 1216-1232.

Tanaka, Y., & Brugliera, F. (2013). Flower colour and cytochromes P450. *Philosophical Transactions of the Royal Society B: Biological Sciences, 368*(1612), 20120432.

Tanaka, Y., & Ohmiya, A. (2008). Seeing is believing: engineering anthocyanin and carotenoid biosynthetic pathways. *Current Opinion in Biotechnology, 19*(2), 190-197. doi: 10.1016/j.copbio.2008.02.015

Tenea, G. N., Cordeiro Raposo, F., & Maquet, A. (2012). Comparative transcriptome profiling in winter wheat grown under different agricultural practices. *Journal of agricultural and food chemistry*, *60*(44), 10970-10978.

Tenllado, F., Martinez-Garcia, B., Vargas, M., & Diaz-Ruiz, J. R. (2003). Crude extracts of bacterially expressed dsRNA can be used to protect plants against virus infections. *Bmc Biotechnology, 3*, 1-11.

Timmons, L., Court, D. L., & Fire, A. (2001a). Ingestion of bacterially expressed dsRNAs can produce specific and potent genetic interference in *Caenorhabditis elegans*. *Gene, 263*(1-2), 103-112.

Timmons, L., Court, D. L., & Fire, A. (2001b). Ingestion of bacterially expressed dsRNAs can produce specific and potent genetic interference in *Caenorhabditis elegans*. *Gene, 263*(1), 103-112. doi: 10.1016/S0378-1119(00)00579-5

Toni, L. S., Garcia, A. M., Jeffrey, D. A., Jiang, X., Stauffer, B. L., Miyamoto, S. D., & Sucharov, C. C. (2018). Optimization of phenol-chloroform RNA extraction. *MethodsX*, *5*, 599-608.

Untergasser, A., Cutcutache, I., Koressaar, T., Ye, J., Faircloth, B. C., Remm, M., & Rozen, S. G. (2012). Primer3--new capabilities and interfaces. *Nucleic acids research, 40*(15), e115-e115. doi:10.1093/nar/gks596

Vega, Y., & Marques, I. (2015). Both biotic and abiotic factors influence floral longevity in three species of *Epidendrum* (Orchidaceae). *Plant Species Biology, 30*(3), 184-192. doi:10.1111/1442-1984.12046

Watanabe, K., Kobayashi, A., Endo, M., Sage-Ono, K., Toki, S., & Ono, M. (2017). CRISPR/Cas9-mediated mutagenesis of the *dihydroflavonol-4-reductase-B* (*DFR-B*) locus in the Japanese morning glory *Ipomoea* (*Pharbitis*) *nil*. *Scientific reports*, *7*(1), 1-9.

Wheeler, L. C., Walker, J. F., Ng, J., Deanna, R., Dunbar-Wallis, A., Backes, A., ... & Smith, S. D. (2022). Transcription factors evolve faster than their structural gene targets in the flavonoid pigment pathway. *Molecular biology and evolution*, *39*(3), msac044.

Whitney, H. M., Bennett, K. M. V., Dorling, M., Sandbach, L., Prince, D., Chittka, L., & Glover, B. J. (2011). Why do so many petals have conical epidermal cells? *Annals of Botany, 108*(4), 609-616. doi:10.1093/aob/mcr065

Wilkins, O., Nahal, H., Foong, J., Provart, N. J., & Campbell, M. M. (2009). Expansion and Diversification of the *Populus* R2R3-MYB Family of Transcription Factors. *Plant Physiology, 149*(2), 981. doi:10.1104/pp.108.132795

Wingard, S. A., & Fromme, F. D. (1928). Tobacco ringspot; a virus disease with a wide host range. *Phytopathology, 18*, 133.

Wong, L.-M., Silvaraj, S., & Phoon, L.-Q. (2014). An Optimised High-Salt CTAB Protocol for Both DNA and RNA Isolation from Succulent Stems of *Hylocereus* sp. *Journal of Medical and Bioengineering Vol, 3*(4).

Wu, X.-M., Lim, S.-H., & Yang, W.-C. (2003). Characterization, expression and phylogenetic study of *R2R3-MYB* genes in orchid. *Plant Molecular Biology, 51*(6), 959-972. doi:10.1023/A:1023050110077

Xie, Y., Chen, P., Yan, Y., Bao, C., Li, X., Wang, L., . . . Guan, Q. (2018). An atypical R2R3 MYB transcription factor increases cold hardiness by CBF-dependent and CBF-independent pathways in apple. *New Phytologist, 218*(1), 201-218. doi:10.1111/nph.14952

Xu, W., Dubos, C., & Lepiniec, L. (2015). Transcriptional control of flavonoid biosynthesis by MYB–bHLH–WDR complexes. *Trends in plant science*, *20*(3), 176-185.

Yamagishi, M., Shimoyamada, Y., Nakatsuka, T., & Masuda, K. (2010). Two R2R3-MYB genes, homologs of petunia *AN2*, regulate anthocyanin biosyntheses in flower tepals, tepal spots and leaves of Asiatic hybrid lily. *Plant and Cell Physiology*, *51*(3), 463-474.

Yoshida, K., Kitahara, S., Ito, D., & Kondo, T. (2006). Ferric ions involved in the flower color development of the Himalayan blue poppy, *Meconopsis grandis*. *Phytochemistry, 67*(10), 992-998. doi: 10.1016/j.phytochem.2006.03.013

Zamore, P. D., Tuschl, T., Sharp, P. A., & Bartel, D. P. (2000). RNAi: Double-Stranded RNA Directs the ATP-Dependent Cleavage of mRNA at 21 to 23 Nucleotide Intervals. *Cell, 101*(1), 25-33. doi: 10.1016/S0092-8674(00)80620-0

Zhang, F., Gonzalez, A., Zhao, M., Payne, C. T., & Lloyd, A. (2003). A network of redundant bHLH proteins functions in all TTG1-dependent pathways of *Arabidopsis Development, 130*(20), 4859. doi:10.1242/dev.00681

Zhang, G.-Q., Xu, Q., Bian, C., Tsai, W.-C., Yeh, C.-M., Liu, K.-W., . . . Liu, Z.-J. (2016). The *Dendrobium catenatum* Lindl. genome sequence provides insights into polysaccharide synthase, floral development and adaptive evolution. *Scientific Reports, 6*(1), 19029. doi:10.1038/srep19029

Zhang, Z., Li, D. W., Jin, J. H., Yin, Y. X., Zhang, H. X., Chai, W. G., & Gong, Z. H. (2015). VIGS approach reveals the modulation of anthocyanin biosynthetic genes by *CaMYB* in chili pepper leaves. *Frontiers in plant science*, *6*, 500.

Zimmermann, I. M., Heim, M. A., Weisshaar, B., & Uhrig, J. F. (2004). Comprehensive identification of *Arabidopsis thaliana* MYB transcription factors interacting with R/B- like BHLH proteins. *The Plant Journal, 40*(1), 22-34.